

HYDROGRAPHISCHE NACHRICHTEN

Fachzeitschrift für Hydrographie und Geoinformation

*Second
International
Issue*

11/2016 HN 105



Selected papers of **HYDRO 2016**
Sea you again ...

Mathias Jonas:

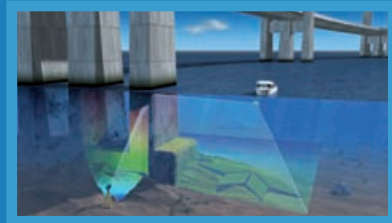
*»I want nothing less than all the
physics of the sea chart«*



OCEAN ENGINEERING IN DEPTH

HYDROGRAPHIC SERVICE

	CONSULTING		MULTIBEAM
	POSITION & MOTION		SIDE SCAN SONAR
	SOFTWARE		INTEGRATION



Dear readers,

Maybe you belong to the visitors who come to HYDRO 2016 in Rostock-Warnemünde at the beginning of November. This isn't unlikely, as we expect more than 300 delegates in Germany's centre of hydrography. Hydrographers from all over the world make the journey in order to keep up-to-date with professional theory and practice. In workshops and boat demos they learn about the most current technological developments. More than 50 expert lectures highlight different aspects of hydrography.

This encounter of the hydrographic community motivated us to publish the second international issue of the *Hydrographische Nachrichten* – entirely in English. In doing so, we want you to enjoy this expert magazine, which has been published by the German Hydrographic Society (DHYG) since 1984.

The special feature of this edition: We publish ten selected conference papers of HYDRO 2016, written by researchers who mainly work in Germany, and practitioners, who apply their knowledge all over the world.

On the first pages you will read an interview with Mathias Jonas, the National Hydrographer of Germany. He wants us to experience hydrography as a great opportunity and push our thoughts and actions beyond confining limits instead of restricting them. Time has come to leave behind the outdated view on our discipline because hydrography

isn't only responsible for the safety of navigation. Hydrography offers so much more, and finds solutions for associated sciences.

This edition shows today's hydrographic border areas. Three articles deal with detailed coastal zone surveys both on land and in shallow water. One paper is about oceanographic measurements, to show hydrodynamic features in the water column. Other topics are navigation with improved electronic sea charts and sophisticated GNSS techniques. Four papers deal with the search of objects – cables, old munition and airplanes – on or under the sea floor.

An interesting essay on the laborious search for a crashed passenger plane shows that hydrography is also very effective publicly. The clear 3D visualisations of the river Elbe, which the Hafen-City University implemented in cooperation with a daily newspaper, demonstrate people's interest in hydrographic information.

We hope that you enjoy the selection of articles – a mixture of vivid essays and expert papers full of formulas. In case you haven't become acquainted with our journal so far, we invite you to read following editions of the *Hydrographische Nachrichten*, in which articles are regularly published in English. You can download the journal under: www.dhyg.de

Yours, *Lars Schiller*



Lars Schiller

Hydrographische Nachrichten HN 105 – November 2016

Fachzeitschrift für Hydrographie und Geoinformation

Official journal of the
German Hydrographic Society – DHYG

Publisher:

Deutsche Hydrographische Gesellschaft e. V.

c/o Sabine Müller
Innomar Technologie GmbH
Schutower Ringstraße 4
18069 Rostock

Internet: www.dhyg.de
E-mail: dhyg@innomar.com
Phone: (0381) 44079-0

ISSN: 1866-9204

Editor-in-chief:

Lars Schiller
E-mail: lars.schiller@dhyg.de

Editorial team:

Stefan Steinmetz, Dipl.-Ing.
Vasiliki Kekridou, M.Sc.
Peter Dugge, Dipl.-Ing.

Scientific advisory board:

Horst Hecht, Dipl.-Met.

Proofreading and translation:

Verena Eisemann,
State-certified translator

The journal is published three times a year, in February, June and October. For DHYG members the subscription is covered by the membership fee.

© 2016

Advertisements:

Full page (210 mm × 297 mm): 300 Euro;
on the inside cover: 400 Euro;
on the outside cover: 600 Euro.
Half page (210 mm × 148 mm): 200 Euro.
Contact: Stefan Steinmetz,
e-mail: sts@eiva.com

Information for contributors:

The submitted paper must not have been published in this form to date. Please submit your text unformatted and without images in the text file itself. The attached images should have a resolution of at least 300 dpi. Automatic hyphenation must be deactivated in the text file and manual hyphenation is not permitted. Decisions regarding paper acceptance and publication time are made by the editorial team. In order for articles to be published, authors have to agree to editorial processing, providing the original meaning is not distorted.



R2SONIC

Multibeam Echosounder



Sonic 2020



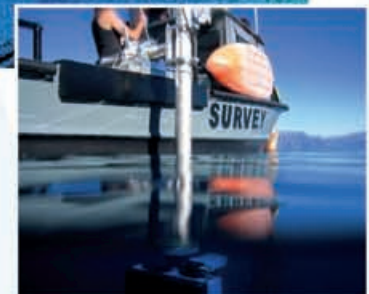
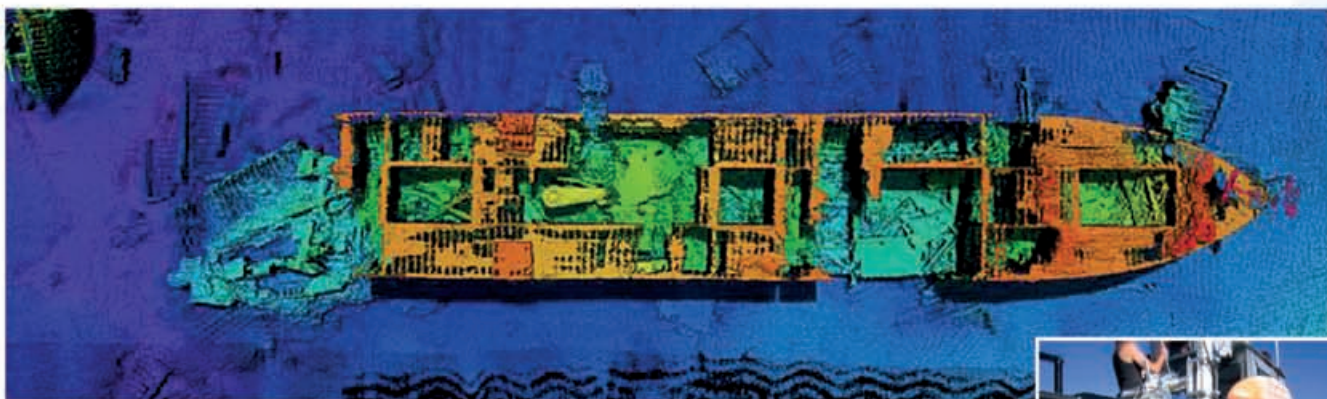
Sonic 2022



Sonic 2024



Sonic 2026



- **Versatile** – Bathymetry with optional TruePix™ Backscatter, Raw Water Column and Forward Looking Sonar imagery
- **Wideband Operation** – Over 20x User Selectable Frequencies from 200 to 400kHz, selectable on the fly, in real-time during survey operations. Optional 700kHz operation with 0.3° x 0.6° beamwidths
- **Highest Resolution & Accuracy** – Focused 0.5° x 1° beamwidths, 60kHz Signal Bandwidth with true range resolution to 1.25 cm
- **Productive** – Selectable swath coverage from 10° to 160°, selectable on the fly, in real-time during survey operations. 1 to 500m range
- **Ease of Operation** – Embedded signal processor and Controller. Sonar user interface from Survey application software PC. Low weight, volume & power consumption (less than 50 Watts).
- **Compelling value** – Latest Advanced Technology. Industry leading 3-year limited warranty. Value priced. Trade-in rebate for older technology systems

■ **R2Sonic** is a leading manufacturer of truly innovative and high quality wideband Multibeam Echosounders with its head office in Austin, Texas. Since first system deliveries in 2009, more than 850 Sonic Multibeam Echosounders have been successfully commissioned to the private and public sectors. That impressively confirms the innovative spirit, superior performance and flexibility of R2Sonic products in general and in particular the appreciation of reliable, light weight, power efficient, and space saving Sonic Multibeam Echosounders by customers all over the world.

■ **Nautilus Marine Service GmbH** based in Buxtehude is the distributor for R2Sonic Multibeam Echosounders in Germany. In addition to sales, Nautilus Marine Service offers assistance to the installation and commissioning of complete hydrographic survey systems including training and maintenance.

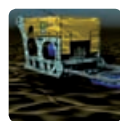
Selected papers of HYDRO 2016



Interview

- 6 »I want nothing less than all the physics of the sea chart«

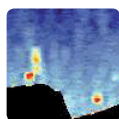
An academic discussion with MATHIAS JONAS



UXO survey

- 40 Offshore unexploded ordnance recovery and disposal

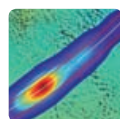
An article by JAN KÖLBEL and DAVID ROSE



Hydrodynamics

- 12 Comparison and characteristics of oceanographic in situ measurements and simulations above submerged sand waves in a tidal inlet

An article by INGO HENNINGS and DAGMAR HERBERS



Aircraft search

- 44 The search for Malaysian Airlines flight MH370

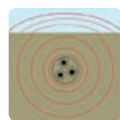
An article by MELANIE BARTH



Coastal zone mapping

- 18 High-resolution, topobathymetric LiDAR coastal zone characterisation

An article by FRANK STEINBACHER et al.



Cable tracking

- 47 The challenge of choosing the right method for surveying power cables

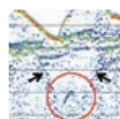
An article by OLIVER ANDERS



Coastal protection

- 22 New techniques in capturing and modelling of morphological data

An article by LUTZ CHRISTIANSEN



Cable survey

- 50 Burial depth determination of cables using acoustics

Requirements, issues and strategies
An article by JENS WUNDERLICH et al.



Coastal zone mapping

- 26 Use of laser bathymetry at the German Baltic Sea coast

An article by WILFRIED ELLMER



3D visualisation

- 56 A new view on the Elbe

Dynamic and interactive 3D views for public information purposes in news media
An article by TANJA DUFEK et al.



Nautical information

- 30 ENC and ECDIS

An article by PETER DUGGE



IHO

- 60 The liberated organisation

An article by MATHIAS JONAS



Advanced GNSS techniques

- 34 Improved positioning of surveying vessels on inland waterways with HydrOs

An article by THOMAS ARTZ et al.



Bereavement

- 62 In memory of DVW President Prof. Dr. Ing. Karl-Friedrich Thöne

An obituary by HAGEN GRAEFF

The next issue of *Hydrographische Nachrichten* will be published in February 2017.
Editorial deadline: 15 January 2017
Advertising deadline: 15 January 2017

»I want nothing less than all the physics of the sea chart«

An academic discussion with MATHIAS JONAS*

Dr. Mathias Jonas is Vice President of the Federal Maritime and Hydrographic Agency. The 55 year old National Hydrographer of Germany and Managing Director of the department »Nautical Hydrography« is responsible for national activities in wreck search, sea survey and the issue of related nautical publications. He represents those tasks in various organs of the International Maritime Organization (IMO) and the International Hydrographic Organization (IHO). In the interview with *Hydrographische Nachrichten* the expert for electronic sea charts talks about his preference for paper and about the future of the printed sea chart. And he believes that dealing with the ocean awakes the good in man.

National Hydrographer | IHO | Baltic Sea | S-100 | universal hydrographic data model | standards | sea chart | paper chart

HN: What does a National Hydrographer do? Are there any clearly defined tasks?

Mathias Jonas: In my function as National Hydrographer I represent the National Hydrographic Office of the Federal Republic of Germany within the IHO.

HN: Does the German National Hydrographer have any different tasks than the one in other countries?

Jonas: In many countries the head of the Hydrographic Office is exclusively responsible for cartographical issues and nautical publications. In Germany, there are more tasks like surveying and the supervision of the fleet as we do not charter surveying capacity but we have our own ships. Insofar, I have quite a broad field of issues compared to other National Hydrographers.

HN: How does the cooperation with the hydrographers of neighbouring countries work?

Jonas: Our bilateral cooperation is good and we coordinate with each other in the bodies of the IHO. The professional exchange is great. However, the Hydrographic Offices of the neighbouring countries are organised in a different way. In Poland and in the Netherlands for example, they belong to the navy, thus they are not part of a civil ministry. Hydrographic surveying and the publication of nautical charts by the navy have a long naval tradition in coastal states based on its strategic importance for the case of operation. Only due to special circumstances in history, hydrography has become part of civil

administration in comparatively few countries. In the old Federal Republic of Germany it happened after World War II; on the other hand, hydrography in the former GDR remained in the responsibility

of the military until the end. In Denmark, the Hydrographic Office is part of the civil administration; however, the survey units are military. In all other Scandinavian countries and Baltic States it is part of the traffic administration. These different structures make cooperation across borders very challenging.

HN: Are there any sensitive issues in the cooperation?

Jonas: The gas pipeline across the Baltic Sea has a certain political dimension in the German-Polish relationship. Of course, hydrography doesn't play a main role in the political process of the pipeline, nonetheless, the topographic circumstances have to be clear. Therefore, it is very important that non-political professionals remain in dialogue. Even in times when the project was politically controversial, we exchanged data and helped each other and kept us informed.

HN: Do you cooperate with our French neighbours as well?

Jonas: We do not only cultivate our regional neighbourhood, but also the bigger one in Europe. For this purpose we founded a working group within the IHO in order to represent the Hydrographic Offices in Europe to a greater extent. The aim is not only the strengthening of our position in terms of ideation but also materially through EU-funds. France has a lot of experience in using EU-funds for projects that's why we aim at closer cooperation. We have launched one project already: Coastal Mapping. With it we demonstrate how high-resolution capturing of offshore areas on both sides of the coastline can be technically improved. In a following project based on the first one, we want to capture the bathymetry of subsequent waters in high resolution up to a depth of 10 metres.

HN: What is a special feature of cooperation in the Baltic Sea region?

Jonas: The Baltic Sea is regarded as our laboratory for marine policy. It is a clearly defined geographic

* The interview was held by Lars Schiller and Thomas Dehling September 23rd, 2016 at the Federal Maritime and Hydrographic Agency (BSH) in Rostock

Translation by Verena Eismann

»Hydrography has a long naval tradition based on its strategic importance for the case of operation. Only due to special circumstances in history, hydrography has become part of civil administration in comparatively few countries«

Mathias Jonas

territory, which is prone to high user pressure with very differing national interests at the same time. Three years ago, all neighbouring states started a common project, the Baltic Sea Bathymetry Database (BSBD). A website offers the link to a bathymetric database that is maintained by Sweden. The result shows what is possible, when all Baltic Sea states cooperate by supplying data and if one party on behalf of all others puts together all data of the Baltic Sea. At the same time, we learned the difficulties of such a project not only from a technical point of view, but also from the administrative one. However, I am very optimistic.

HN: Do you coordinate with the neighbouring countries the usage of the different Baltic Sea areas?

Jonas: Spatial planning in the Baltic Sea plays an important role. The process of authorising wind energy plants, cable routes and pipelines gives us a clear idea of our neighbour's interests. Together we discuss which sea area is suitable for which usage. This allocation of usage and protection areas doesn't belong to the still prevailing concept of hydrography, but it is based on it. It is very nice to see how similarities and mutual trust become stronger through cooperation.

HN: Since January 2014 you are Vice President of the Federal Maritime and Hydrographic Agency. What has changed within the agency since you have started?

Jonas: I am very much interested in topics that are not related directly to nautical hydrography. When I represent the agency I must have knowledge of

the entire range of topics, whether it is about flag states administration, maritime spatial planning or oceanography. All this has influence on my view of hydrography because I need to reflect on the relationship of these topics and hydrography. I have already given up the idea that hydrography is all about sea charts. My American colleagues say that it should not be »chart-driven« anymore, but »data-centred« and I cannot agree more. The Federal Maritime and Hydrographic Agency has broadened its hydrographic spectrum from the mere producing point of view to the entire ocean knowledge. We administer the available

data and information in such a flexible way so we can satisfy all requests and user interests without restrictions. The concept of hydrography is in a developing process. Apart from ground topography and geology, data of water column, salinity and dynamics belong to it because all of them are interdependent. Some time ago a TV reporter asked me for a briefest description how the state of the Baltic Sea is. My answer was only three sentences long. However, at the same time I thought that the question deserved more profundity, the presentation and relation of each individual aspect.

HN: You talk about nautical hydrography, and your department in the Federal Maritime and Hydro-

»The concept of hydrography is in a developing process. Apart from ground topography and geology, data of water column, salinity and dynamics belong to it because all of them are interdependent«

Mathias Jonas



Published up to now:

Horst Hecht (HN 82),
 Holger Klindt (HN 83),
 Joachim Behrens (HN 84),
 Bernd Jeuken (HN 85),
 Hans Werner Schenke (HN 86),
 Wilhelm Weinrebe (HN 87),
 William Heaps (HN 88),
 Christian Maushake (HN 89),
 Monika Breuch-Moritz (HN 90),
 Dietmar Grünreich (HN 91),
 Peter Gimpel (HN 92),
 Jörg Schimmeler (HN 93),
 Delf Egge (HN 94),
 Gunther Braun (HN 95),
 Siegfried Fahrentholz (HN 96),
 Gunther Braun, Delf Egge, Ingo
 Harre, Horst Hecht, Wolfram
 Kirchner und Hans-Friedrich
 Neumann (HN 97),
 Werner und Andres Nicola
 (HN 98),
 Sören Themann (HN 99),
 Peter Ehlers (HN 100),
 Rob van Ree (HN 101),
 DHyG-Beirat (HN 102),
 Walter Offenborn (HN 103),
 Jens Schneider von Deimling
 (HN 104)

»The Baltic Sea is regarded as laboratory for marine policy. It is a clearly defined geographic territory, which is prone to high user pressure with very differing national interests at the same time«

Mathias Jonas

graphic Agency carries that title. How do you differ between nautical hydrography and hydrography?

Jonas: The German name of our agency is »Bundesamt für Seeschifffahrt und Hydrographie«. »Seeschifffahrt« means maritime traffic or shipping, everyone has a vague idea of what this is. However, the German term »Hydrographie« does not only stand for the department »Nautical Hydrography« but also for the department »Marine Sciences«, directed by Dr. Bernd Brüggge. Therefore, we call the combination of hydrographic surveying and nautical cartography »nautical hydrography«.

HN: What are you responsible for as head of the department »Nautical Hydrography«?

Jonas: There are four areas. One of it is the surveying ships with special technology, which are also used in the marine sciences for monitoring the environment. Then, the entire field of hydrographic surveying including marine geodesy, Thomas Dehling is head of that department. Another one is cartography, which is information processing for obtaining a certain product. Finally, graphic technology with two big offset printing machines. All in all, 230 employees work in these four areas. In comparison to other departments in this building they are part of a common production. Collecting data, processing and interpreting them and finally manufacturing the product. Only selling the charts, books and data sets is not our issue. My experience is that this special working process has a positive influence on the social and professional cooperation.

HN: How do you share the work with President Mrs Breuch-Moritz?

Jonas: The entire responsibility remains with the President of course. She gave me the task to represent all question regarding hydrography. In the daily working routine we take decisions with the heads of all four departments.

HN: Let's look back in time. At the end of the 1970s you began as merchant seaman. After the Service at the Armed Forces of the German Democratic Republic you studied Nautical Engineering. What attracted you to the sea in younger years?

Jonas: I could answer that being born and raised in Rostock, a sea-related job is inevitable. I could also tell you about our family tradition. One of my ancestors,

Olerich Gottfried Jonas, moved from the island of Usedom to the formerly Hanseatic city Anklam in order to become a fisherman. All other descendants were fishermen too, except my grandfather and father, who were heating engineers. However, all these answers are not really true because as a child I surely didn't see it this way. I guess I was a romantic person who wanted to travel the world. That wasn't so easy in the former GDR. Seafaring

was definitely the only possibility to leave the country legally and see the world. I chose the job according to my desire.

HN: In the end you didn't spent too much time on board of ships. Instead you went to the Maritime Academy of Rostock-Warnemünde.

Jonas: Counting all seafaring days together I spent quite a few years on merchant ships. For the Federal Maritime and Hydrographic Agency I was head of mission on the »Gauss« a couple of times. Spending your life on sea is a very special life plan. You must be the type of person for it and do without social relations. I admit that this was very hard for me.

HN: What did you do at the Universities of Rostock and Hamburg?

Jonas: In Rostock I was scientific assistant and taught navigation at the radar simulator, but mainly I was involved in research projects. We invented the first computer-based assistant system for ships, for example the advance calculation of man-over-board rescue manoeuvre. From today's point of view it sounds quite simple, but at that time it was new. We were really successful and the former company Krupp Atlas took over our product – that was still before the German reunification. On a specialist trade fair in Southampton we received an award. After the reunification Professor Jens Froese, who was head of SUSAN at that time, looked for young people, also in Rostock, with new ideas and ambition. That's how I came to ISSUS at Hamburg University of Applied Sciences. There I continued to develop user interfaces for integrated navigation systems.

HN: How did you come to the Federal Maritime and Hydrographic Agency?

Jonas: In September 1993, on behalf of Professor Froese I took part in a presentation on a study about the feasibility of future integrated navigation systems. During the following discussion I mentioned fervently our research on that topic at ISSUS. A few weeks later, at the beginning of 1994, I was employed for electronic sea charts. Right at that time a Russian company wanted to offer an electronic sea chart on the German market. I was just in time with my computer knowledge and nautical background. Four weeks later, I went to London to participate in a working group on that topic.

HN: So, you would say that it was a gradual approach to hydrography?

Jonas: Yes, indeed. I was responsible for the legal type approval of electronic chart systems. For almost nine years I worked in this sector, which encompassed the technical check of electronic sea chart systems, satellite navigation receiver and integrated navigation systems. All that offered a good basis for switching to hydrography in 2004.

HN: In a press release of the Federal Maritime and Hydrographic Agency it says that you are a professional for »digital hydrography«. What does it mean?

Jonas: Currently, we experience a great transformation from the analogous to the digital era, as well in all fields of hydrography: Measurement technology, data processing, the product itself and in sales. That's what the term means.

HN: What is your attitude toward paper in this digital era?

Jonas: I grew up in a low-stimulus country. As a child I used to read a lot and definitely I am a »book person«. In the end, paper is a medium with advantages and disadvantages; it doesn't need electricity. You can read the newspaper in the tub. The printing resolution is very good. For a lot of information, paper is a very good medium, which on top doesn't cost a lot. However, for distributing ever changing geoinformation fast enough and across great distances you need a digital medium.

HN: Do you think the printed sea chart can still be improved?

Jonas: Maybe the cuttings of sea charts can be individualised. The current cutting is always a result of balancing the manageable total amount of charts of an area and the desired detail of the resulting scales. In order to solve this compromise, a procedure would be necessary with which you can select a certain area from a database and print it on paper according to a true to scale automated generalisation. If you stick to the chart

contents that are included in the electronic sea chart, then you could print on board. However, you should know that there is no 1:1 relation in an ENC between the all-encompassing compendium of paper-based sea chart contents and the attributed objects.

HN: You mean the tailored true-to-scale sea chart for the individual user? The assurance of the electronic sea chart shall be transferred to the printed version?

Jonas: Yes, this could be a possibility to improve the paper sea chart. The demand in our digital world is questionable. Probably the effort to realise it surpasses its benefit.

HN: Nonetheless, the paper sea chart and the electronic one are based on the same surveying data. How much closer to reality is the electronic sea chart?

Jonas: We have an increasing gap between the information we can survey and what we offer on charts. Not a lot of depth information is left of a multibeam measuring. Out of thousand measur-

»Paper doesn't need electricity. You can read the newspaper in the tub. For a lot of information, paper is a very good medium, which on top doesn't cost a lot. However, for distributing ever changing geoinformation fast enough and across great distances you need a digital medium«

Mathias Jonas

The new SWIFT_{SVF}

The ultimate handheld profiler - performance doesn't have to come at a price



- Sound Velocity, Temperature, Density & Salinity Profiles
- High accuracy sensor technology for exceptional data quality
- Titanium Construction for unmatched durability
- Less than 2kg for ease of handling and 2m/s drop rate
- Inbuilt GPS for geo-located data
- Simple switch and LED indicators for 'twist and go' deployments
- Long life USB rechargeable battery
- Bluetooth Smart communications for cable-free data transfer
- iOS App and DataLog X2 software for control and data display

'Professional and Affordable'

VALEPORT
in our element

Tel: +44 (0) 1803 869292
sales@valeport.co.uk

www.valeport.co.uk



ing data we obtain a depth number, a contour line. On the input side however, there is much more information. We need to close this gap by presenting the information we have. The dilemma is that electronic sea charts use modern technology, but the presentation of the contained information remains on the level of paper based charts. Consequently, the available data is reduced; that is true not only for the topography but also for the reference systems and the reduction of soundings. We know far more about the current water level than shown in the systems.

HN: Why don't you bring the knowledge together?

Jonas: So far, out of technical reasons we can only put together separate data sets for certain applications. In case we are able to achieve that for all information sources, the result needs to be presented differently than it is the case today. The current presentation is still based very much on the paradigms of the paper based sea chart, which emphasises the optical aspect. In future we will define automatic processes that will interpret data contents and offer action plans. For this we have to bring together technically all information and make them interoperable.

HN: You regulate the IHO data formats in order to be successful?

Jonas: Yes, this takes place in cartography, only to a smaller extent in surveying. The Hydrographic Standards and Service Committee (HSSC), which I manage, coordinate eight working groups, which deal with the infrastructure of technical standards. For a long time, specialists focused on electronic sea charts: Data exchange, data presentation and data encryption. Eleven years ago, we decided to establish a universal hydrographic data model called S-100. It will offer the possibility to present data of all domains – ground topography, wind, waves, sea disturbance, but as well weather and traffic information – in one single data model. All

the information is available in one device. I think in strategic steps, as it is my task to keep professionals motivated so we don't lose the common goal out of sight.

HN: There are people that regard standards very sceptically. What are your arguments to convince them?

Jonas: Very often, standards are pushed ahead by companies and implemented with significant market power. Our intergovernmental organisation works differently. Together with the industry we achieved a worldwide common standard. There is no electronic sea chart data producing state, which doesn't stick to the standard. I am convinced that this concept is applicable to other areas as well with the aid of the universal hydrographic data model, if the standard is technically manageable and carried by the authority of the IHO.

»We have an increasing gap between the information we can survey and what we offer on charts. We need to close this gap by presenting the information we have«

Mathias Jonas

HN: Your task is then to make the data model known to the different data suppliers?

Jonas: That's correct. My first success is that the national Ice Services of the northern hemisphere already use an S-100 compatible format for the sea ice charts. Currently, I am in dialogue with the technical specialists of the International Cable Protection Committee (ICPC). The global data exchange will depend on high-performance cable connections across the oceans. For the cable layout, the maintenance and operation an S-100 compatible format could be very useful as well as for securing and passing data.

HN: So you are serious about opening the current concept of electronic sea charts to other user groups?

Jonas: The popular notion that hydrography is for navigation of surface seafaring only, is outdated. I want nothing less than all the physics of the sea chart. This data set must include all relevant physical characteristics of the ocean ground, water body and the water surface dynamics. Furthermore, all information on human activity above and under water must be taken into account. From my point of view this guiding principle should be the future base for standardisation efforts of the IHO.

HN: The IHO wants to draw public attention to hydrography with the »World Hydrography Day«. What else can be done?

Jonas: I am not sure if we should address the public. In view of our goals it could be more efficient to contact the expert public, which deals professionally with the ocean. We should convince them to support our goals and solutions. Our aim must be to use hydrography visibly. My project of the all physical sea chart would be suitable and maybe we are able to reposition hydrography in future under the aspect »engineering the blue«.

HN: What do you expect of the DHyG?

Jonas: I really enjoy paying my contribution to the DHyG; the *Hydrographische Nachrichten* alone are worth it. The society works on a very high professional level as can be seen in the organisation of this year's HYDRO conference and the annual newcomer awarding. Maybe the DHyG could intensify its contact to the international industry with the aim to make the technology site Germany more popular and attract students to study hydrography at the HCU.

HN: How do you write a course book – *The Electronic Chart* – in a team?

Jonas: We started in 1998 with a German version. Beforehand, all the authors discussed which topics to choose, how to deal with overlapping and repetitions and how to link the chapters. We talked about an author's freedom and decided in how far we accept something, which doesn't fit into one's own point of view. We started this tasks based on honesty. For the announced fourth edition, we included into our team two young experts from Germany and England. We belong to three generations now. One, which conceptually developed

this system, one, which implemented it (I count myself to this generation), and one, which uses this technology as a standard.

HN: In 2014, Rostock started the project »A city reads Uwe Johnson's ›Jahrestage«». Why did you join this event and recited a chapter in the radio?

Jonas: Johnson wasn't published in the former GDR, that's why I didn't know his work. Maybe the *Jahrestage* wouldn't have attracted me because Johnson isn't an easy to read author. To broadcast a spoken text is a special form of absorbing it. You read the given lines over and over again and with an increased perception for the rhythm of the language. I really enjoyed being part of this city project.

HN: What would you like to be able to do?

Jonas: I would like to play the piano.

HN: What do you know without being able to prove it?

Jonas: I believe that we narrow our perception if we regard things only from the technical point of view and their usage. That's what I don't like about globalisation because this is not in our human nature. The all-encompassing mechanisation hasn't brought any moral development globally. I believe that dealing with the ocean can help to develop a humanistic attitude. We all are fascinated by the ocean, the great expanse, which has mobilised the inventiveness and forces of mankind. I am sure that

taking over responsibility for the ocean will lead us to a more respectful behaviour with our community.

HN: Finally, I would like to repeat the reporter's question: Mr. Jonas, how do you see the state of the Baltic Sea?

Jonas: The Baltic Sea is in better shape than many of us believe, but it isn't as good as it should be. Currently, the greatest problems are still the phosphates and nitrates that the agriculture brings into the sea. Shipping traffic will increase. We must guarantee safe seafaring, prevent the introduction of foreign animals in ballast water and stick consequently to the valid emissions of ship exhaust gases. Designated protected areas must be excluded from economic use. This demands counselling from the economy, regulation by administrations and the courage to implement unpopular measures. All political assurances are useless if we don't implement the knowledge that we have about the ocean. If we succeed then we are able to keep the Baltic Sea sound even under a high usage pressure. 

»Our aim must be to use hydrography visibly. My project of the all physical sea chart would be suitable and maybe we are able to reposition hydrography in future under the aspect ›engineering the blue«

Mathias Jonas

**HYDRO
2016**

on-water
equipment
demos

NICOLA
ENGINEERING GmbH
HYDROGRAPHIC SURVEY

Comparison and characteristics of oceanographic in situ measurements and simulations above submerged sand waves in a tidal inlet

An article by INGO HENNINGS and DAGMAR HERBERS

Ocean colour and its transparency are related to turbidity caused by substances in water like organic and inorganic material. One of the essential climate variables (ECV) is ocean colour. However, this implies the correct interpretation of observed water quality parameters. Acoustic Doppler Current Profiler (ADCP) data of the three-dimensional current-field, echo intensity, modulation of suspended sediment concentration (SSC), and related water levels and wind velocities have been analysed as a function of water depth above submerged asymmetric compound sand waves during a tidal cycle in the Lister Tief of the German Bight in the North Sea.

Authors

Dr. Ingo Hennings and Dagmar Herbers are Research Scientists at the Geomar Helmholtz Centre for Ocean Research Kiel, Germany.

ihennings@geomar.de
dherbers@geomar.de

ADCP | SSC – suspended sediment concentration | TSM – total suspended sediment | asymmetric compound sand wave | dynamic buoyancy density | action density

1 Introduction

It is well known that a strong coherence exists between fluctuations of turbidity, phytoplankton, and suspended sediment concentration (SSC) induced by disturbances of tidal current velocities. Substantial phenomena of SSC during two tidal cycles at two anchor stations in the southern North Sea were described by Joseph (1954). There he showed that a phase shift of 30 to 45 minutes happened between turbidity and current velocity maximum.

In situ observations in the past showed that submerged sand waves and internal waves associated with vertical current components can be sources of enhanced SSC in the water column above sea bottom topography. Often, such SSC features can come up to the water surface in shallow tidal seas of the ocean. The study presented by Hennings et al. (2002) showed that in a stratified two water

layer system, simultaneous reductions in the near-surface water temperature and beam transmittance have been recorded, whereas fluorescence data are increased above sand waves. A good linear relationship between water depth and total suspended sediment (TSM) data derived from Moderate Resolution Imaging Spectroradiometer (MODIS) measurements above sand ridges in the southern Yellow Sea was found by Tao et al. (2011). The TSM concentration was proportional to the inverse water depth; high TSM concentrations were located above shallow parts of sand ridges. It was shown by Hennings and Herbers (2014) that strong currents flowing over steep bottom topography are able to stir up the sediments to form both a general continuum of SSC and localised pulses of higher SSC in the vicinity of the causative bed feature itself. Tide-dependent variations in the formation and dynamics of suspended sediment patterns coupled to mean flow and turbulence above asymmetric bed forms were examined by Kwoil et al. (2014).

2 Measurements conducted during a tidal cycle

The study area of the Lister Tief is a tidal inlet of the German Bight in the North Sea bounded by the islands of Sylt to the south and Rømø to the north. The positions of analysed runs along transect AB in the Lister Tief are presented in Fig. 1. Tide gauge station List is located 4.8 km southerly of transect AB. The seabed morphology in the Lister Tief is a complex configuration of continuously changing different bed forms. The submerged compound sand waves investigated in this study are four-dimensional in space and time. Small-scale as well as megaripples are superimposed on sand waves as

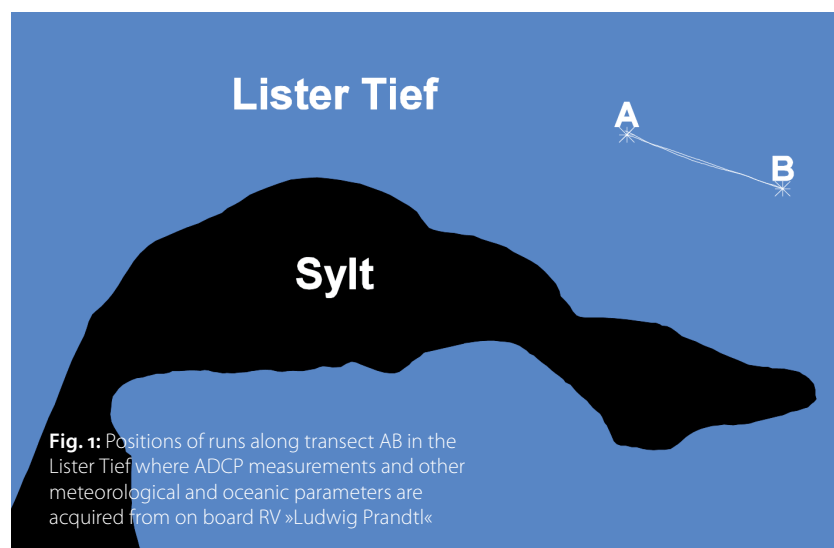


Fig. 1: Positions of runs along transect AB in the Lister Tief where ADCP measurements and other meteorological and oceanic parameters are acquired from on board RV »Ludwig Prandtl«

presented here and already discussed in Van Dijk and Kleinhans (2005) as well as in Hennings and Herbers (2006). Analysed flood dominated sand waves have stoss slopes of the order of 2° and lee slopes up to 31° .

Water levels measured at tide gauge station List, wind and current velocities, vertical current components w , echo intensities E_3 of fore beam No. 3 measured by ADCP and calculated SSC modulations expressed as $\log((\delta c / c_0)_3)$ of beam No. 3 as a function of water depth are presented. The constant SSC equilibrium term is defined by c_0 and δc is the time-dependent perturbation term of the local SSC c . All parameters are measured and calculated over submerged asymmetric compound sand waves on the sea bottom during several runs along transect AB.

As an example, measurements during run 51 are shown in Fig. 2 for ebb tidal current phase. The duration of the measurement time is indicated by a vertical black line in Fig. 2a. Each run has been rotated by an angle of 19° in order to direct the current component u perpendicular to the sand wave crest. Hence, the v -component of the current field is minimised and can be neglected as a first approximation. The rotation point is marked at the highest sand wave crest along the profile named as reference crest, shown in Fig. 2c to 2e. The current vectors shown in Fig. 2b are water depth averaged velocity values. Time interval of both, wind and current velocity arrows, is 30 s. Especially Fig. 2d illustrates the resuspension expressed by E_3 in progress at ebb tides.

2.1 Time dependent measurements of vertical water depth averaged data

The base of Fig. 3 is a data set measured on 10 August 2002 between 0516 UTC and 0740 UTC while the research vessel was sailing against the ebb tidal current direction over asymmetric flood orientated submerged sand waves along transect AB. Fig. 3a shows the water level recorded at the tide gauge station List as a function of time. Herein, the acquisition times of five analysed single runs are marked. In Fig. 3b wind speeds are represented by arrows in a geocoded coordinate system. All other data are shown as a function of time and position in east-west direction. Fig. 3c to 3f illustrate time series of vertically averaged values for current component u (east direction, indicated by a compass symbol with a red stick in Fig. 3c), echo intensity E_3 of fore beam No. 3 measured by ADCP, vertical current component w , and calculated SSC modulations expressed as $\log((\delta c / c_0)_3)$ of beam No. 3. The water depth profiles of the asymmetric sand waves are shown in Fig. 3g to 3h.

Wind speeds between 5.8 m s^{-1} and 7.5 m s^{-1} from northerly directions were measured (Fig. 3b). Negative, enhanced and positive values of u , E_3 , and w , respectively, show phase relationships with sand wave crests of the sea bed. In contrast, enhanced $\log((\delta c / c_0)_3)$ shows a phase relationship

with the sand wave troughs of the sea bed. The parameters u , w , and $\log((\delta c / c_0)_3)$ are only weakly time dependent. All signatures of u , E_3 , w , and $\log((\delta c / c_0)_3)$, respectively, show spatially dependent variations in x -direction above the sand waves.

3 Theory of hydrodynamics above submerged sand waves

The focus of this section is the understanding and mathematical description of dynamic buoyancy density, total energy density, and action density above submerged asymmetric sand waves due to semi-diurnal lunar M_2 tidal motion. The dynamic buoyancy density A_d is defined by

$$A_d = \frac{\tilde{A}_d}{F \cdot z_b} \approx \frac{1}{2} \cdot \rho \cdot (c_a - 1) \cdot \bar{u}^2 \quad (1)$$

where \tilde{A}_d is the dynamic buoyancy in the water column of volume $V(x,y,z)$ with the horizontal and

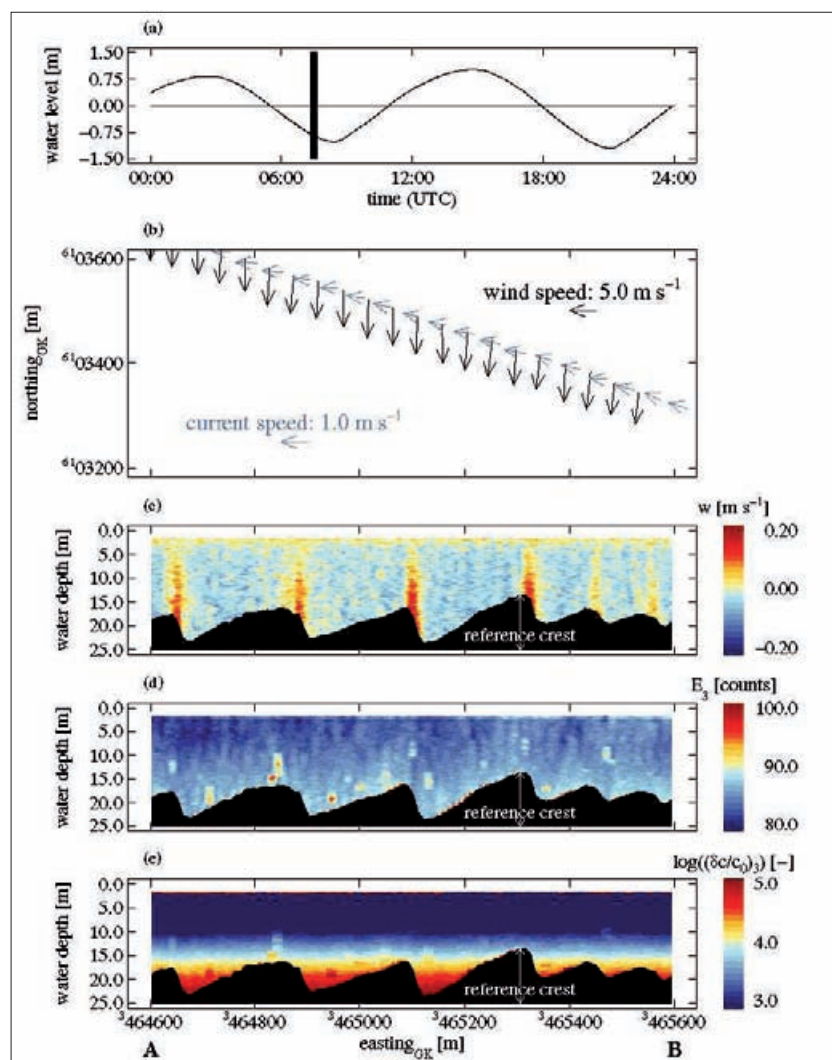


Fig. 2: Analysed data of ADCP of fore beam No. 3 as a function of position and water depth above asymmetric sand waves of run 51 along transect AB during ebb tidal phase between 0721 UTC and 0740 UTC on 10 August 2002; **a)** time series of water levels measured at the tide gauge station List; **b)** wind and current velocities, the two horizontal arrow-scales indicate a wind speed of 5.0 m s^{-1} and a current speed of 1.0 m s^{-1} , respectively; along-track presentations of **c)** vertical current component w of the three-dimensional current field; **d)** echo intensity E_3 ; and **e)** calculated SSC modulation $\log((\delta c / c_0)_3)$. The timing of the measurement is marked by a vertical black line in a). The position of the reference crest is indicated at the highest sand wave crest of the run

vertical space coordinates x , y , and z , z_b is the local water depth, F is the infinitely thin horizontal plane element, ρ is the water density, c_a is the dimensionless lift coefficient, and \bar{u} is the vertical average current velocity perpendicular to the sand wave crest. The dimensionless lift coefficient c_a is defined by Dätwyler (1934) for a flat plate as

$$c_a = \frac{\pi}{\sin(\pi \cdot \beta)} \left(\frac{\beta}{1 - \beta} \right)^{1-2\beta} \quad (2)$$

and

$$\beta = \frac{\alpha}{\pi} \quad (3)$$

with α the slope angle of the stoss or lee plane of the sand wave. Both, stoss as well as lee sides of the sand wave were approximated by a flat plate. However, here c_a was subtracted by 1 in equation

(1), whereas Dätwyler (1934) normalised c_a by 1. The reason is here that both upwelling (positive) as well as downwelling (negative) values of c_a can arise above sand waves. As a first approximation, for the downforce at the lee side of the sand wave, the negative value (downforce coefficient) of the lift coefficient c_a is used here. Kinematic molecular viscosity and roughness effects at the sea bed are neglected.

The gradient of the dynamic buoyancy density perpendicular to the sand wave crest is derived as

$$\frac{\partial A_d}{\partial x} \approx (c_a - 1) \cdot \rho \cdot \bar{u} \frac{\partial \bar{u}}{\partial x} \quad (4)$$

Total energy density E is the sum of the potential energy density E_p and the kinetic energy density E_k .

$$E = E_p + E_k = \rho \cdot g \left(z_R - \frac{1}{2} z_b \right) + \frac{A_d}{(c_a - 1)} \quad (5)$$

where g is the acceleration due to gravity and z_R is the reference water depth at the trough of sand wave.

The action density N is defined by

$$N = \frac{E}{\omega'} \quad (6)$$

where ω' is the radial frequency of the semi-diurnal lunar M_2 tidal wave with

$$\omega' = \frac{2\pi}{T} \quad (7)$$

where T is the period of the semi-diurnal lunar M_2 tidal wave.

Using equations (4) to (6), the gradient of the action density N perpendicular to the sand wave crest is derived as

$$\frac{\partial N}{\partial x} = \frac{\rho}{\omega'} \left(-\frac{1}{2} g \frac{\partial z_b}{\partial x} + \bar{u} \frac{\partial \bar{u}}{\partial x} \right) \quad (8)$$

Equation (8) shows that the gradient of the action density caused by the semi-diurnal M_2 tidal wave is anti-proportional to the slope of the sea bed $\partial z_b / \partial x$ and proportional to the product of the vertical averaged current speed and its gradient $\bar{u} \cdot (\partial \bar{u} / \partial x)$, respectively.

Assuming that the vertical averaged current speed \bar{u} perpendicular to the sand wave crest obeys the continuity equation

$$\bar{u} \cdot z_b = \text{const} = c \quad (9)$$

and inserting equation (9) into equation (8) for $\partial \bar{u} / \partial x$, the following expression is derived

$$\frac{\partial N}{\partial x} = -\frac{\rho}{\omega'} \frac{\partial z_b}{\partial x} \left(\frac{g}{2} + \frac{\bar{u}^2}{z_b} \right) \quad (10)$$

where $\partial N / \partial x$ is proportional to \bar{u}^2 and $(z_b)^{-1}$.

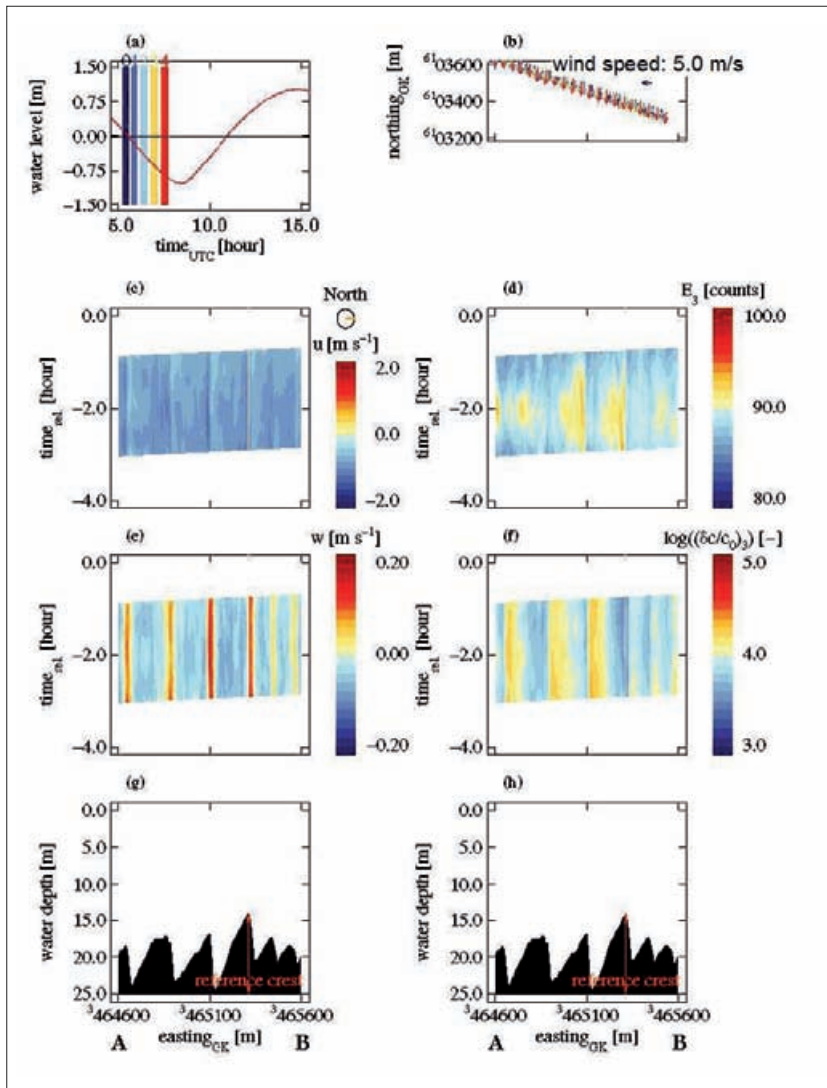


Fig. 3: **a)** Time series of water level measured at tide gauge station List with acquisition times marked by No. 0 to 4 of 5 selected runs analysed during ebb tidal current phase from B to A while the research vessel is sailing against the current direction on 10 August 2002; **b)** measured wind velocities; the horizontal arrow-scale indicates a wind speed of 5.0 m s⁻¹; **c)** time series of measured current component u ; the east direction is marked by a red stick within the compass symbol; **d)** time series of echo intensity E_3 of fore beam No. 3 measured by the ADCP; **e)** time series of measured vertical current component w ; **f)** time series of calculated SSC modulation expressed as $\log((\delta c / c_0)_3)$ of beam No. 3; and **g) – h)** measured water depth profile of asymmetric submerged sand waves on the sea bed along transect AB

4 Evaluation and results of simulations

For all simulations a sand wave length $L = 220$ m and a sand wave height $h_c = 6$ m are selected. These parameters are typical values measured in the southern part of Lister Tief (see section 2). Simulations of the sand wave profile with water depth z_b , slope of the sea bed $\partial z_b / \partial x$, vertical averaged tidal current speed \bar{u} and its gradient $\partial \bar{u} / \partial x$, respectively, dynamic buoyancy density A_d , gradient of the dynamic buoyancy density $\partial A_d / \partial x$, kinetic energy density E_k , potential energy density E_p , action density N , and gradient of the action density $\partial N / \partial x$ as a function of space variable x are shown in Fig. 4a to 4e for ebb tidal current phase of asymmetric flood orientated sand waves. Typical values for the spatial resolutions $\Delta x = 10$ m and $\Delta y = 1$ m, $z_R = 25$ m, gentle slope of sand wave $\alpha_g = 2^\circ$, steep slope of sand wave $\alpha_s = 9^\circ$, $\rho = 1020$ kg m⁻³, $\bar{u} = 0.7$ m s⁻¹ at x with $z_b = z_R$, $\bar{u} = 0.95$ m s⁻¹ at $x = 0$ m (sand wave crest), $g = 9.82$ m s⁻², and $T = 12.42$ hours are calculated or inserted by using equations (1) to (10).

The sea bed profile with water depth z_b which defines the asymmetric sand wave in black and the slope of the sea bed $\partial z_b / \partial x$ in red are shown in Fig. 4a.

The tidal current velocity $u = \bar{u}$ is presented in black in Fig. 4b during ebb tidal current phase. Due to the continuity equation (9) \bar{u} acquires its maximum absolute value at the sand wave crest. The gradient of the tidal current speed $\partial u / \partial x = \partial \bar{u} / \partial x$ is shown in red in Fig. 4b. A relative strong divergence flow $\partial \bar{u} / \partial x = 0.007$ s⁻¹ is calculated at the steep slope of the sea bed.

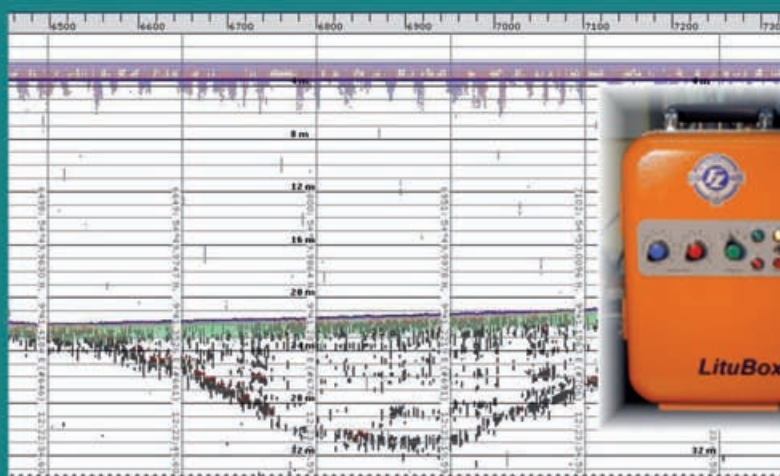
The dynamic buoyancy density A_d , shown in black in Fig. 4c, strongly depends on the slope of the sea bed; a maximum negative value $A_d = -50$ N (downwelling) is calculated at the gentle slope of the sea bed and a maximum positive value $A_d = 160$ N (upwelling) is calculated at the steep slope of the sea bed during ebb tidal current phase. A reversal of A_d is obtained during flood tidal current phase. These simulations agree with ADCP measurements of vertical positive and negative components w of the tidal current velocity shown in Fig. 2c. The gradient of the dynamic buoyancy density $\partial A_d / \partial x$ presented in Fig. 4c in red show low and high negative values at both the gentle as well as the steep slope of the sea bed during ebb tidal current phase. Again, a reversal of $\partial A_d / \partial x$ took place during flood tidal current phase. Maximum values of $\partial A_d / \partial x = -2.6$ N m⁻¹ are associated with maxi-

References

- Dätwyler, Gottfried (1934): Untersuchungen über das Verhalten von Tragflügelprofilen sehr nahe am Boden; Diss.-Druckerei A.-G. Gebr. Leemann & Co., Zürich, 110 p.
- Hennings, Ingo; Margitta Metzner; G.-P. de Loor (2002): The influence of quasi resonant internal waves on the radar imaging mechanism of shallow sea bottom topography; *Oceanologica Acta*, 25, pp. 87–99
- Hennings, Ingo; Dagmar Herbers (2006): Radar imaging mechanism of marine sand waves of very low grazing angle illumination caused by unique hydrodynamic interactions; *Journal of Geophysical Research*, 111 C1008, 15 p.
- Hennings, Ingo; Dagmar Herbers (2014): Suspended sediment signatures induced by shallow water undulating bottom topography; *Remote Sensing of Environment*, 140, pp. 294–305
- Joseph, J. (1954): Die Sinkstoffführung von Gezeitenströmen als Austauschproblem; *Archiv für Meteorologie, Geophysik und Bioklimatologie, Serie A* 7, pp. 482–501 ...



Hydrographic Echo Sounders



Dr. Fahrentholz GmbH & Co. KG, Grasweg 4-6, 24118 Kiel, Germany
Phone ++49 431 542049 fz@fahrentholz.de www.fahrentholz.de

Finanzamt Kiel-Nord, Steuer-Nr. 19 288 01703, VAT-USt-Id: DE 812 388 842
Amtsgericht Kiel: HA # 3776, Geschäftsführer: Dr. Siegfried Fahrentholz
Komplementär: Dr. Fahrentholz Verwaltungs GmbH, Amtsgericht Kiel: HB # 4608
EAR: Fahrentholz-Sounder: WEEE-Reg # DE43104036

Kwoll, Eva; Marius Becker; Christian Winter (2014): With or against the tide: The influence of bed form asymmetry on the formation of macroturbulence and suspended sediment patterns; *Water Resources Research*, 50, pp. 7800–7815

Tao, Zui; Ziwei Li; Bangyong Qin (2011): Ocean sand ridges in the Yellow Sea observed by satellite remote sensing measurements; *Remote Sensing, Environment and Transportation Engineering, International Conference, 24–26 June 2011, Nanjing, China; Institute of Electrical and Electronics Engineers (IEEE)*, pp. 528–531

Van Dijk, Thiënne A. G. P., Maarten G. Kleinhans (2005): Processes controlling the dynamics of compound sand waves in the North Sea, Netherlands; *Journal of Geophysical Research*, 110 F04S10, 15 p.

imum values of $\partial u / \partial x = \partial \bar{u} / \partial x$ as it is also expressed by equation (4).

The potential energy density E_p shown in red and the kinetic energy density E_k presented in black in Fig. 4d, respectively, are always positive and have same magnitudes during ebb as well as flood tidal current phases. However, the potential energy density E_p is a factor of about 349 to 500 J m^{-3} stronger than the kinetic energy density E_k . Maximum values of E_p and E_k are corresponding with the sand wave crest where the current speed maximises.

The action density N shown in Fig. 4e as a black curve, is always positive and has the same magnitudes during ebb as well as flood tidal current phases with maximum $N = 1.13 \cdot 10^9 \text{ J s m}^{-3}$ at the sand wave crest. The total action density N in the water column presented in Fig. 4e is higher at the spatial longer gentle slope region than at the shorter steep slope region of sand waves. Therefore, more suspended sediment particles are moving upwards which is also shown by the measure-

ments of E_3 shown in Fig. 2d. The gradient of the action density $\partial N / \partial x$ coloured in red in Fig. 4e is positive at the gentle slope and negative at the steep slope of the sand wave during ebb as well as flood tidal current phases. Maximum values of $\partial N / \partial x = -6.0 \cdot 10^6 \text{ N s m}^{-3}$ are related to maximum and high values of $\partial z_b / \partial x$, $\partial u / \partial x = \partial \bar{u} / \partial x$, and $\partial A_d / \partial x$, respectively.

5 Conclusions

Based on in situ measurements of several oceanographic and meteorological parameters acquired in the Lister Tief, theory and simulations regarding the hydrodynamics above submerged asymmetric sand waves the following conclusions are drawn:

- Sand suspensions strongly depend on wave activity for high concentrations in the water column. Wave orbital motions close to the sea bed are induced by measured wind speeds between 11.7 m s^{-1} and 13.3 m s^{-1} from southeasterly direction to stir up sand particles.
- Bursts of w and E_3 may be triggered at disturbances like megaripples superimposed on sand waves by current wave interaction at high current and wind speeds observed of opposite directions and measured at high spatial resolution.
- During moderate wind speeds between 5.8 m s^{-1} and 7.5 m s^{-1} from northerly directions, negative, enhanced and positive values of u , E_3 , and w , respectively, show a definite phase relationship with the crest and upper gentle slope regions of sand waves during ebb tidal current phase while the research vessel is sailing with or against the current direction. In contrast, enhanced $\log((\delta c / c_0)_3)$ shows a phase relationship with trough regions of sand waves during ebb tidal current phase.
- Intense ejections caused by tidal current velocity transport higher SSC near the bottom boundary layer at the sand waves superimposed by megaripples towards the free water surface. Such hydrodynamic upwelling mechanism above sand waves creates distinct SSC signatures in remote sensing data visible in air- and space-borne optical imagery.
- During well developing flood and ebb tidal currents the intensities of u , w , and $\log((\delta c / c_0)_3)$ are only weakly time dependent. In contrast, E_3 shows time dependence.
- The ADCP in situ measurements are to be consistent with simulations based on the applied theory.
- The action density N and its gradient $\partial N / \partial x$ due to semi-diurnal tide motion are the most important hydrodynamic parameters, which characterise comprehensively the dynamics of suspended sediment concentration (SSC) above submerged asymmetric sand waves. †

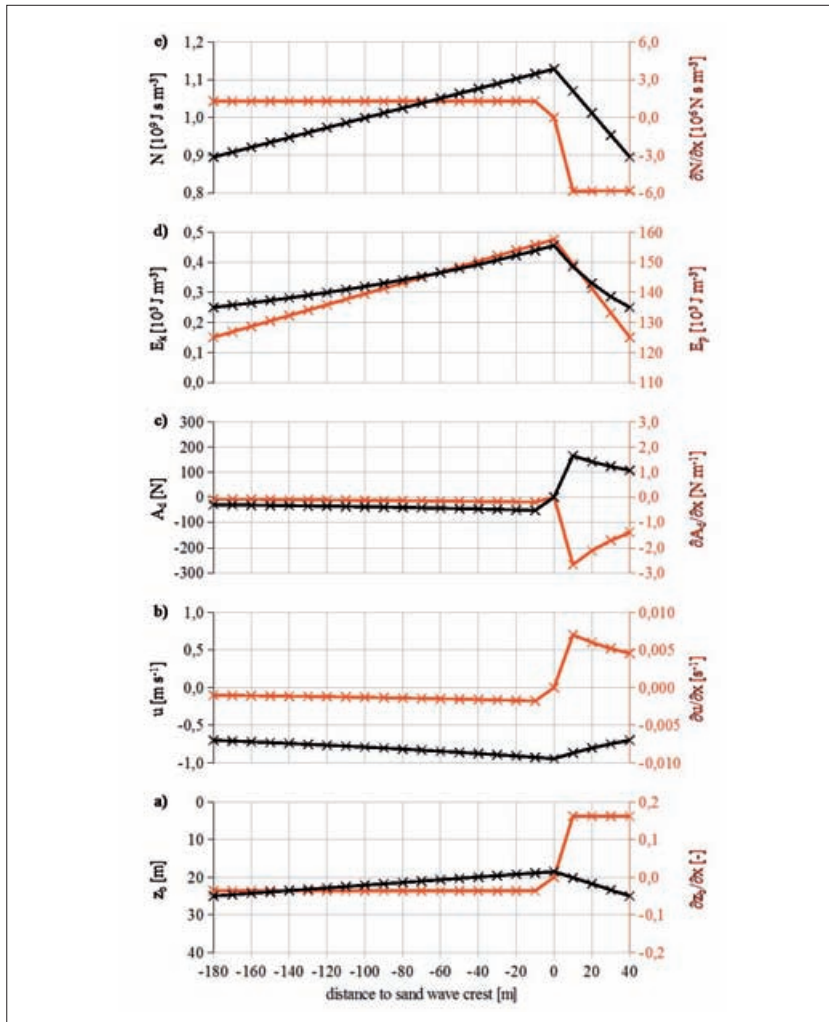
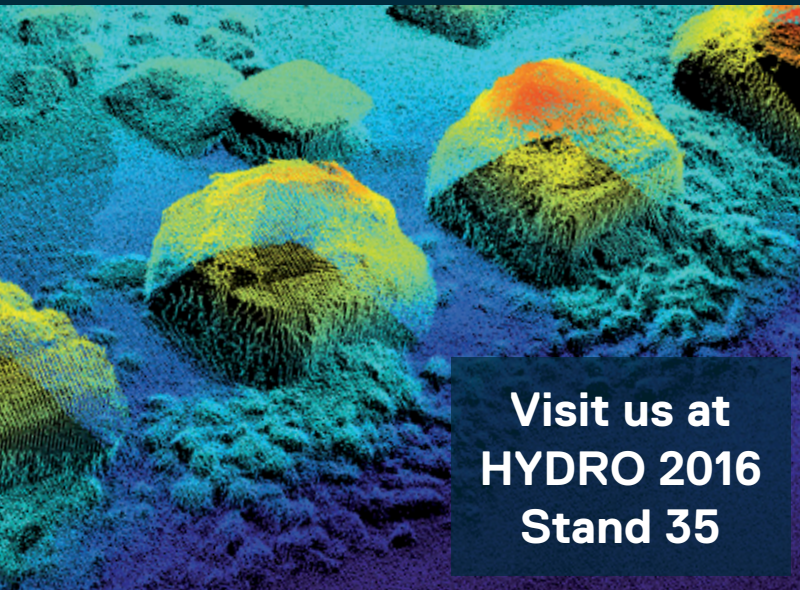


Fig. 4: Simulations of oceanographic parameters applying equations (1) to (10) for ebb tidal current phase (current is directed from right to left) as a function of space variable x ; **a)** sand wave profile with water depth z_b in black and slope of the sea bed $\partial z_b / \partial x$ in red, **b)** tidal current velocity $u = \bar{u}$ in black and gradient of the tidal current velocity $\partial u / \partial x = \partial \bar{u} / \partial x$ in red, **c)** dynamic buoyancy density A_d in black and gradient of the dynamic buoyancy density $\partial A_d / \partial x$ in red, **d)** kinetic energy density E_k in black and potential energy density E_p in red, and **e)** action density N in black and gradient of the action density $\partial N / \partial x$ in red

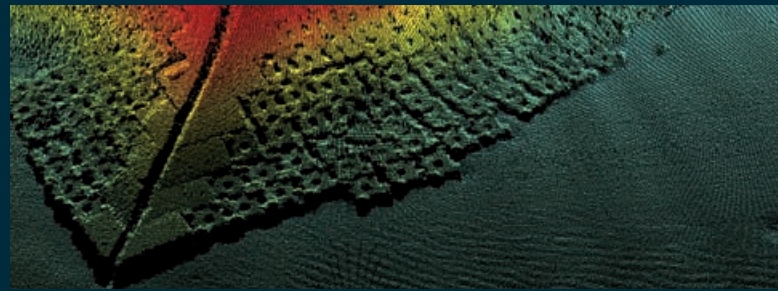


KONGSBERG

BRINGING CLARITY TO THE WORLD BELOW



Visit us at
HYDRO 2016
Stand 35



Kongsberg Solutions for

- Hydrographic Mapping
- Harbour Survey & Inspection
- Acoustic Positioning
- Acoustic Communication and Control
- Fishery Research & Fish Finding
- Search and Rescue

High-resolution, topobathymetric LiDAR coastal zone characterisation

An article by FRANK STEINBACHER, RAMONA BARAN, MIKKEL S. ANDERSEN, ZYAD AL-HAMDANI, LAURIDS R. LARSEN, MARTIN PFENNIGBAUER and VERNER B. ERNSTSEN

Coastal and tidal environments are valuable ecosystems, which, however, are under pressure in many areas around the world due to globalisation and/or climate change. Detailed mapping of these environments is required in order to manage the coastal zone in a sustainable way. However, historically these transition zones between land and water are difficult or even impossible to map and investigate in high spatial resolution due to the challenging environmental conditions. The new generation of airborne topobathymetric light detection and ranging (LiDAR) potentially enables full-coverage and high-resolution mapping of these land-water transition zones. We have carried out topobathymetric LiDAR surveys in the Knudedyb tidal inlet system in the Danish Wadden Sea and the Rødsand lagoon connected to Fehmarnbelt. Here, we present the preliminary results of these two surveys which were carried out at two locations with different environmental settings. We demonstrate the potential of using airborne

topobathymetric LiDAR for seamless mapping of land-water transition zones in challenging coastal environments, e.g. in an environment with high water column turbidity and continuously varying water levels due to tides as well as in an environment characterised by a very heterogeneous surface sediment composition.

topobathymetry | LiDAR | coastal zone | HydroVISH | point cloud classification

1 Introduction

Coastal and tidal environments are valuable ecosystems, which are highly impacted by globalisation, climate change, and human encroachment in many areas around the world. Detailed mapping of these environments is required in order to manage the coastal zone in an economically sustainable manner, but traditionally used methods are not sufficient to gain full coverage, comprehensive and high-resolution spatial data of these shallow water areas (e.g., Steinbacher et al. 2013; Dobler et al. 2013). This is particularly due to highly variable environmental conditions of the land-water transition zone impeding an efficient monitoring. Furthermore, the results often have a very low spatial resolution, are expensive and time consuming. In contrast, by using a new generation of laser scanning equipment (green wavelength 532 nm)

airborne topobathymetric laser scanning can provide measurements of the land surface and the river bed or seabed within a single measurement process (Fig. 1). The measurements have both a very high accuracy (\pm centimetres) and a very high resolution (about 20 to 30 points/m²) (Andersen et al. 2016). Contrary to previous methods, which are mostly cross-section/profile based or only consider subareas, the comprehensive spatial information gained by the new LiDAR technique signifies an enormous and game changing advancement in the recording of underwater information. Among other factors the penetration depth of the laser beam crucially depends on the turbidity of the water body. At ideal viewing conditions, the sea/river bed can be detected down to about 10 to 11 m depth.

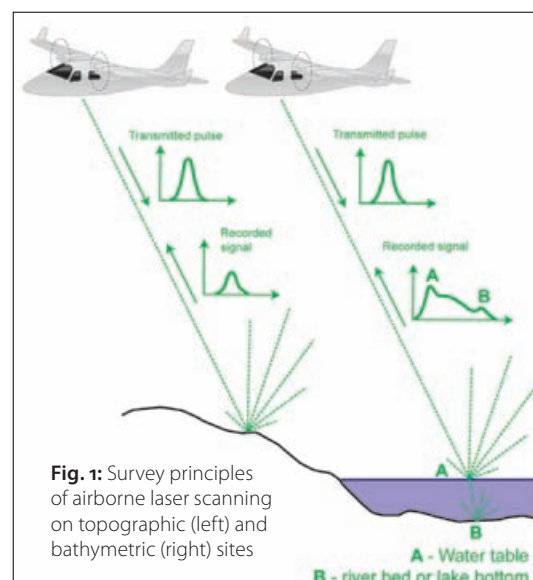
Thus, we performed topobathymetric LiDAR surveys in the Knudedyb tidal inlet system, a coastal environment in the Danish Wadden Sea which is part of the Wadden Sea National Park and UNESCO World Heritage, and in the Rødsand lagoon, which is a NATURA2000 site located in close vicinity of the planned Fehmarnbelt fixed link (for locations Fig. 2 and 3). These two surveys were conducted in order to:

- Derive characteristic properties of the morphology, surface sediment, the vegetation and the water column in land-water transition zones like rivers, lakes, wetlands, estuaries and coasts;
- Improve the understanding of the dynamics of these properties in shallow water ecosystems, which are under pressure due to changing environmental conditions driven by climate change;
- Develop tools for quantifying geological resources, habitat distributions and system-indicators in land-water transition zones, developed

Authors

Frank Steinbacher and Ramona Baran work for Airborne HydroMapping GmbH in Innsbruck, Austria. Mikkel S. Andersen and Verner B. Ernstsen are from the Department of Geosciences and Natural Resource Management, University of Copenhagen, Denmark. Ziad Al-Hamdani is from the Geological Survey of Denmark and Greenland (GEUS), Copenhagen, Denmark. Laurids R. Larsen works for NIRAS in Allerød, Denmark. Martin Pfennigbauer is from RIEGL Laser Measurement Systems GmbH in Horn, Austria.

info@ahm.co.at



in and for a GIS in order to optimise application by end-users.

2 Project sites and airborne survey

The Knudedyb tidal inlet system is located at the west coast of Denmark in the Danish Wadden Sea, and is part of the Wadden Sea National Park and belongs to the UNESCO World Heritage (Fig. 2). The coastal area is strongly influenced by tides with a mean tidal range of 1.6 m (Pedersen and Bartholdy 2006), and is characterised by a manifold environment in terms of biodiversity, geodiversity, and complexity of coastal processes (sediment transport and morphologic changes). The Knudedyb site was surveyed two times on 19 April 2014 and 30 May 2014 at low tide under clear weather conditions and offshore winds using the VQ820G sensor (RIEGL LMS; Fig. 2). About 118 scan strips were acquired during both surveys: 37 strips in the first run and 81 strips in the second. The strips were adjusted with respect to each other to derive an internally consistent point cloud (internal accuracy of 6 to 10 cm given as standard deviation). Subsequently, the point cloud was georeferenced to terrestrially measured reference planes (accuracy of 4 to 9 cm given as standard deviation).

The Rødsand lagoon is located at the south coast of Lolland and is connected to the Fehmarnbelt; it is a NATURA2000 site located in close vicinity of the planned Fehmarnbelt fixed link (Fig. 3). The lagoon is approximately 30 × 8.5 km wide. In the offshore area near the lagoon two offshore wind parks are established (Rødsand 1 & 2). The lagoon is bordered by a broad sand barrier at its southern edge extending from Gedser in the east towards the west, intersected by three inlets. This sand barrier plus several N-S traverses across the Rødsand lagoon were surveyed on 7 September 2015 at clear and relatively calm water conditions as well as clear weather using the VQ880G sensor (RIEGL LMS; Fig. 3 and 4). In total, 35 scan strips were acquired yielding 70 single strips due to simultaneous forward and backward recording of the VQ880G. The strips were adjusted to each other to gain an internally consistent point cloud similar to the Knudedyb tidal inlet data (internal accuracy of ca. 5 cm given as standard deviation).

3 Point cloud processing using HydroVISH

3.1 Noise filtering

The further point cloud processing of the topobathymetric LIDAR data was done using the HydroVISH software package developed by AHM. Prior to point cloud classification, flaw echoes (noise) need to be removed from the raw point cloud (Fig. 5). These echoes were recorded because the sensor setting was extremely sensitive in order to capture as many echoes from the water surface as well as achieving a best possible penetration. For each point of the point cloud, the point density within a 0.75 m radius was evaluated and a point

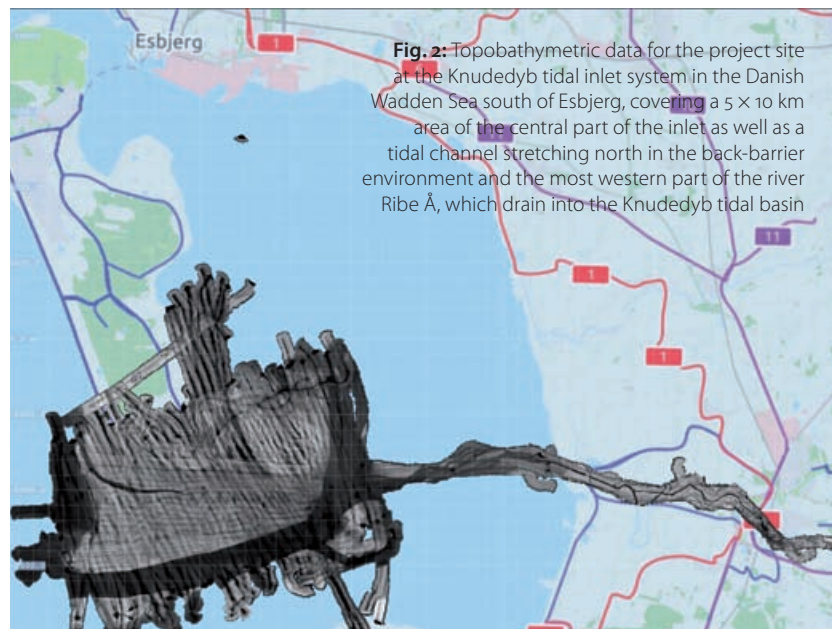
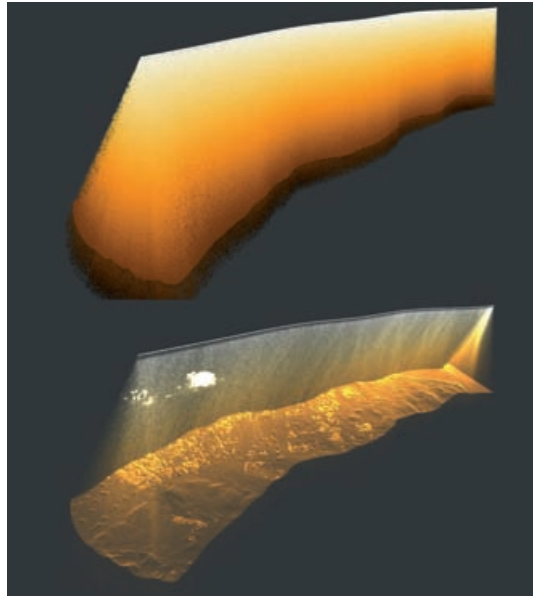


Fig. 5: Flaw echoes for a scan strip from the Knudedyb tidal inlet system



References

Andersen, Mikkel S.; A. Gergely; Ziad Al-Hamdani; Frank Steinbacher; Laurids R. Larsen; Verner B. Ernstsen (2016): Processing and accuracy of topobathymetric LiDAR data in land-water transition zones; *Hydrology and Earth System Sciences*, doi:10.5194/hess-2016-3, in review

Dobler, Wolfgang; Ramona Baran; Frank Steinbacher; Marcel Ritter; Manfred Niederwieser; Werner Bengler; Markus Aufleger (2013): Die Verbindung moderner und klassischer Gewässervermessung; *Hydrographische Nachrichten*, HN 95, pp. 16–22

Mandlbürger Gottfried; Martin Pfennigbauer; Norbert Pfeifer (2013): Analyzing near water surface penetration in laser bathymetry – a case study at the river Pielach; *ISPRS Annals of the Photogrammetry, Remote Sensing and Spatial Information Sciences*, Volume II-5/W2, pp. 175–180

Pedersen, J. B. T.; Jesper Bartholdy (2006): Budgets for fine-grained sediment in the Danish Wadden Sea; *Marine Geology*, 235, pp. 101–117

Steinbacher, Frank; Ramona Baran; Wolfgang Dobler; Markus Aufleger; Lutz Christiansen (2013): Combining Novel and Traditional Survey Technologies to Monitor Coastal Environments: Airborne Hydromapping and Sonar Data along the Baltic Sea Coastline, Schleswig-Holstein, Germany; in: *Proceedings of the 35th IAHR World Congress*, Tsinghua University Press, Beijing

was identified as flaw echo, if the number of point neighbours was less than five within the given radius. The cleaned point cloud was subsequently classified.

3.2 Point cloud classification

First of all, the point cloud was mapped onto a 0.5 × 0.5 m grid using the deepest point per grid cell to classify terrain (terrain on land and water ground), and the highest point per grid cell to classify the rest (water body, buildings, vegetation). The differentiation among the two follows a height- and slope criterion. By intersecting the two grid data sets, the water land boundary was approximated. After manual correction of the raster classification, all rest raster points located within the water-land boundary are classified as water body including water surface, and all terrain raster points located within the water-land boundary are classified as water ground. The results of the raster classification are then transferred to the point cloud and controlled manually.

3.3 Water surface model and refraction

The laser beam is reflected and refracted at the boundary between air and water. The fact that light is about 25 % slower in water than in air ($c_{air} = 299,710 \text{ km/s}$, $c_{water} = 225,000 \text{ km/s}$) requires the application of a refraction- and runtime correction for all measurement points located below the water surface. Therefore, the water surface needs to be modelled based on all classified water-surface points. Those spread over a 20 to 30 cm thick band around the true water table and only the uppermost points (99 % quantile) were considered as valid points to model the actual water surface (Mandlbürger et al. 2013). The water-surface model was defined by element sizes of 1.5 m to 5 m, where the centre of each grid cell had the elevation $z = q_{0.99}$. The raster points were triangulated for the final water-surface model, which was then extrapolated towards the water-land boundary.

For applying the refraction correction three data sets are required: the point cloud with time stamp for each measurement point, the trajectory with time stamp for each point of the trajectory and the triangulated water-surface model. First of all, a pair of points with the same time stamp (P from the trajectory, and Q from the point cloud) and the vector between these two points was evaluated to determine the point, where the beam P-Q intersects the water surface S (Fig. 6). Therefore, the beam's entering angle can be determined in order to correct the beam with respect to the refraction angle. Moreover, the beam's length S-Q below water can be calculated in order to apply the runtime correction with respect to the refraction index. Using a refraction index of 1.33 for water and 1.000292 for air, the runtime correction was derived by:

$$\begin{aligned} & \text{Beam length under water unrefracted} \\ & \times (1/\text{refraction index water}) \\ & = \text{Beam length under water refracted.} \end{aligned}$$

The angle correction was calculated according the Snell's refraction law:

$$\begin{aligned} & \text{Refraction index air} \\ & \times \sin(\text{angle between beam in air and water surface}) \\ & = \text{Refraction index water} \\ & \times \sin(\text{angle between water surface and beam in water}). \end{aligned}$$

The difference prior and after application of the refraction and runtime correction is shown in Fig. 7 for an exemplary cross-section. Corrected water-ground points (in blue) are located above their original position (in red). Terrain points above the water surface are not affected by this correction.

Fig. 6: Schematic illustration for refraction calculation

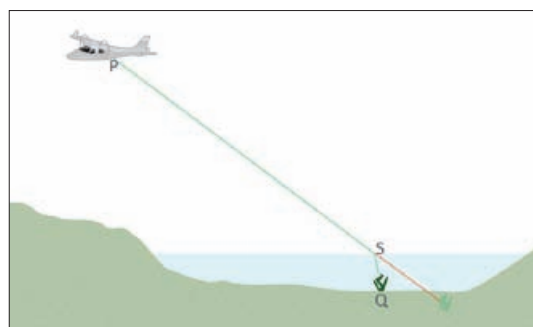
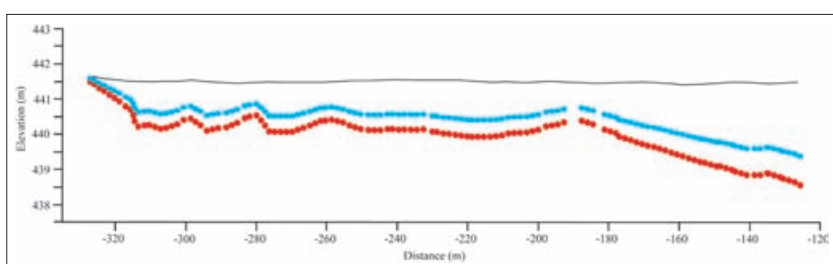


Fig. 7: Simplified cross-section to illustrate location of points prior (red) and after (blue) applying the refraction. Water table is marked in black



3.3 Digital terrain modelling

Finally, in order to generate high-resolution digital terrain models (DTMs) for both project sites the classified terrain points were mapped onto a 0.5 × 0.5 m grid using the mean elevation of all terrain points per grid cell (compare with Fig. 8). The DTMs serve as base for detailed mapping purposes.

es as well as morphologic analysis and comparison with terrestrially measured data.

4 Preliminary results and discussion

Based on object detection Andersen et al. (2016) have demonstrated that the vertical accuracy and precision of the LiDAR data on land was ± 8 cm with a 95% confidence level; while the vertical precision below the water surface was ± 4 cm. Andersen et al. (2016) determined the horizontal mean error to ± 10 cm. Hence, the overall vertical and horizontal precision is within sub-decimetre scale. The same objects, a cement block ($250 \times 125 \times 80$ cm) located on land as well as a steel frame ($92 \times 92 \times 30$ cm) positioned in a shallow water area (Fig. 9), were also used to assess the feature-scale detection. The two objects, which were clearly visible in the point cloud, were modelled based on different approaches (triangulation vs. grid) and subsequently detailed morphological analysis (slope, etc.; Fig. 10) were conducted. The results indicate that such sharp-edged, sharp-cornered, and steep-angled features are smoothed, e.g. underestimation of slope angles (Fig. 10). This smoothing is mostly due to the footprint size of the topobathymetric LiDAR system (about 40 cm). Nevertheless, decimetre-scale features are well detected by airborne LiDAR topobathymetry. Hence, the preliminary results demonstrate that airborne topobathymetric LiDAR is a valuable tool to bridge land and water environments as well as to bridge morphological scales, thereby closing the gaps between terrestrial and marine surveys and between the mapping of individual morphological features and complete landscapes.

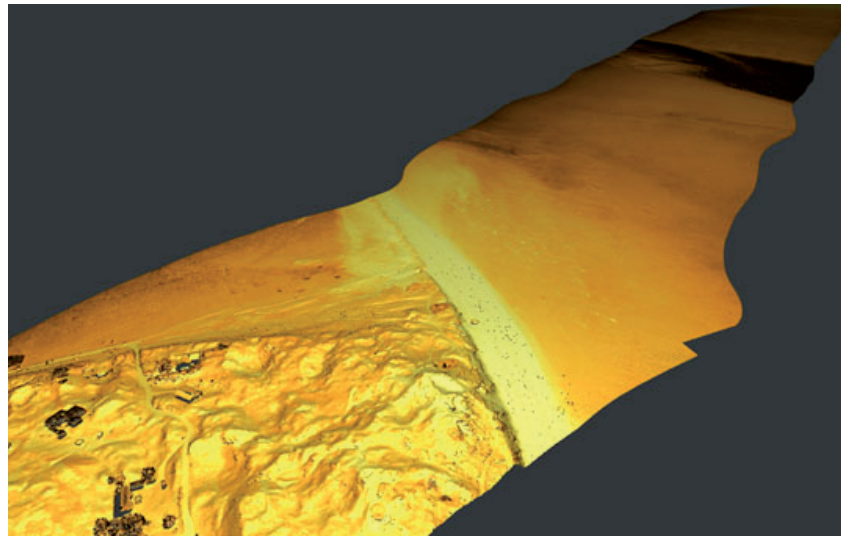


Fig. 8: DTM section from the Knudedyb tidal inlet system showing the complex and manifold morphologic patterns

5 Conclusions

The results of our study underpin that topobathymetric surveying is a highly efficient and valuable tool for monitoring complex coastal areas. In tidal influenced areas with extremely variable water surface conditions, the seabed can be well detected at low tide down to depths of about 3 to 4 m (Knudedyb site), whereas in calm and clear water conditions within the Rød-sand lagoon the seabed was detected down to depths of 6 to 7 m. Moreover, small scale under-water features (decimetre- to metre-scale) can be readily identified in the data allowing detailed and area-based analysis of sediment transport and morphologic changes and to evaluate specific habitat characteristics and distribution. [↕](#)

Fig. 9: Small-scale objects at Knudedyb project site. Both objects are visible in the point cloud and are modelled based on triangulation and rasterisation

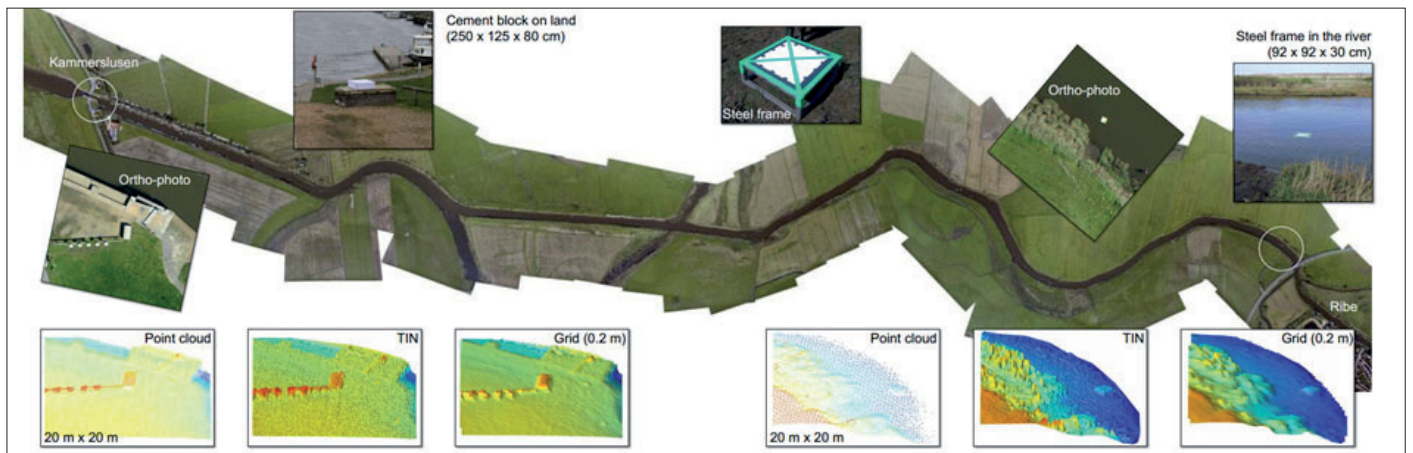
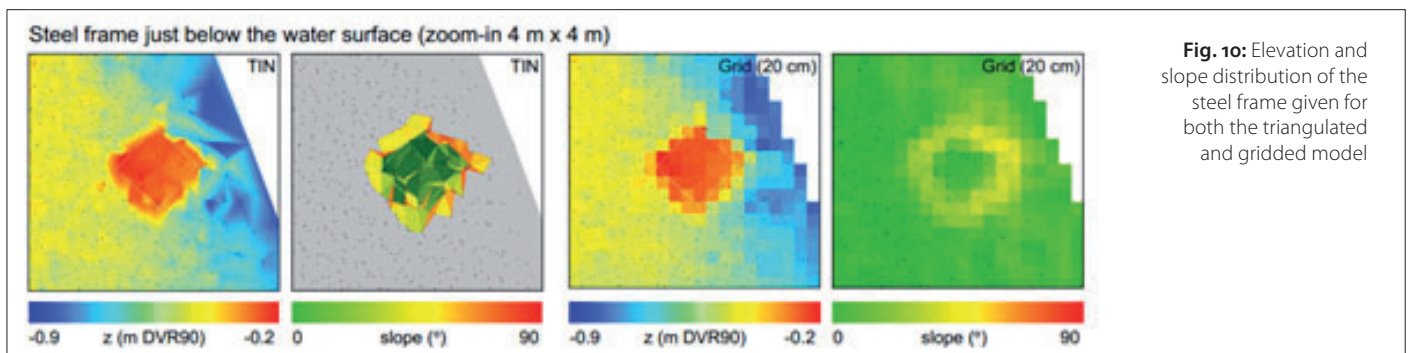


Fig. 10: Elevation and slope distribution of the steel frame given for both the triangulated and gridded model



New techniques in capturing and modelling of morphological data

An article by LUTZ CHRISTIANSEN

Since 2014 the techniques of LiDAR bathymetry have been used for capturing morphological data in Schleswig-Holstein. Round 2000 km² have already been surveyed with these techniques. Data gaps only occur locally in tide ways or low-lying areas, which are needed to be filled by hydrographic surveys. But compared with the bathymetric LiDAR, these surveys have a substantially lower density of points. Hence, it is difficult to merge these data to a morphological model. As a consequence it is necessary to densify the hydrographic data to create a homogeneous model. The mathematical method of Coons patches is suitable for this purpose. The gaps inside the area of hydrographic survey are filled with data points in desired density. The bathymetric information is then calculated using bilinear interpolation. As a result a data set which has a similar point density as the bathymetric LiDAR is created. After the preparation a homogeneous morphological model can be generated by triangulation, based on bathymetric LiDAR on the one hand and hydrographic surveys on the other hand.

Author

Lutz Christiansen is Survey Manager at the Schleswig-Holstein Agency for Coastal Defence, National Park and Marine Conservation (LKN.SH).

lutz.christiansen@lkn.landsh.de

coastal protection | LiDAR bathymetry | morphological data model | Coons patches

1 Introduction

Schleswig-Holstein, the most northern state of Germany, is called »the land between the seas« because it is placed between the Baltic Sea with a coastline of approximately 640 kilometres on the east side and the North Sea with a coastline of approximately 550 kilometres at the west side of the state (Fig. 1).

This location between the seas justifies that coastal protection is a main task. Without buildings of coastal protection, 25 % of the area and 12 % of the inhabitants of Schleswig-Holstein would be threatened of storm surge and floods.

For coastal protection knowledge about the development of the morphology of the coastal areas is necessary. Therefore, an area-wide survey above and below the mean sea level has been conducted and an analysis of the acquired data has been done.

2 Previous survey

Both seas have different conditions which are considered by implementing a survey. The Baltic Sea is stamped by the last ice-age with fjords and shallow shore areas. A nearly constant water level in the height of the mean sea level is predominant. Variations are only in the impact of wind. The North Sea is stamped after the last ice-age by the growth of the Wadden Sea offshore the coastline which is daily formed by two tides. The water level varies between round three metres from the high tide to the low tide.

Both coastal regions are shallow water areas. In focus of coastal protection are the areas between the coastline and seawards the depth line of ten metres below the mean sea level. Because of these natural conditions an area-wide survey is seen to be difficult.

The region of the North Sea, including the Wadden Sea, has been primarily surveyed by ships until now using the high tide completed by airborne LiDAR scanning at the low tide.

The region of the Baltic Sea until now has been primarily surveyed by ships and boats with a small draught following by terrestrial survey on feet up to the waterline and then completed by airborne LiDAR scanning.

3 LiDAR bathymetry as a new method of survey

Since 2014 the Schleswig-Holstein Agency for Coastal Defence, National Park and Marine Conservation (LKN.SH) has been using the method of LiDAR bathymetry for the survey of the coastal regions above and below the mean sea level. Only lower areas are additionally hydrographical surveyed by ships.

The known method of airborne LiDAR scanning applies red LiDAR light, which is able to capture terrain and water surfaces. The technique of LiDAR



Fig. 1: The state Schleswig-Holstein

bathymetry uses additional green LiDAR light, which is able to penetrate into the water body and capture the seafloor (Fig. 2).

3.1 Expected depths

For the depth of penetration the turbidity of the water body is decisive. This is declared as Secchi depth. Also the power of the systems is important which is described as a factor of the Secchi depth.

On the coast of the Baltic Sea the Secchi depth varies between three metres at the fjords and five metres at the open sea.

On the coast of the North Sea the values of Secchi depths varies at the Wadden Sea between nought and one and a half metres and seaside the Wadden Sea nearly three metres.

In spite of the small Secchi depth the technique of LiDAR bathymetry is very suitable because the ground of all water areas left on the tide land at the low tide are captured.

This is not possible by using airborne LiDAR scanning. The red LiDAR light cannot penetrate into the water body.

The systems of LiDAR bathymetry on the market are divided into two categories. The one system is able to reach the one to one and a half (1 : 1.5) of the Secchi depth, the other system is able to reach the two and a half to three (2.5 : 3) of the Secchi depth.

With this information of the manufactures and the knowledge of the Secchi depths of the areas the reachable depths of the survey are estimated (Fig. 3).

3.2 Results of LiDAR bathymetry in coastal areas

Between 2014 and 2016 around 2,000 km² have been covered by LiDAR bathymetry. The whole coastal area of the Baltic Sea with 650 km² and approximately 50 % of the Wadden Sea with 1,350 km² have been captured until now.

In all regions the expected depths are nearly reached.

The following examples of the west coast of the island of Sylt, the Wadden Sea and a coastal area of the Baltic Sea show this:

- At the west coast of the island Sylt the whole sand reef down to eight metres is captured (Fig. 4).
- At the Wadden Sea the ground of all water areas on the tideland is captured (Fig. 5).
- In the Baltic Sea detailed under-water structures down to five metres are captured (Fig. 6).

3.3 Accuracy of data of LiDAR bathymetry

The accuracy of data of LiDAR bathymetry are defined by comparison with terrestrial and hydrographical surveys realised nearly at the same time. The results are nearly between one and two decimetres in height, which conforms with the ac-

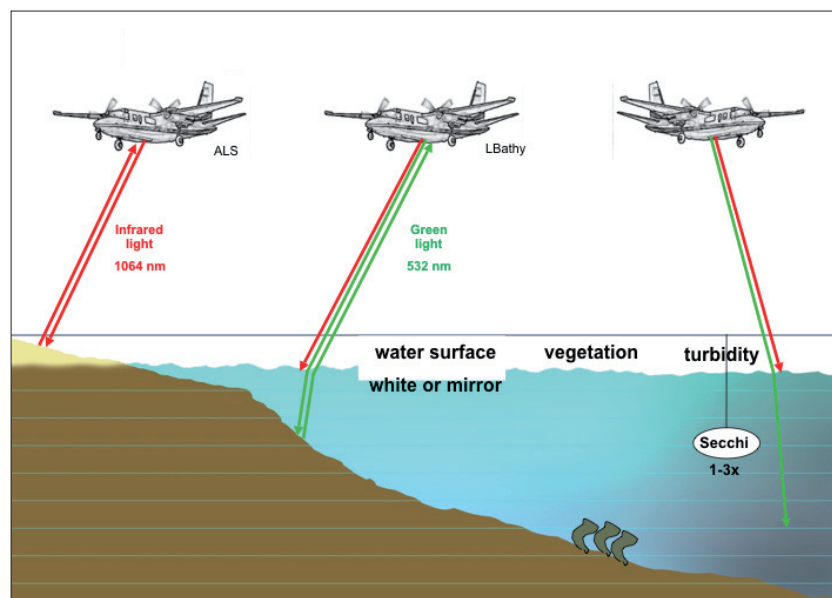


Fig. 2: Principle and limitations of LiDAR bathymetry



Fig. 3: Secchi depths at the North Sea and the Baltic Sea

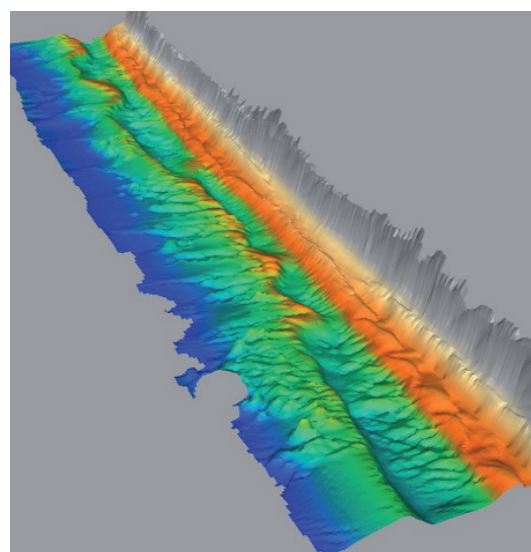


Fig. 4: Results of LiDAR bathymetry down to eight metres at the west coast of the island Sylt

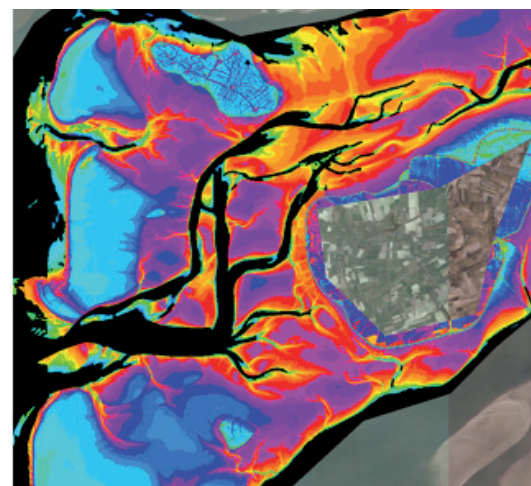


Fig. 5: Results of LiDAR bathymetry of the Wadden Sea, the most turbidity area. Only the tide ways are not captured

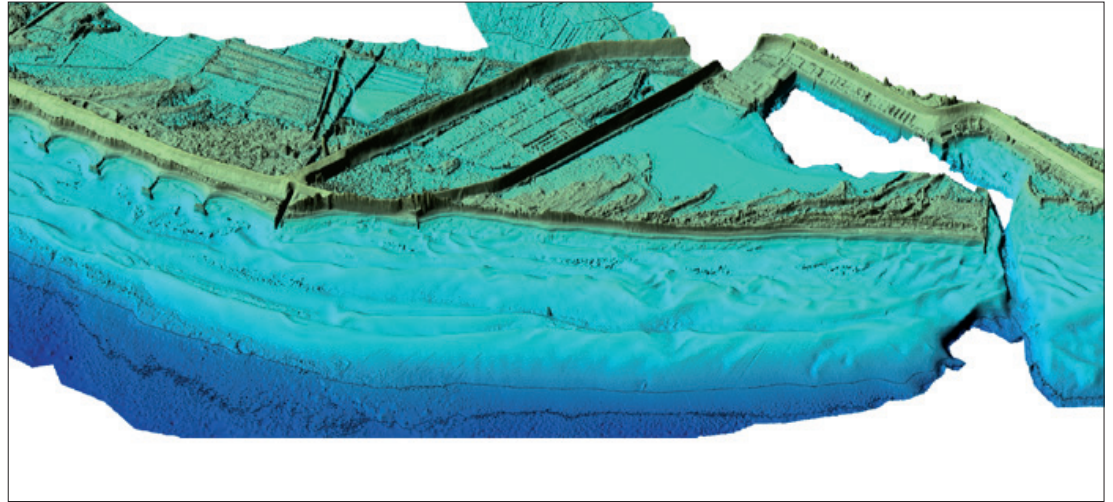


Fig. 6: Results of LiDAR bathymetry down to five metres of the Baltic Sea

curacy of the hydrographic survey as Fig. 7, 8 and 9 show.

4 Modelling of line-based survey data

After a first implemented survey by LiDAR bathymetry at the shallow water areas the remaining deeper channels of the tide ways are hydrographically surveyed by using a single-beam system.

The LiDAR data are area-wide homogeneous spreaded with at least one point per squaremetre. These data are unproblematically converted into a plausible morphological model.

The line-based hydrographical data with an usually line distance of one hundred metres and one data point per running metre is very problematically converted into a plausible morphological model because of the inhomogeneous data distribution.

Therefore, it is a goal of the LKN.SH to create a homogeneous data distribution of line-based surveys and to generate a plausible morphological model.

This is possible by using Coons patches.

4.1 Coons patches for higher data density

Especially the car industry needs algorithms to generate free formed surfaces by CAD (Krömker 2008).

Approximation algorithms of Bézier curves and Bézier surfaces are known. These were developed by P. Bézier at Renault.

Steven Anson Coons (1912 to 1979) was a pioneer of developments in computer graphics. He worked among others at Ford. His developed Coons patches are based on an interpolation algorithm (Bungartz et al. 2013, p. 91). Inside of mostly four squared polygons a higher data density takes place by bilinear interpolation (Fig. 10).

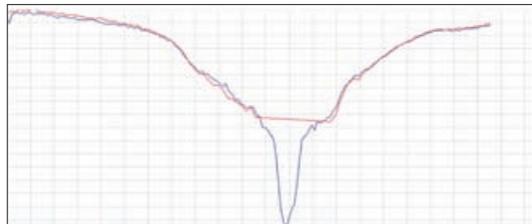


Fig. 7: Accuracy of LiDAR bathymetry (red line) in the Wadden Sea in comparison with hydrographic survey data (blue line)

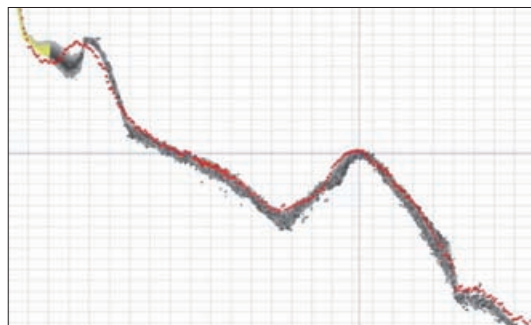


Fig. 8: Accuracy of LiDAR bathymetry (grey points) at the west coast of Sylt in comparison with hydrographic survey data (red points)

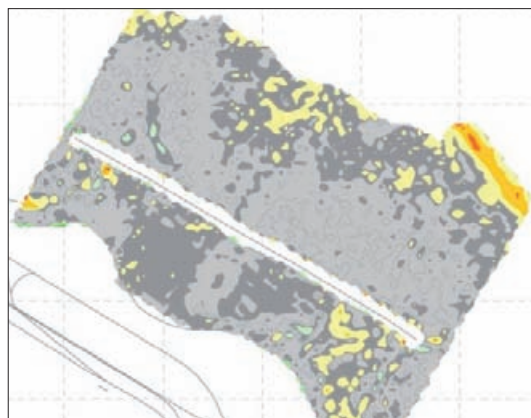


Fig. 9: Accuracy of LiDAR bathymetry depicted in a difference model LiDAR bathymetry vs. hydrographic/terrestrial survey. Grey: 0 to 10 cm, dark grey: 10 to 20 cm

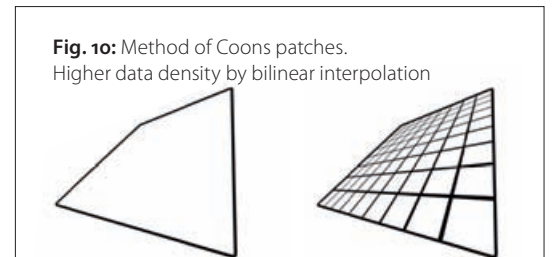


Fig. 10: Method of Coons patches. Higher data density by bilinear interpolation

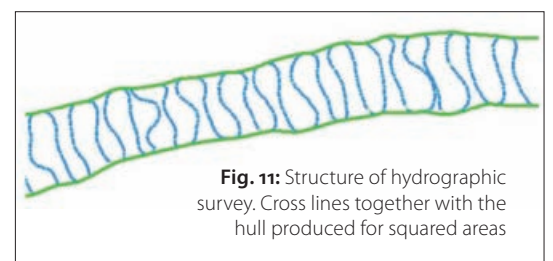
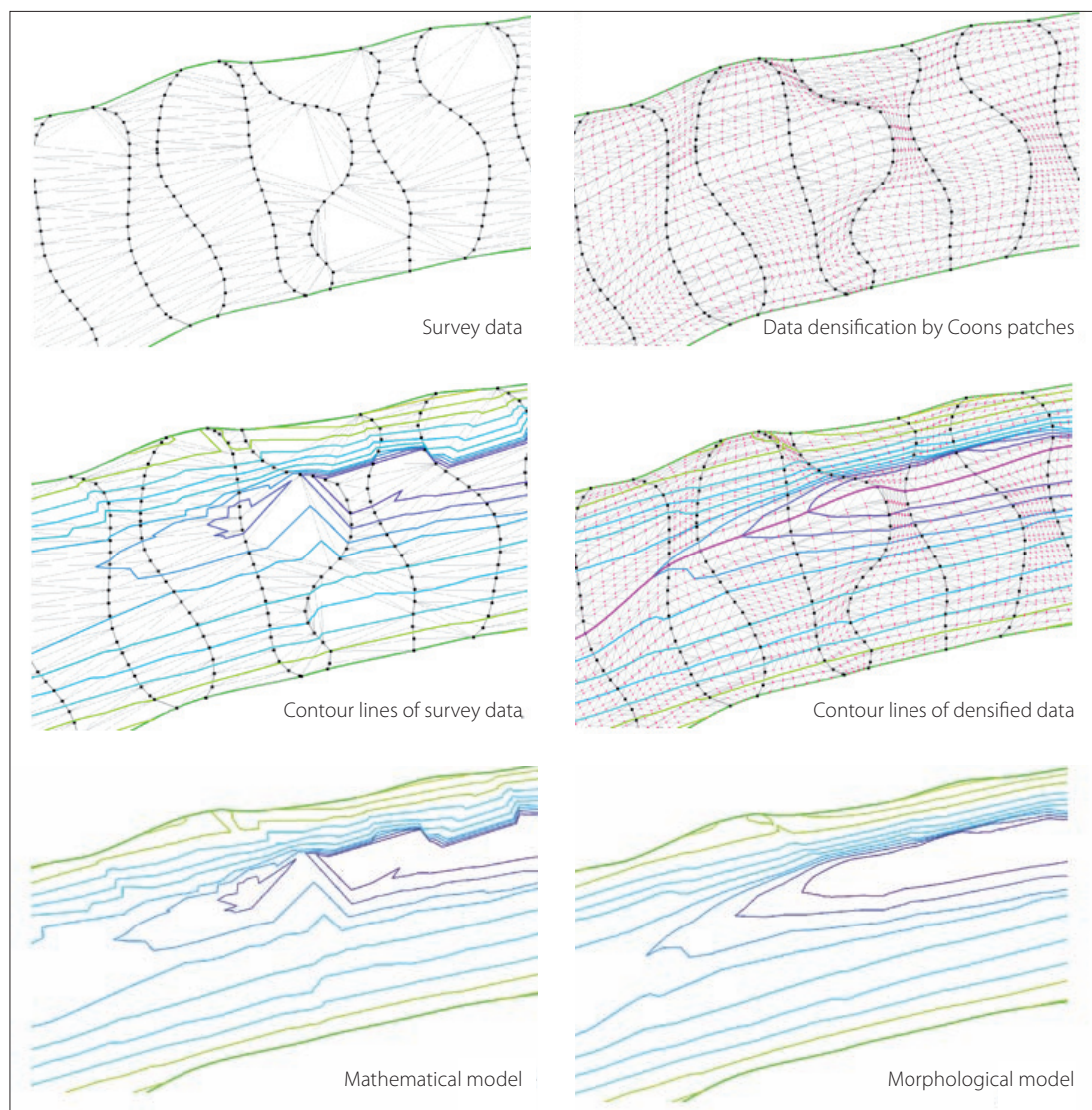


Fig. 11: Structure of hydrographic survey. Cross lines together with the hull produced for squared areas



References

- Krömker, Susanne (2008): Skript Computergraphik II, SS2008, Kapitel 6 Splines; www.iwr.uni-heidelberg.de/groups/ngg/CG2008/Txt/Kapitel6.pdf, last access 19.09.2016
- Bungartz, Hans-Joachim; Michael Griebel; Christoph Zenger (2002): Einführung in die Computergraphik – Grundlagen, Geometrische Modellierung, Algorithmen; Vieweg+Teubner-Verlag, 344 p.

Fig. 12: Comparison of the mathematical model with only the survey data (left) and the morphological model additional with the Coons data (right)

4.2 Transfer to line-based survey of channels

In the survey of channels the definition of the measuring lines are perpendicular to the direction of flow.

The hull line, composed of the ending points of each measuring line, encloses the area which is represented by the inside-placed data points.

Thus, four squared polygons are produced which allow bilinear interpolation inside. The algorithm of Coons patches are utilised here (Fig. 11).

An improvement of the polygonal partitioning is given by embedding morphological structure lines like the deepest line of the channel bed or lines of change of inclination. These optimise the morphological accuracy of the model.

4.3 Using of Coons patches

As a result virtual data will be formed with a homogeneous data distribution and assigned high information by bilinear interpolation of the surveyed data.

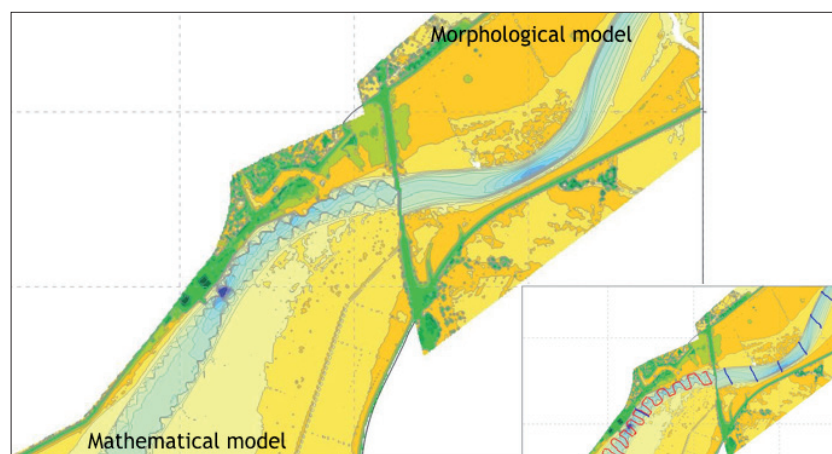
By using the original data and the Coons data a plausible morphological terrain model is generated. Fig. 12 and 13 illustrate the differences between mathematical and morphological model.

5 Conclusions

For an area-wide survey of shallow water areas along the coast the technique of LiDAR bathymetry is very effectively usable. This method replaces the difficult realisation of hydrographic survey which is only necessary as addition in deeper areas.

In a hydrographic survey with single-beam technique it is possible to generate a homogeneous data density by using Coons patches. More plausible morphological terrain models are creatable. [↗](#)

Fig. 13: Demonstration of the difference between the mathematical model and the morphological model at a part of the River Eider



Use of laser bathymetry at the German Baltic Sea coast

An article by WILFRIED ELLMER

The German coastal waters are quite shallow. The idea arose to use airborne laser bathymetry (ALB) for hydrographic surveying of near-shore areas of the German Baltic Sea. Since these waters are relatively turbid, it became necessary to investigate to what extent modern ALB systems could be of practical use in an area large enough for hydrographic purposes especially in the Baltic Sea. The basic questions to be answered by the project were: Which areas can be measured by this method? And how expensive will this be in relation to traditional methods? From 2012 to 2014, four test surveys have been accomplished in an area north of the city of Wismar. During these surveys, many relevant questions were solved.

Author

Dr. Wilfried Ellmer is deputy head of the surveying and geodesy section of the German Maritime and Hydrographic Agency (BSH) in Rostock.

wilfried.ellmer@bsh.de

ALB | laser bathymetry | Baltic Sea | Secchi depth

1 The state of hydrography in Germany

1.1 Hydrographic surveying in Germany

The German Maritime and Hydrographic Agency is mandated to conduct hydrographic surveys in the coastal waters and the EEZ of two different areas:

- North Sea, there are very busy approaches to Hamburg, Bremerhaven, and Wilhelmshaven, with large shallow areas shaped by strong tidal currents, the Wadden Sea area. Due to these currents the water is very turbid, large parts with Secchi depths of less than 0.5 m. The depths of shallow areas are changing very much, so they have to be resurveyed very frequently, partly every year. The deeper areas of up to 70 m are to be resurveyed once in 25 years only.
- Baltic Sea, also quite shallow, up to 50 m. The tidal range is less than 30 cm, so the structure of the bottom is much less dominated by strong currents. Most parts will be resurveyed once in 10 or 25 years only, but it is necessary to achieve full bottom coverage. The visibility of the water is much better than in the North Sea, sometimes better than 5 m.

Surveying is done by single-beam and multibeam echo sounding. In areas of frequent resurvey activities, single-beam echo sounding is the standard procedure.

Wreck search is a very important task in German waters. The obstructions database contains about 2,000 positions. Every year nearly 30 new obstructions are found, and 200 positions have to be revisited in order to examine changes of the position and the least depth; especially in the strong tidal currents of the Wadden Sea, one has to take into account that even large objects may move.

1.2 The question of airborne laser bathymetry

In former times, airborne laser bathymetry (ALB) was assumed to be unsuitable for hydrographic surveys in German waters due to the poor water-

visibility conditions. A test flight in 2008 showed poor results, and seemed to validate this assumption. However, recent developments of new ALB systems may lead to better results, and made it necessary to investigate the potential of this technology, and to verify, whether or not ALB has the potential to replace the traditional techniques or at least to complement them.

A project was started in order to answer this question, and to decide on further actions. The basic questions to be answered by the project were:

- Where does it make sense to use ALB for hydrographic surveys?
- How expensive will this be in relation to traditional methods?

The criteria for these answers are those of S-44 (IHO 2008).

2 The laser bathymetry project

2.1 The structure of the project

The project took place in the years 2012 to 2014. Each year one flight was planned and a call for tender was issued. The area to be surveyed was chosen north of the island of Poel, an area with different structures, with some stones, and with depths from zero to a depth well exceeding the capabilities of modern ALB in order to reach the system's maximum depth capability.

The Institute of Photogrammetry and Geo-Information (IPI) of Leibnitz University of Hannover took over a scientific cooperation in the frame of the project. One person processed the ALB data and prepared a report (Niemeyer et al. 2015). Additionally, some Bachelor and Master theses were written on special aspects of the project. Attached to the project a board was installed with representatives of some other German institutions interested in that topic. The board met every year to exchange information on the project and on other activities pertaining to ALB. Coastal protection authorities were especially interested in the project and gave input on their activities (Christiansen 2016). This was very important since ALB cam-

campaigns for data production can only be financed through cooperation of all institutions active in the same area.

2.2 The flight campaigns

The 2012 campaign was planned with three main criteria:

- High resolution (much higher than the 2008 tests);
- In some areas, the tracks had to be in three heights: the optimum, 20 % more, and 20 % less of the optimum;
- The measurements were to be made in fall 2012.

The survey took place in October/November 2012. Some of the measurements could not be processed, so it became necessary to repeat the relevant tracks in April 2013. The sensor was a Riegl VQ-820-G. The Secchi depth was 6.8 m.

The main results in short (Wischow 2013):

- A depth of 5 to 6 m could be reached, in April 6 to 7 m;
- Obstructions could not be found;
- There are some gaps in the data, partly in the same places as with the 2008 test flight.

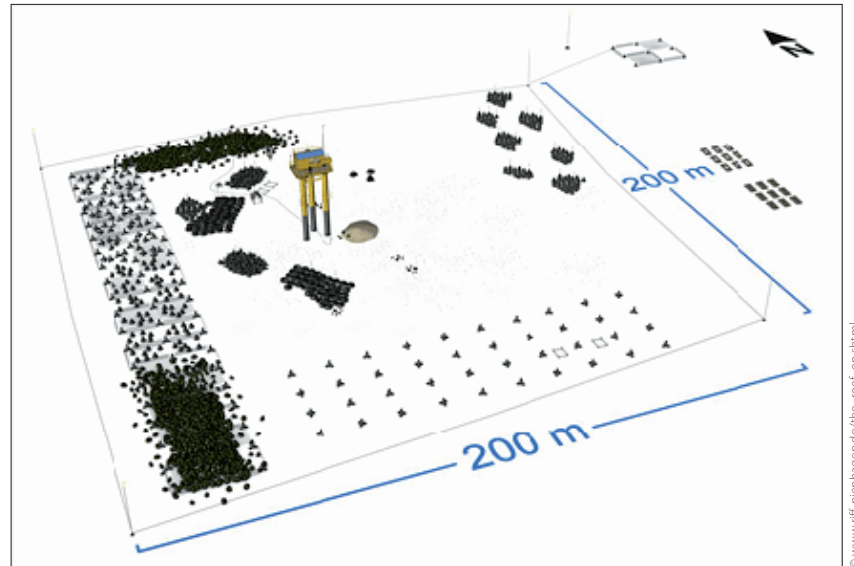
The 2013 campaign was planned with three main criteria:

- Two different resolutions: High resolution in the shallow areas, and a depth of 2 × Secchi depth with less resolution;
- The measurements were to be made in fall 2013;
- Additionally to the area north of Poel, two little areas further east had to be surveyed, artificial reefs Nienhagen and Rosenort.

The survey took place in September 2013 in two campaigns, first with Hawkeye II, later with Chiroptera in the shallow areas. The Secchi depth was 7 to 9 m.

The main results in short (Sánchez Gámez 2014):

- With Chiroptera a depth of 9 to 10 m could be reached, with Hawkeye II the depth range of 7 to 14 m was covered;



© www.riff-nienhagen.de/the_reef_en.shtml

Fig. 1: Reef Nienhagen

- Obstructions again could not be found, even the relative large reefs in Nienhagen (Fig. 1) and Rosenort;
- The object classes »vegetation« and »obstruction« could not be separated.

The 2014 campaign was planned again with the same main criteria. The main difference was the request to fly in spring 2014. Due to the long-time required for the procurement, the planning took place before the results of the 2013 flight had been delivered.

The survey had initially been planned with the new Hawkeye III, which would have been able to do the high-resolution and the deeper survey in one flight. However, in spring 2014 the system was not available, so the flight was performed in May 2014 with Chiroptera. In September 2014, six selected tracks were resurveyed with Hawkeye III, and seven at the position of the reefs. The Secchi depth was 6 m only in May and in September, somewhat more at the reefs. The areas of the survey are to be seen in Fig. 2.

The main results do not differ much from those of 2013 (Warnke 2015). Even the new Hawkeye III

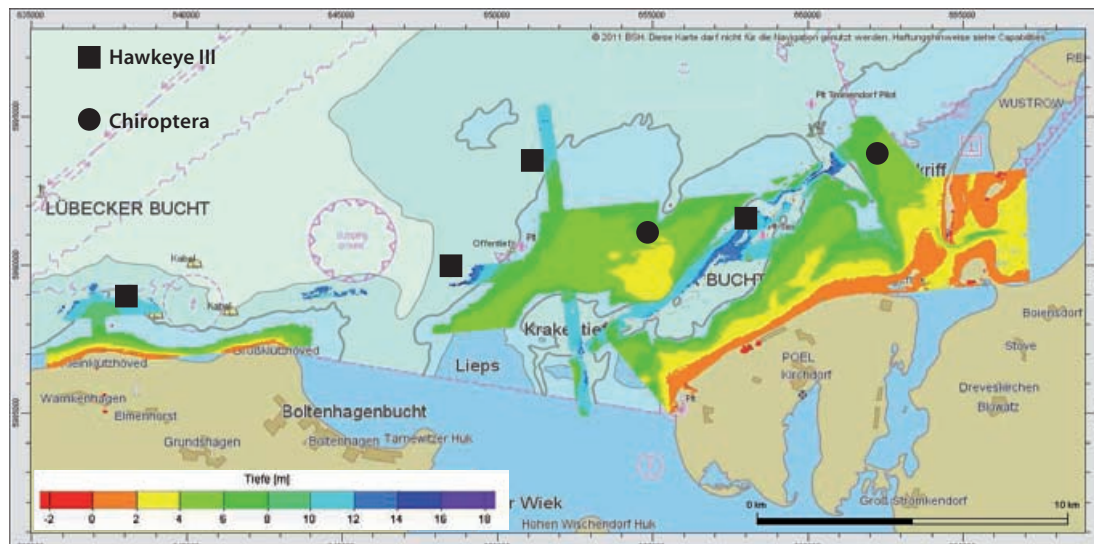


Fig. 2: Area and depths of 2014 campaigns

References

- Christiansen, Lutz (2016): New techniques in capturing and modelling of morphological data; HYDRO 2016 paper, Hydrographische Nachrichten, HN 105, pp. 20–23
- Helsinki Commission (2010): HELCOM Ministerial Declaration on the implementation of the HELCOM Baltic Sea Action Plan; Helsinki Commission, Baltic Marine Environment Protection Commission, Moscow, 20 May 2010
- Hübner, Tony (2014): Visualisierung von Secchi-Tiefen in der Ostsee zum Zwecke der Laserbathymetrie; Bachelor thesis, Hochschule Neubrandenburg
- IHO (2008): IHO standards for hydrographic surveys; Special Publication No. 44, 5th edition, Monaco
- Niemeyer, Joachim; Yujin Song; Tomasz Kogut; Christian Heipke (2015): Untersuchungen zum Einsatz der Laserbathymetrie in der Seevermessung; Projektbericht, Institut für Photogrammetrie und Geoinformation, Leibniz Universität, Hannover
- Sánchez Gámez, Pablo (2014): Comparison of Laser Bathymetry with Single beam and Multibeam data in the southwestern Baltic Sea; Master thesis, HafenCity Universität, Hamburg
- Warnke, Kai (2015): Untersuchung zur Qualität flugzeuggestützter Laserbathymetriedaten in Küstengewässern der Ostsee; Master thesis, Technische Universität Dresden
- Wischow, Philippe (2013): Vergleich von flugzeuggestützten Laserbathymetriedaten mit Vertikal- und Fächerecholotdaten; Bachelor thesis, HafenCity Universität, Hamburg

does not produce results that significantly deviate from the results of Chiroptera and Hawkeye II.

2.3 The investigation of Secchi depths

In order to extrapolate the findings to the whole German coast of the Baltic Sea, it is necessary to investigate the Secchi depths of the whole German waters (Hübner 2014). These depths vary much during the year. There are two time windows of special interest:

- Spring time has the best Secchi depths, but the time window is smaller and depends much on the weather conditions of the months before.
- Fall time has slightly worse Secchi values, but the time is longer and better to predict.

The spatial variation is very large (0.5 to 9 m). This leads to a consideration of the relationship (depth/Secchi depth) instead of the Secchi depth itself. The result of this investigation is a chart (Fig. 3) showing areas of:

- $0.7 \times$ Secchi depth for Riegl VQ-820-G or similar;
- $1.3 \times$ Secchi depth for Chiroptera or similar;
- $2.0 \times$ Secchi depth for Hawkeye III or similar.

3 Conclusion

3.1 The findings of the project

The main conclusion is that bathymetric airborne laser scanning will not replace traditional hydrographic surveys as such, but will be an important supplement in shallow areas with minor importance for mariners. It is a strong improvement against single-beam hydrographic survey, since the survey is compliant with S-44 order 1b instead of order 2 (IHO 2008). Within the German part of the Baltic Sea, 2,500 km² may be surveyed with ALB with full coverage up to a relation depth/Secchi depth of 1.3 and with minor resolution up to a relation of 2 (Fig. 3).

These areas are mostly to be resurveyed every

25 years. It makes sense to do the survey in parts of this area in order to limit the size of data sets to be processed. In order to improve the efficiency it is necessary to coordinate a flight campaign with all stakeholders of the area to be surveyed, especially between the hydrographic office, the coastal engineers, the coastal protection authorities, and the ordnance survey.

There are still some questions remaining, especially:

- The detection of obstructions,
- Data gaps due to vegetation or other material with bad backscattering.

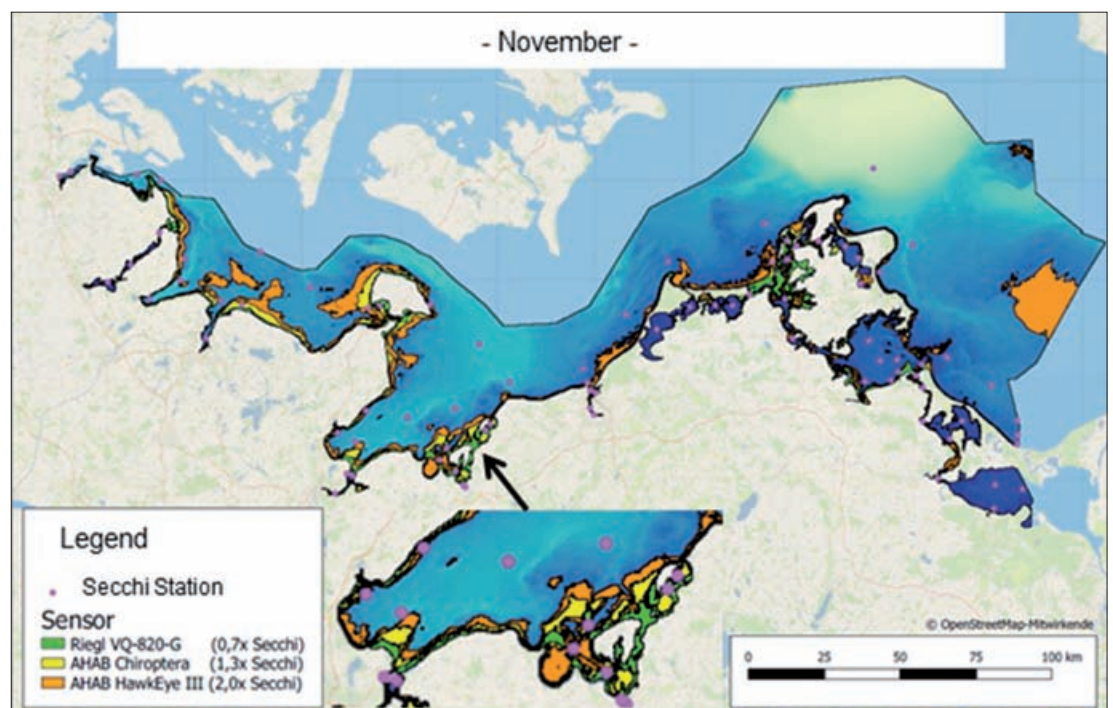
Solving these questions would significantly improve the use of ALB for hydrographic purposes. Particularly at the German Baltic Sea coast, lots of stones, dangerous for shipping, could be detected.

3.2 The next step

Following this project it becomes necessary to update the general plan of surveys in the Baltic Sea. An area of 2,500 km² may be described as ALB area. This gives the possibility to concentrate the multi-beam capacity to other areas where the frequency of surveys must be increased in order to improve the safety of shipping (Helsinki Commission 2010). The next steps will be to arrange the financing and the coordination of the projects.

The ALB campaign will be organised with a public call for tenders. The project has shown that the area should be described between some distance landwards from the coastline up to a line described by the relation depth/Secchi depth. Thus, it is necessary to organise shipborne Secchi measurements together with shipborne control check lines very close to the ALB measurements. The time of survey should be open, but with good communication in order to coordinate the flights with the shipborne measurements. [↕](#)

Fig. 3: Possible areas for ALB in November



... und die Realität kommt einfach an den Arbeitsplatz.



Die Lösung aus einer Hand: Nutzung von 3D-Punkt-
wolken und Panoramabildern in Ihrer gewohnten GIS-
oder CAD-Umgebung. Webbasierte Anwendungen für
eine Vielzahl unterschiedlicher Anwender in Ämtern
und Abteilungen durch einfaches und intuitives Daten-
handling. Machen Sie Schluss mit Kompatibilitäts-
problemen bei 3D- und Visualisierungsdaten und
nutzen Sie die Möglichkeiten von Scan2Map für Präsen-
tationen, zum Arbeiten und Vermessen am Rechner
und für aktuelle Kartendarstellungen.

Mobile Mapping



Mit modernsten mobilen Datenerfassungs- und Vermessungs-
systemen wie dem Trimble® MX7, MX2 und MX8 werden präzise
die räumlichen Daten erfasst. Laserscanning in Kombination mit
Bildaufnahmen oder reine Bildaufnahmen mit kalibrierten Kameras.

- Flächendeckende und präzise georeferenzierte Punktwolken und / oder 360°-Panoramabilder
- Aufbereitung der Daten entsprechend der Datenschutzvorschriften
- Komplett aufbereitete Daten

Content Manager

Mit dem Content-Manager lassen sich sowohl die Mobile Mapping-
Daten als auch weitere Daten von UAV, aus klassischen Bildflügen,
terrestrischen Scans oder Planungsdaten importieren. Auf Basis
unterschiedlicher Hintergrundkarten kann der Nutzer die Daten
organisieren und kontrollieren.

Scan2Map für eine optimale Nutzung der Panoramabilder und Punktwolken

- Visualisieren und Bearbeiten von „unendlich“ großen Punktwolken
- Darstellen der aufgenommenen Panoramabilder und Überlagerung mit den Punktwolken
- Analyse- und Viewer-Funktionen / Datennutzung auf mobilen Endgeräten
- Arbeiten und digitalisieren in Echtzeit in der gewohnten GIS- oder CAD-Umgebung durch Nutzung von Plugins
- Nutzung unterschiedlicher Suchfunktionen und Hintergrundkarten zur optimalen Navigation und Orientierung

Publisher-Tool

Über das Publisher-Tool lassen sich die Mobile Mapping-Daten
sehr einfach und intuitiv webbasiert auf Standardrechnern
nutzen und können somit einer Vielzahl von Mitarbeitern zur
Verfügung gestellt werden. Der Publisher bietet zahlreiche
Messfunktionalitäten in den Punktwolken und Panoramabildern.

Nutzung der Plugins

Durch die Plugins für verschiedene GIS- oder CAD-Systeme kann
der Nutzer in seiner gewohnten Arbeitsumgebung zusätzlich auf die
Mobile Mapping-Daten zugreifen und diese mit den vorhandenen
Informationen überlagern. Über die Plugins lassen sich im Zielsystem
Objekte mit allen erforderlichen Attributen erzeugen oder anpassen.

Nachfolgende Plugins stehen derzeit zur Verfügung, weitere können erstellt werden:

AutoCAD Map / ArcGIS / QGIS / Geocortex

Ihr Mehrwert

- Weniger Ortstermine durch aktuelle Bild- und Scandaten
- Optimierte Entscheidungsprozesse durch Visualisierung von Bestands- und Planungsdaten
- Messfunktion in den Bild- und Scandaten
- Nutzung der Daten in verschiedenen Fachbereichen

... und vor allem:

**Sie haben
einen Ansprechpartner!**

ENC and ECDIS

An article by PETER DUGGE

Electronic Navigational Charts (ENC) and Electronic Chart Display and Information Systems (ECDIS) are typically created at different places: ENC by various hydrographic offices, ECDIS by various industrial ECDIS manufacturers. When in use, ENC and ECDIS form a closely interconnected »community« with its members strongly dependent on each other when creating results which aim to support the navigator as efficiently as possible. Recognising the complexity of the standardisation task a great deal of success has been achieved in creating a worldwide community of producers and users of ECDIS and ENC providing a global coverage for the international maritime community.

However, gaps exist between worlds of ENC and ECDIS with regard to the standards and methods applied when producing and using ENC and ECDIS. Some of these discrepancies between the worlds of ENC and ECDIS have the potential to mislead the navigator and other users.

Author

Peter Dugge is Lead of Design and Management of Lean Mission, Navigation and Charting Systems at Atlas Elektronik GmbH in Bremen.

peter.dugge@atlas-elektronik.com

ENC | ECDIS | bathymetry | zooming in | S-57

1 ENC

ENC is the actual chart data prepared by hydrographic authorities for use with appropriate systems to support safe navigation.

ENC is neither software nor hardware – quite like a text file is neither software nor hardware, but »just« the actual user data.

The content, structure and format of ENC is standardised by the International Hydrographic Organization with their Special Publication No. 57 *IHO Transfer Standard for Digital Hydrographic Data* and its components (IHO 2000; IHO 2014).

ENC is »... issued for use with ECDIS on the authority of government-authorized hydrographic offices« (IMO 1995).

ENCs are object-oriented vector charts, hence providing not only pixel-information allowing to produce chart images (like raster charts such as ARCS do), but machine-readable real-world information such as depth values and light-sect-

2 ECDIS

Together with appropriate ENC ECDIS is a tool to support safe navigation at sea (Hecht et al. 2006; IMO 1995).

Generally ECDIS is understood to be a system consisting of »just« hardware and software but no chart data – quite like a computer with just a word processor is just hardware and software but does not contain any user data.

When the development of an ECDIS is finalised, it is thoroughly checked against tests stated in IEC 61174 *Operational and performance requirements, methods of testing and required test results* (IEC 2015) which – after successful tests – is the basis for the official type-approval of an ECDIS and its use for navigation on-board of seagoing ships (Hecht et al. 2006).

ECDIS is developed and produced mainly by commercial ECDIS manufacturers. An ECDIS typically consists of a computer with interfaces for navigation sensors, a monitor and a keyboard (Fig. 1).

ECDIS is not just a »display« system just creating chart images with a symbol on top showing own ship's position, but also provides »information« functions such as automatic route checks against charted depths.

3 ENC and ECDIS

Based on the understanding stated in chapters 1 and 2, ENC issued by or on behalf of hydrographic offices and ECDIS developed and produced by manufacturers form together a »Real-Time Geographic Information System« consisting of data, hardware and software – like all geographic information systems do (Bill and Fritsch 1994, p 5).

The fact, that in this sense neither ENC nor ECDIS alone provide any real use, is reflected by the following definitions in the *IMO Performance Standards for ECDIS* (IMO 1995):

- ENC »means the database (...) issued for use with ECDIS«;
- ECDIS »means a navigation information system (...) displaying (...) information« from a SENC, with SENC being the ENC imported into the ECDIS.

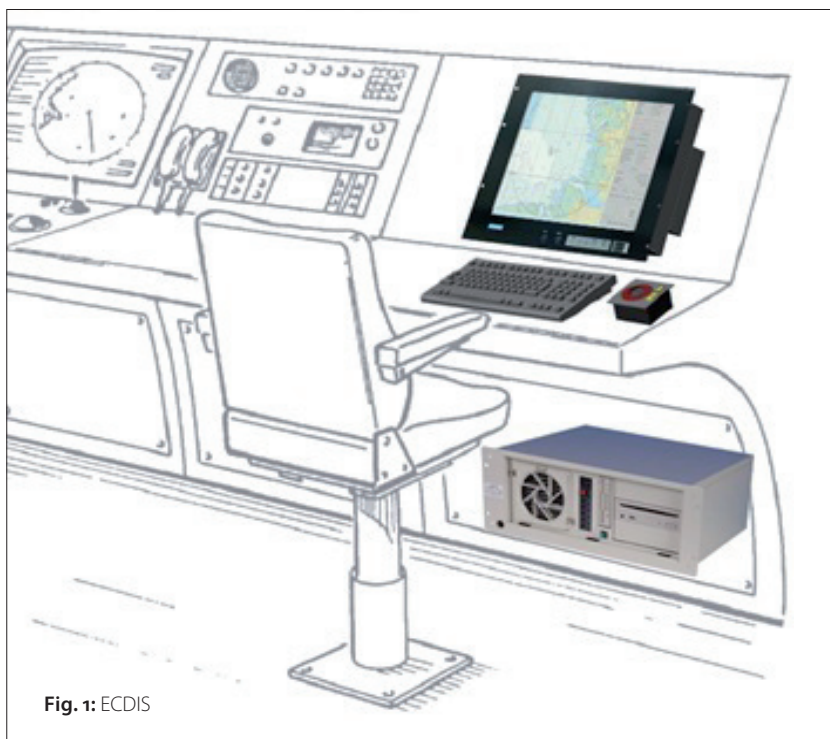


Fig. 1: ECDIS

It is quite obvious that the data and the hardware and software must fit well together in order to provide a tool useful to the navigator.

With ENC and ECDIS this is achieved by following a set of rules carefully adjusted to each other and constantly maintained based on the feedback of hydrographic offices, ECDIS manufacturers and navigators. This set of rules consists of:

- mainly S-57 and its components for the data (IHO 2002; IHO 2016)
- and IEC 61174 for the hardware and software (IEC 2015).

With the purpose of ENC and ECDIS being civil sea surface navigation and therefore ENCs providing worldwide coverage, ECDIS with ENCs is the only GIS known to the author with worldwide coverage of up-to-date, quality controlled, object-oriented vector charts commercially accessible for a clearly defined purpose, and with public standards allowing production and update for data and hardware and software independently from each other.

Other chart product specifications than those for ENCs regularly applied to provide for worldwide chart coverage are either used with raster charts (such as ARCS), used with gridded data (such as DTED used to exchange elevation data), proprietary formats (such as Shape from ESRI), used for products largely accessible to the military only (such as DNC, MGCP and AML), used with largely outdated information (such as VMap), or used with crowd-sourced information which is not quality-controlled by an authority (OpenStreetMap, OpenSeaMap).

Consequently, official sea charts are also used for applications other than civil navigation – e.g. the military (Dugge 2016; Offenborn 2016). It is actually its unique combination of features which makes ENCs attractive for users other than navigation, too, but only, if the related standards are carefully

- obeyed when actually producing ENCs and developing and producing ECDIS and other GIS using ENCs,
- maintained to meet anticipations of users.

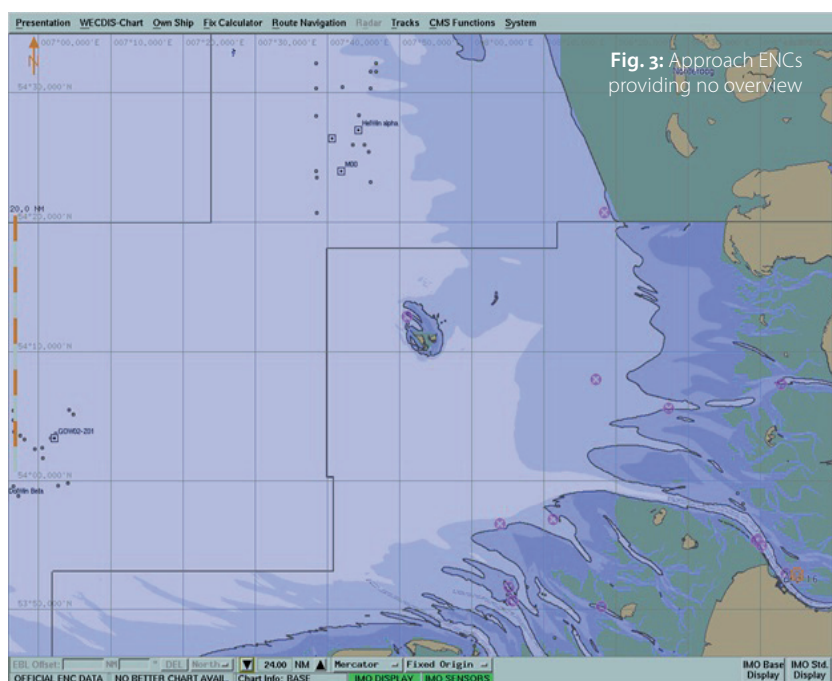
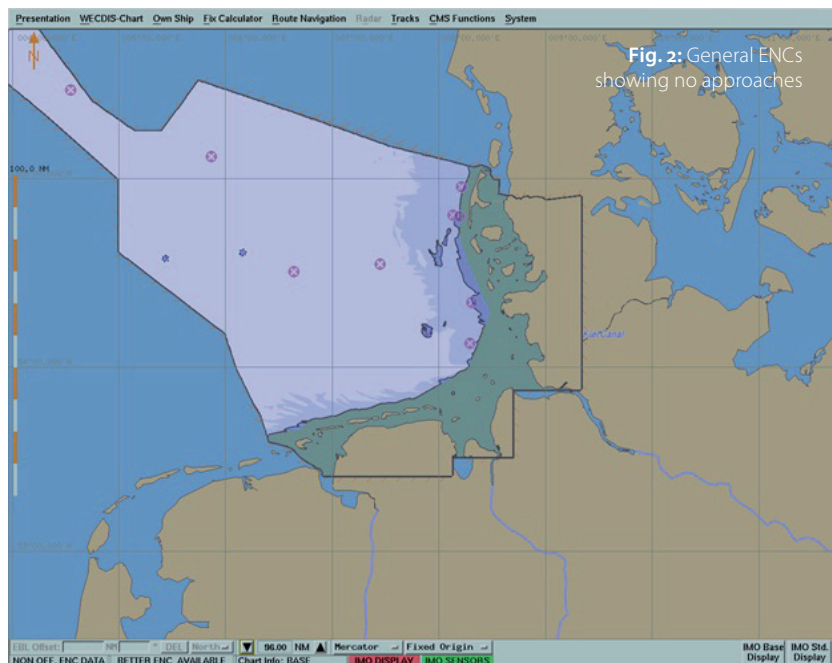
If this is not the case, the appearance of ENCs on an ECDIS or other GIS has the potential to deviate from the expectations of the user as being detailed with the following examples.

4 Medium scale bathymetry

Some hydrographic offices have decided to show bathymetry for some areas only on the more detailed charts – no medium scale bathymetry is provided for these areas.

As an example, this is shown with some electronic charts for the German Bight. The German Bight is a sea area situated north-west of Germany in the North Sea with a size of roughly 100 nm x 100 nm.

Fig. 2 shows the General ENC covering the German Exclusive Economic Zone on an ECDIS at a



display range of 96 nm (with the »display range« being the range from the centre of the display to its top). It can be clearly seen that the entire coastal waters are covered by a greenish area. Greenish stands for »intertidal areas«, sea areas that fall dry at low water.

In this chart no approaches leading to any harbour such as Hamburg or Bremen are indicated.

When using this chart on an ECDIS a Caution Area is shown warning the mariner to use a more detailed chart to navigate these areas.

When zooming in, charts carrying more detail – so-called »Coastal« ENCs – will appear. These, too, do not indicate any approaches to harbours.

Only when zooming in further, »Approach« ENCs showing major approaches eventually appear (Fig. 3).

However – as the sea area being displayed

Abbreviations

- ARCS – Admiralty Raster Chart Service
- AML – Additional Military Layers
- DNC – Digital Nautical Chart
- DTED – Digital Terrain Elevation Data
- IEC – International Electrotechnical Commission
- MGCP – Multinational Geospatial Coproduction Program
- SENC – System Electronic Navigational Chart
- VMap – Vector Map

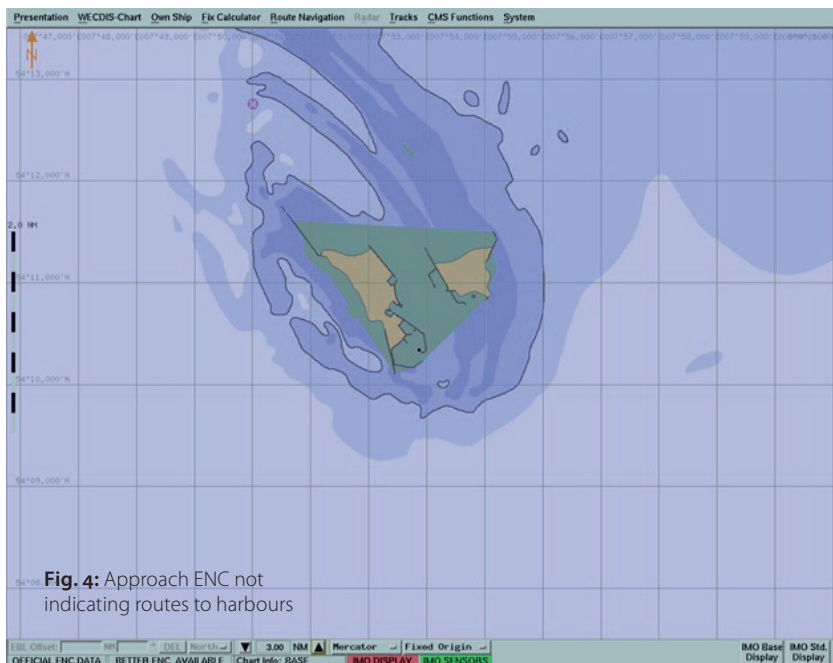


Fig. 4: Approach ENC not indicating routes to harbours

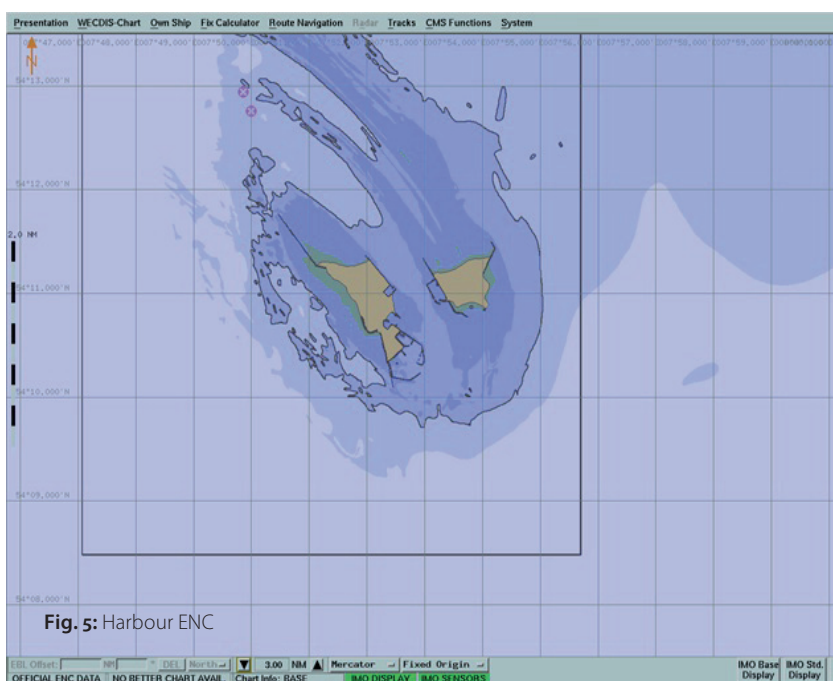


Fig. 5: Harbour ENC

References

Bill, Ralf; Dieter Fritsch (1994) : Grundlagen der Geo-Informationssysteme, Band 1; Wichmann, Heidelberg
 Dugge, Peter (2016): Kartographie für Marine-Führungssysteme; Hydrographische Nachrichten, HN 103, pp. 6–10
 Hecht, Horst; Bernhard Berking; Gert Büttgenbach; Mathias Jonas; Lee Alexander (2006): The Electronic Chart – Functions, Potential and Limitations of a New Marine Navigation System; GiTC, Lemmer
 IEC (2015): IEC 61174, Maritime navigation and radiocommunication equipment and systems – Electronic chart display and information system (ECDIS) - Operational and performance requirements, methods of testing and required test results; IEC, Geneva ...

shrinks – the overview gets lost. It does not become clear immediately which of the approaches shown must be taken to travel from one particular harbour to another one.

Zooming in further shows – e.g. at Heligoland (Fig. 4) – that even now no indications are given with the Approach ENC on how to reach a harbour, as the area of Heligoland is covered by an artificial »cartographic« intertidal area not representing the actual feature.

Only when switching to the harbour chart (which is the most detailed chart for this area), this oversized intertidal area is resolved and the mariner can see from which direction the harbour entrance can be approached (Fig. 5).

With these effects of showing no bathymetry at medium-scale displays in some areas the question arises:

What does this method of using »cartographic« intertidal areas mean to the mariner using ECDIS and to other users of ENCs?

Based on a background of uses of ENCs in ECDIS and other GIS the following can be stated:

- The overview gets lost with showing no indications of approaches on charts covering large areas.
- When executing route checks on an ECDIS, many ECDIS will individually check all charts available from coastal usage to the most detailed usage and will provide all alarms to the user. This means that all route checks in these navigable waters covered with »cartographic« intertidal areas will result in a false check results.
- For many other uses of ENCs the last decimetre of depth is not relevant. This applies e.g. to sonar propagation predictions, tactical SAR planning or simulation of currents. Hence, medium-scale charts are used. However, if these are wrong by many metres and virtually close existing waterways, they cannot be used for such applications.

To summarise it can be concluded: The geographic information provided for and loaded into a GIS should not be distorted due to mere cartographic reasons.

5 Vanishing details when zooming in

When zooming in it is the user's expectation that more details appear in the chart window than was visible before.

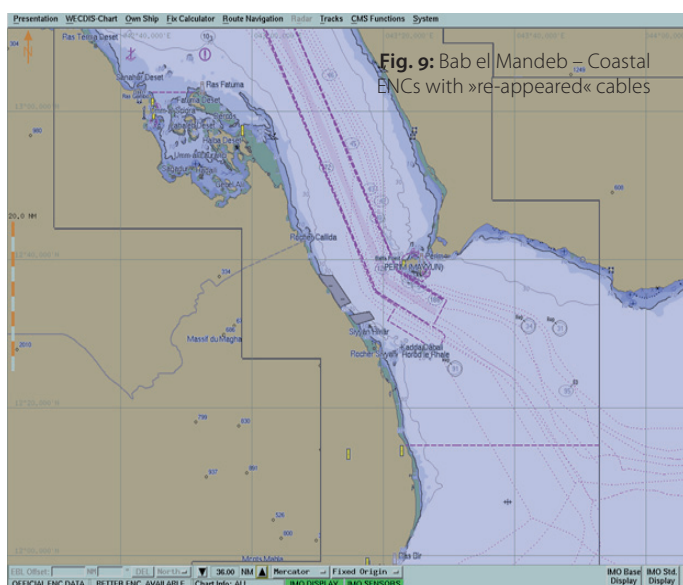
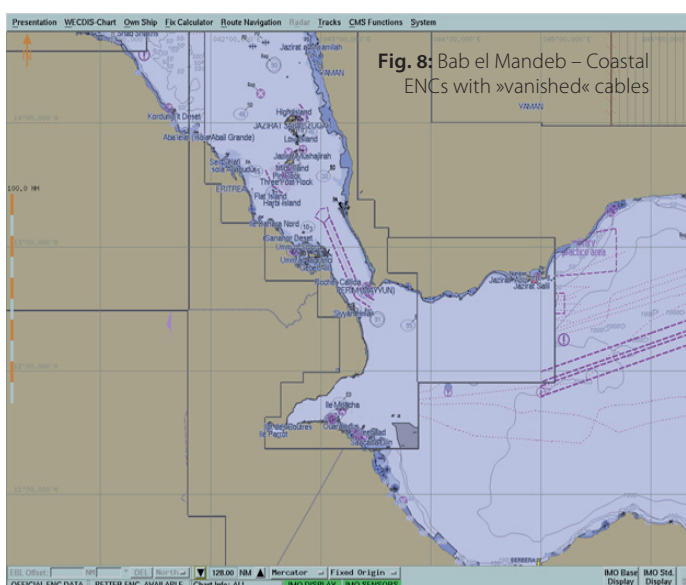
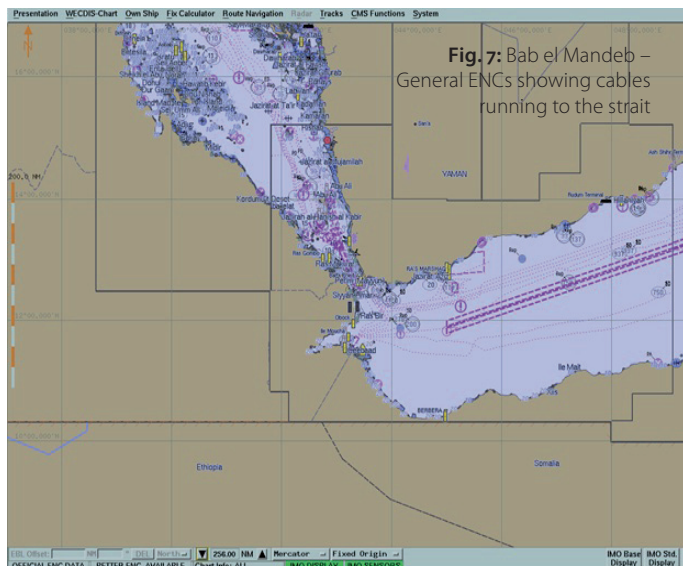
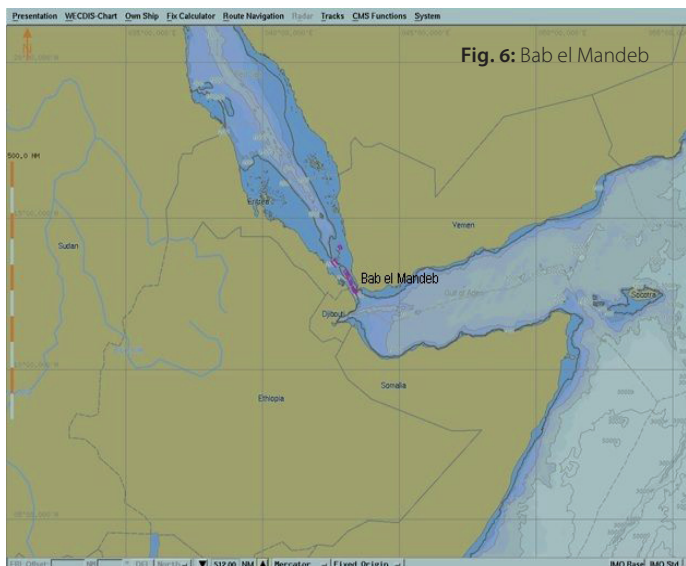
However, in many areas the charts provided are designed in such a way that details vanish when zooming in on an ECDIS.

As an example, charts for the sea area of Bab el Mandeb are chosen (Fig. 6). Bab el Mandeb is a busy Sea Line of Communication situated between Djibouti and Yemen forming the southern entrance of the Red Sea. ENCs for this area is issued by the hydrographic offices of the UK and France.

Fig. 7 shows a chart picture with no surprises which is generated by the ECDIS at a display range of 256 nm. It is somewhat cluttered, but a good overview is given showing e.g. cables running to and from Bab el Mandeb. General ENCs are used for this image.

When zooming in to a range of 128 nm, Coastal ENCs (bordered by grey solid lines) are drawn on top of the General ENCs (Fig. 8). However, rather than showing more details, fewer details are shown: where the Coastal ENCs are drawn, no cables can be seen anymore – they are visible only in the area which is not covered by the Coastal ENCs.

Route planning along a cable becomes virtually impossible at this scale. Only when zooming in to a range of 36 nm the cables are shown again (Fig. 9).



However, only a small area is shown now – an overview of where the cables come from and run to is not provided at this display scale.

The same effect can be observed when zooming in further: Approach ENCs appear and the cables vanish in the areas of the Approach charts which are expected to show more details than the Coastal charts.

And – once again – only when zooming in further do the cables »re-appear«.

For many users the examples with the »vanishing« cables shown here may not be of great relevance. But the same effect has been observed with other objects such as anchorage areas. Their picture, too, vanishes in parts when zooming in in some areas and only re-appears when zooming in further – hence not given an overview of the complete set of anchorage areas.

To summarise what it means when details vanish when zooming in:

- The anticipations of the user are not met – hence he or she gets lost.
- No tactical – in other words medium-scale – planning is possible.

As a conclusion it is preferred to have no vanishing details when zooming in using ENCs.

6 Recommendations

ENC and ECDIS together form a real-time GIS based on a common set of carefully adjusted and maintained rules.

The following is recommended to be considered when producing ENCs in order to increase acceptance by meeting anticipations of users of ECDIS and to promote usages of ENC other than navigation:

- No distortion of geographic information to achieve cartographic effects;
- No vanishing details when zooming in.

It is hoped that these recommendations contribute to the harmonisation efforts of the maritime community to lessen the gaps between the worlds of ENC and ECDIS. Furthermore, this explanation aims at contributing to the usability of ENCs not only with ECDIS but also in other environments such as tactical displays, hence contributing to a common maritime picture of various stakeholders creating commercial benefits for the production of ENCs. ⚓

IHO (2000): IHO Transfer Standard for Digital Hydrographic Data; Special Publication No. 57, IHB, Monaco
 IHO (2002): IHO Transfer Standard for Digital Hydrographic Data, S-57 Maintenance Document, Number 8; IHB, Monaco
 IHO (2014): IHO Transfer Standard for Digital Hydrographic Data, Supplementary Information for the Encoding of S-57 Edition 3.1 ENC Data (S-57 Supplement No. 3); IHB, Monaco
 IHO (2016): IHO S-57 Edition 3.1 Encoding Bulletins; www.iho.int/mtg_docs/enc/enc_prod/S-57EncodingBulletins.htm, last accessed on 19 August 2016
 IMO (1995): IMO Performance Standards for Electronic Chart Display and Information Systems (ECDIS), Resolution A.817(19); IMO, London
 Offenborn, Walter (2016): »Die Hydrographie leistet viel für die Marine« – Interview; Hydrographische Nachrichten, HN 103, pp. 30–37

Improved positioning of surveying vessels on inland waterways with HydrOs

An article by THOMAS ARTZ, ANNETTE SCHEIDER, MARC BREITENFELD, THOMAS BRÜGGEMANN, VOLKER SCHWIEGER and HARRY WIRTH

Surveying vessels are equipped with GNSS receivers or GNSS-INS coupled systems respectively to determine their position. By receiving and processing a correction signal, which is provided by a network of continuously operating reference stations, they determine a precise GNSS real-time kinematic (GNSS-RTK) solution. Thereby, the multibeam echo sounder observations can be georeferenced in order to produce a map of the channel bottom. One crucial point of the entire workflow is the quality of the vessel position which is highly influenced by the surrounding topography. For instance, bridges or buildings can cause multipath effects, refraction or a complete loss of signal reception. Often, even the correction signals cannot be received. Then, no RTK solution can be determined. To mitigate such gaps in the GNSS-RTK trajectory, an adjustable multi-sensor system called Integrated Hydrographic Positioning System (HydrOs) was developed as a joint project of the German Federal Institute of Hydrology (Bundesanstalt für Gewässerkunde) and the Institute of Engineering Geodesy at the University of Stuttgart.

Authors

Dr. Thomas Artz is Head of the team for Hydrographic Surveying at the German Federal Institute of Hydrology (BfG).

Annette Scheider is Research Associate at the Institute of Engineering Geodesy, University of Stuttgart.

Marc Breitenfeld is Trainee for Public Service in the field of Cadastral Surveying and Mapping Authorities in Germany.

Thomas Brüggemann works in the team for Hydrographic Surveying at the German Federal Institute of Hydrology (BfG).

Prof. Dr. Volker Schwieger is Professor and Head of the Institute of Engineering Geodesy, University of Stuttgart.

Prof. Harry Wirth is Professor at the Institute of Metrology and Analysis Technique, Jade University of Applied Sciences in Oldenburg.

artz@bafg.de

GNSS | positioning | Extended Kalman Filter | hydrographic multi-sensor system | outlier testing

1 Introduction

In Germany, the Federal Waterways and Shipping Administration (Wasserstraßen- und Schifffahrtsverwaltung, WSV) has to guarantee certain water depths in waterways to ensure a smooth flow of the inland shipping and its security, i.e. basically, to allow mariners to calculate the optimal load in shallow waters. As a river's channel bottom is subject to fluctuations on time scales from days to years, the waterways have to be permanently monitored. For this purpose, echo sounding measurements are regularly performed under the patronage of the WSV. These measurements have to be georeferenced, in order to create a map or a digital terrain model of the channel. For this purpose, the absolute position of the vessel has to be known with an accuracy of at least 1 dm for the height component and 3 dm for the horizontal position, respectively.

The primary technique to determine the vessel's position at the epoch of the echo sounding measurements, and thus, to achieve the georeferencing, is the Global Navigation Satellite System (GNSS). Typically, GNSS receivers are augmented with an Inertial Measurement Unit (IMU) and a heading system to measure the orientation of the vessel in a terrestrial reference frame simultaneously. In this process, a precise Real Time Kinematic GNSS solution (GNSS-RTK) is achieved by receiving and processing a correction signal being provided by a network of continuously operating reference stations and resolving the ambiguities on-the-fly. Within the WSV, the German SAPOS Highly Precise Real-time Positioning Service (HEPS) is used. According to the SAPOS documentation (GeoBasis-DE 2015), the accuracy of this service is below 2 cm for the horizontal and 3 cm for the vertical component. Unfortunately, the solution might be significantly deteriorated

from (partial) shading due to the surrounding topography, e.g., hills, buildings, trees, or bridges. Multipath effects and loss of the correction data reception could also lead to further degradations, and, in the worst case, to a complete loss of the precise differential GNSS solution. For the purpose of monitoring inland waterways ensuring the safety of shipping traffic, this is a serious problem. Thus, the need for a more precise and most importantly more reliable positioning is obvious.

To improve the situation, i.e., to mitigate gaps in the GNSS-RTK trajectory, the Integrated Hydrographic Positioning System (HydrOs) was developed as a joint project of the department for Geodesy of the German Federal Institute of Hydrology (Bundesanstalt für Gewässerkunde, BfG) and the Institute of Engineering Geodesy (IIGS, University of Stuttgart) (Breitenfeld et al. 2014; 2015; Scheider et al. 2016). HydrOs is an integrated multi-sensor system using the entire available hardware equipment on board to determine a more reliable and robust position of the vessel. HydrOs also contains advanced models describing hydrological and vessel depending effects, e.g., a water flow model, and a squat model. For processing the measurements of the on-board sensors and the model data, an Extended Kalman Filter (EKF) (e.g., Gelb 1974) and complementary outlier tests were implemented.

2 System design

HydrOs is composed of several components, which are schematically shown in Fig. 1a. It shows the hardware components (solid boxes) which are installed on the vessel, and the models (dashed boxes). The basic core of HydrOs is the EKF with its integrity checks and outlier elimination capabilities. The output of HydrOs are coordinates, velocities and attitude information.

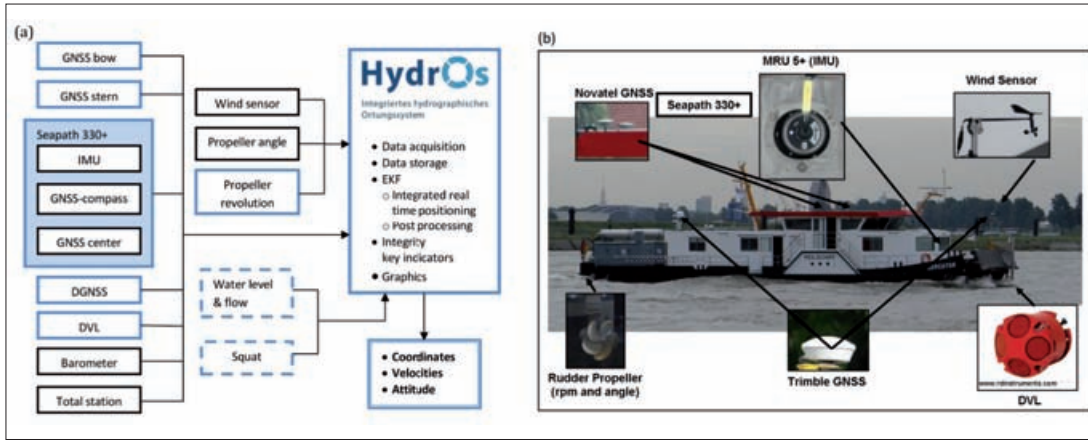


Fig. 1: (a) Sensor integration and data flow (according to Breitenfeld et al. 2014). The components which are currently adapted to the prototype are depicted in blue. The other components have just been tested. (b) Hardware components mounted to the WSV surveying vessel »Mercator« (Breitenfeld et al. 2014)

2.1 Input sensors and models

Various on-board components can be used to derive information on the motion of the vessel. For the HydrOs prototype on board of the surveying vessel »Mercator« (Fig. 1b), several GNSS receivers were used. In the test scenario, two geodetic two-frequency receivers were installed which are capable of determining a high accurate RTK solution by using SAPOS HEPS correction data. Furthermore, an integrated GNSS/INS unit (Seapath 330+) served as IMU and as GNSS compass and it also determined a RTK solution. To measure flow velocities, a Doppler Velocity Log (DVL) was appended to the measurement system. Finally, sensors were mounted to capture information about the turning rates and the direction of the two rudder propellers. However, different sensors like cameras or terrestrial laser scanners might be used in future as well. A time stamp (HydrOs reference time) is added to each incoming measurement message. The reference time is realised by synchronising the computer time with the GNSS time signal which can be extracted from the NMEA-ZDA strings according to the NMEA-0183 standard of the National Marine Electronics Association (NMEA 2016; DIN 2011). Further information on the hardware design is given by Scheider et al. (2014).

In addition to the hardware components, various models are used as input to the filtering process. The one-dimensional hydrodynamic model FLYS (FLYS 2016) is integrated to take water levels into account. Furthermore, a squat model has been derived empirically (Scheider et al. 2014) as state-of-the-art models (e.g., Briggs 2006) tend to assume too pessimistic values.

2.2 Trajectory estimation

Extended Kalman Filter

The Kalman Filter (Kalman 1960) is a linear recursive algorithm with state equations

$$x_{k+1} = T \cdot x_k + B \cdot u_k + C \cdot w_k \quad (1)$$

and measurement equations

$$l_{k+1} = A \cdot x_{k+1} + \varepsilon_{k+1} \quad (2)$$

Here, x_k represents the state vector, l_k is the measurement vector, u_k represents the system input

vector, w_k represents the process noise and ε_k the measurement noise respectively. The two noise terms are normally distributed $N(0, \Sigma_{ww})$. The matrices T , B and C describe the linear mapping of the individual variables to the following epoch. The matrix A describes the projection of the parameters into the observation space. If the prerequisites of linearity and Gaussian distribution are not fulfilled, the Kalman Filter is not the optimal estimator. To overcome the non-linearity, e.g., the Extended Kalman Filter makes use of non-linear equations ($f_{k+1,k}$, $t_{k+1,k}$, $b_{k+1,k}$, $c_{k+1,k}$ and a_{k+1}), leading to the non-linear state and measurement equations

$$x_{k+1} = f_{k+1,k}(t_{k+1,k}(x_k), b_{k+1,k}(u_k), c_{k+1,k}(w_k)) \quad (3)$$

$$l_{k+1} = a_{k+1}(x_{k+1}) + \varepsilon_{k+1} \quad (4)$$

However, the stochastic terms still have to be Gaussian. To expand the Kalman Filter to the EKF, a first-order linearisation has to be performed

$$T_{k+1,k} = \left. \frac{\partial f_{k+1,k}(t_{k+1,k}(x_k), b_{k+1,k}(u_k), c_{k+1,k}(w_k))}{\partial x_k} \right|_{x_k = \hat{x}_k} \quad (5)$$

$$B_{k+1,k} = \left. \frac{\partial f_{k+1,k}(t_{k+1,k}(x_k), b_{k+1,k}(u_k), c_{k+1,k}(w_k))}{\partial u_k} \right|_{u_k} \quad (6)$$

$$C_{k+1,k} = \left. \frac{\partial f_{k+1,k}(t_{k+1,k}(x_k), b_{k+1,k}(u_k), c_{k+1,k}(w_k))}{\partial w_k} \right|_{w_k} \quad (7)$$

$$A_{k+1} = \left. \frac{\partial a_{k+1}(x_{k+1})}{\partial x_{k+1}} \right|_{x_{k+1} = \bar{x}_{k+1}} \quad (8)$$

which leads to the linearised model

$$\bar{x}_{k+1} = T_{k+1,k} \cdot \hat{x}_k + B_{k+1,k} \cdot u_k + C_{k+1,k} \cdot w_k \quad (9)$$

$$l_{k+1} = A_{k+1} \cdot x_{k+1} + \varepsilon_{k+1} \quad (10)$$

Thus, the prediction can be calculated via the non-linear state equations

$$\bar{x}_{k+1} = f_{k+1,k}(t_{k+1,k}(\hat{x}_k), b_{k+1,k}(u_k), c_{k+1,k}(0)) \quad (11)$$

and its covariance matrix by error propagation of equation (9)

$$\Sigma_{\bar{x},k+1} = T_{k+1,k} \cdot \Sigma_{\hat{x},k} \cdot T_{k+1,k}^T + B_{k+1,k} \cdot \Sigma_{uu} \cdot B_{k+1,k}^T + C_{k+1,k} \cdot \Sigma_{ww} \cdot C_{k+1,k}^T \quad (12)$$

Subsequently, the so-called innovation and the corresponding covariance matrix

References

Breitenfeld, Marc; Harry Wirth; Annette Scheider, Volker Schwieger (2014): Development of a Multi-Sensor System to optimize the Positioning of Hydrographic Surveying Vessels; Proceedings on 4th International Conference on Machine Control & Guidance, 19–20 March 2014 in Braunschweig

Breitenfeld, Marc; Harry Wirth; Thomas Brüggemann; Annette Scheider; Volker Schwieger (2015): Entwicklung von Echtzeit- und Postprocessingverfahren zur Verbesserung der bisherigen Ortung mit Global Navigation Satellite Systems (GNSS) durch Kombination mit weiteren Sensoren sowie hydrologischen Daten; BfG-Bericht, Bundesanstalt für Gewässerkunde, <http://doi.bafg.de/BfG/2015/BfG-1856.pdf>

Briggs, Michael J. (2006): Ship Squat Predictions for Ship/Tow Simulator. Coastal and Hydraulics Engineering Technical Note CHETN-1-72; U.S. Army Engineer Research and Development Center, Vicksburg, MS

Caspary, Wilhelm; Jian-Guo Wang (1998): Redundanzanteile und Varianzkomponenten im Kalman Filter; Zeitschrift für Vermessungswesen, 123, pp. 121–128

DIN (2011): DIN 6162-1 – Navigations- und Funkkommunikationsgeräte und -systeme für die Seeschifffahrt – Digitale Schnittstellen – Teil 1: Ein Datensender und mehrere Datenempfänger; Beuth Verlag, Berlin

FLYS (2016): Flusshydrologischer Webdienst; www.bafg.de/DE/os_Wissen/01_InfoSys/flys/flys.html, last accessed on 5 July 2016

Gelb, Arthur (1974): Applied Optimal Estimation; The M.I.T. Press, Cambridge, Massachusetts

GeoBasis-DE (2015): SAPOS® Precise Positioning in Location and Height; www.sapos.de/files/SAPOS-Broschuere-2015-eng.pdf, last accessed on 5 July 2016

Kalman, Rudolph-Emil (1960): A New Approach to Linear Filtering and Prediction Problems; Transactions of the ASME-Journal of Basic Engineering, 82, pp. 35–45

Koch, Karl-Rudolf (2004): Parameterschätzung und Hypothesentests in linearen Modellen; Dümmeler Verlag, Bonn

Langeley, Richard B. (1999): Dilution of Precision; GPS world, 10(5), pp. 52–59

NMEA (2016): www.nmea.org/content/nmea_standards/nmea_0183_v_410.asp, last accessed on 5 July 2016

Pelzer, Hans Georg (1987): Deformationsuntersuchungen auf der Basis kinematischer Bewegungsmodelle; Allgemeine Vermessungs-Nachrichten, 94(2), pp. 49–62 ...

$$d_{k+1} = l_{k+1} - a_{k+1} \cdot \bar{x}_{k+1} \quad (13)$$

$$\Sigma_{dd,k+1} = A_{k+1} \cdot \Sigma_{\bar{x}\bar{x},k+1} \cdot A_{k+1}^T + \Sigma_{ll} \quad (14)$$

are calculated. Finally the update

$$\hat{x}_{k+1} = \bar{x}_{k+1} + K_{k+1} \cdot d_{k+1} \quad (15)$$

$$\Sigma_{\hat{x}\hat{x},k+1} = \Sigma_{\bar{x}\bar{x},k+1} - K_{k+1} \cdot \Sigma_{dd,k+1} \cdot K_{k+1}^T \quad (16)$$

is performed via the Kalman-Gain matrix

$$K_{k+1} = \Sigma_{\bar{x}\bar{x},k+1} \cdot A_{k+1}^T \cdot \Sigma_{dd,k+1}^{-1} \quad (17)$$

Determination of redundancy values

Within the EKF solution, there is a certain amount of redundancy due to components of the state vector, the system input, the process noise, and the observations. To derive the covariance matrix of the residuals and the redundancy values, Caspary and Wang (1998) introduced pseudo observations expanded by true deviations, e.g., $\epsilon_{\hat{x},k} = \hat{x}_k - x_k$

$$l_{x,k+1} = \hat{x}_k + \epsilon_{\hat{x},k} \quad \Sigma_{\hat{x}\hat{x},k} = \Sigma_{l_x l_x, k+1} \quad (18)$$

$$l_{u,k+1} = u_k + \epsilon_{u,k} \quad \Sigma_{uu} = \Sigma_{l_u l_u, k+1} \quad (19)$$

$$l_{w,k+1} = w_k + \epsilon_{w,k} = E(w_k) \quad \Sigma_{ww} = \Sigma_{l_w l_w, k+1} \quad (20)$$

$$l_{l,k+1} = l_{k+1} = A_{k+1} \cdot \bar{x}_{k+1} + \epsilon_{l,k+1} \quad \Sigma_{ll} = \Sigma_{l_l l_l, k+1} \quad (21)$$

Based on these pseudo observations, residuals and their covariance matrices can be deduced (Wang 2009)

$$\begin{bmatrix} \hat{v}_{x,k+1} \\ \hat{v}_{u,k+1} \\ \hat{v}_{w,k+1} \\ \hat{v}_{l,k+1} \end{bmatrix} = \begin{bmatrix} \Sigma_{\hat{x}\hat{x},k} \cdot T_{k+1,k}^T \cdot \Sigma_{\bar{x}\bar{x},k+1}^{-1} \cdot K \cdot d_{k+1} \\ \Sigma_{uu} \cdot B_{k+1,k}^T \cdot \Sigma_{\bar{x}\bar{x},k+1}^{-1} \cdot K \cdot d_{k+1} \\ \Sigma_{ww} \cdot C_{k+1,k}^T \cdot \Sigma_{\bar{x}\bar{x},k+1}^{-1} \cdot K \cdot d_{k+1} \\ -\Sigma_{ll} \cdot \Sigma_{dd,k+1}^{-1} \cdot d_{k+1} \end{bmatrix} \quad (22)$$

$$\begin{aligned} \Sigma_{\hat{x}\hat{x},k+1} &= \\ \Sigma_{\hat{x}\hat{x},k} \cdot T_{k+1,k}^T \cdot A_{k+1}^T \cdot \Sigma_{dd,k+1}^{-1} \cdot A_{k+1} \cdot T_{k+1,k} \cdot \Sigma_{\hat{x}\hat{x},k} & \quad (23) \end{aligned}$$

$$\begin{aligned} \Sigma_{uu} \cdot B_{k+1,k}^T \cdot A_{k+1}^T \cdot \Sigma_{dd,k+1}^{-1} \cdot A_{k+1} \cdot B_{k+1,k} \cdot \Sigma_{uu} & \quad (24) \end{aligned}$$

$$\begin{aligned} \Sigma_{ww} \cdot C_{k+1,k}^T \cdot A_{k+1}^T \cdot \Sigma_{dd,k+1}^{-1} \cdot A_{k+1} \cdot C_{k+1,k} \cdot \Sigma_{ww} & \quad (25) \end{aligned}$$

$$\Sigma_{\hat{v}\hat{v},k+1} = (I - A_{k+1} \cdot K) \cdot \Sigma_{ll} \quad (26)$$

which are necessary to derive the redundancy values (Wang 2009)

$$r_{x,k+1} = \text{diag}\{\Sigma_{\hat{x}\hat{x},k} \cdot T_{k+1,k}^T \cdot A_{k+1}^T \cdot \Sigma_{dd,k+1}^{-1} \cdot A_{k+1} \cdot T_{k+1,k}\} \quad (27)$$

$$r_{u,k+1} = \text{diag}\{\Sigma_{uu} \cdot B_{k+1,k}^T \cdot A_{k+1}^T \cdot \Sigma_{dd,k+1}^{-1} \cdot A_{k+1} \cdot B_{k+1,k}\} \quad (28)$$

$$r_{w,k+1} = \text{diag}\{\Sigma_{ww} \cdot C_{k+1,k}^T \cdot A_{k+1}^T \cdot \Sigma_{dd,k+1}^{-1} \cdot A_{k+1} \cdot C_{k+1,k}\} \quad (29)$$

$$r_{l,k+1} = \text{diag}\{I - A_{k+1} \cdot K\} \quad (30)$$

and finally, the whole redundancy of the solution by summing up the individual redundancy values. These values are used within HyDrOs to analyse the impact of any observation on the solution and to investigate its controllability.

Outlier elimination

The EKF solution can be erroneous, due to outliers or errors in the functional or stochastic modelling,

which is expressed in discrepancies between the predicted state \bar{x}_{k+1} and new observations l_{k+1} . To detect such discrepancies, the empirical variance factor

$$s_{0,j...l}^2 = \frac{\sum_{i=j}^l d_{k-i}^T \cdot \Sigma_{dd,k-i}^{-1} \cdot d_{k-i}}{\sum_{i=j}^l r_{k-i}} \quad (31)$$

is tested. It should be noted, that a local variance factor for the k th epoch is derived with $j = l = 0$. Using $l = k - 1$ leads to a global variance factor for all epochs until the most recent one, while $j < k$ yields a regional variance for $l - j + 1$ epochs. Thus, the null and alternative hypothesis read

$$H_0: E\{s_{0,k}^2\} = E\{s_{0,j...l}^2\} \quad (32)$$

$$H_A: E\{s_{0,k}^2\} \neq E\{s_{0,j...l}^2\}$$

i.e., does the local variance differ significantly from the global or regional one. Thus, the test statistics are (Pelzer 1987)

$$T = \frac{s_{0,k}^2}{s_{0,j...l}^2} = \frac{d_k^T \cdot \Sigma_{dd,k}^{-1} \cdot d_k}{r_k \cdot s_{0,j...l}^2} \sim F_{r_k, f, 1-\alpha} \quad (33)$$

f : degree of freedom in $s_{0,j...l}^2$

$r_k = n_{l_{k+1}}$: degree of freedom in $s_{0,k}^2$

$F_{r_k, f, 1-\alpha}$: quantile of Fisher distribution with level of significance α

A hypothesis test is performed to detect an outlier in observation i within an observation group g by using following null and alternative hypothesis (Koch 2004, p. 329)

$$H_0: v_{g,i,k} = 0 \quad (34)$$

$$H_A: v_{g,i,k} \neq 0$$

and the corresponding test statistics for a standardised residual i is

$$T = \frac{v_{g,i,k}}{\sigma_{v_{g,i,k}}} \sim N(\alpha_0, 0, 1) \quad (35)$$

α_0 : level of significance for a single observation given the entire level of significance α
 $N(\alpha_0, 0, 1)$: quantile of normal distribution

As one outlier is searched for in n observations, the level of significance has to be adapted

$$\alpha_0 \approx 1 - (1 - \alpha)^{1/n} \approx \frac{\alpha}{n \cdot (n_{\hat{x}_k} + n_{u_k} + n_{w_k} + n_{l_k})} \quad (36)$$

Finally, the null hypothesis is accepted if $-N(1 - \frac{\alpha_0}{2}, 0, 1) \leq T \leq N(1 - \frac{\alpha_0}{2}, 0, 1)$ or

$$|T| \leq N(1 - \frac{\alpha_0}{2}, 0, 1)$$

is fulfilled. As the standardised residuals can be calculated for all four groups of pseudo-observations, outliers can be detected in \hat{x}_k , u_k , w_k and l_{k+1} . The corresponding test statistics for the real observations are, e.g.,

$$\begin{aligned} T_{l_i,k+1} &= \frac{\hat{v}_{l_i,k+1}}{\sigma_{\hat{v}_{l_i,k+1}}} \\ &= \frac{e_i^T \cdot \Sigma_{ll} \cdot \Sigma_{dd,k}^{-1} \cdot d_k}{\sigma_0 \cdot \sqrt{e_i^T \cdot \Sigma_{ll} \cdot \Sigma_{dd,k}^{-1} \cdot \Sigma_{ll} \cdot e_i}} \end{aligned}$$

$$= \frac{e_i^T \cdot \Sigma_{dd,k}^{-1} \cdot d_k}{\sigma_0 \cdot \sqrt{e_i^T \cdot \Sigma_{dd,k}^{-1} \cdot e_i}} \quad (38)$$

with $i = \{1, 2, \dots, n_{l_i}\}$ (Wang 2008). Similarly, the test statistics can be derived for the other groups of pseudo observations (Breitenfeld et al. 2015). The test is performed iteratively starting with the largest standardised residual. If an outlier is detected for a (pseudo) observation, the respective observation is down-weighted, the affected matrices are recalculated and the next largest observation is tested until the null hypothesis is accepted.

Alternatively, the hypothesis test in HydrOs can be performed with studentised residuals. For this purpose, σ_0 is replaced with the empirical variance $s_{0,k}^2$ of the k th epoch. Thus, quantiles of the tau-distribution have to be used (Koch 2004, p. 332).

3 Results of the field tests

To evaluate the capability of the HydrOs system on the surveying vessel »Mercator«, several test runs were performed on the River Rhine and the channel to the port of Duisburg (Hafenkanal). The test area and the corresponding trajectories are depicted in Fig. 2. Four surveys have been performed: (1) without any shading (red), (2) with one bridge (yellow), (3) with one bridge and low vessel dynamics (green), and (4) only on parts of the red trajectory with high dynamics. Although these four surveys took place, only the results from the trajectory in the channel (green) are presented here. Furthermore, GNSS gaps have been simulated by cutting out two pieces of 62 s and 100 s, respectively. In contrast to the evaluation of real gaps, this procedure enables a comparison to the original results.

3.1 Reliability and controllability

The HydrOs solution incorporates several almost redundant measurements leading to a huge controllability of the observations. This can, e.g., be demonstrated by the redundancy values (Fig. 3) which are derived from the covariance matrix of the residuals. These numbers indicate whether a gross error shows up in the residuals of its corresponding observation or if it influences all other residuals, which can occur for small redundancy values. Thus, the redundancy values should be larger than 0.5 for a good controllability. As it can be seen in Fig. 3, the GNSS measurements are highly redundant with partial redundancies above 0.9. Therefore, filtering out individual GNSS observations does not destabilise the solution. The only observation type which is prone to undetected gross errors is the roll velocity (ω_x).

Due to the large redundancy, outliers can be easily detected. Here, a level of significance of 95 % is used as bigger problems might arise due to accepting a false null hypothesis, i.e., non-detection of outliers. Fig. 4 shows speed over ground measurements of a GNSS receiver prior to a GNSS gap. Obviously, the scatter of the time series increases

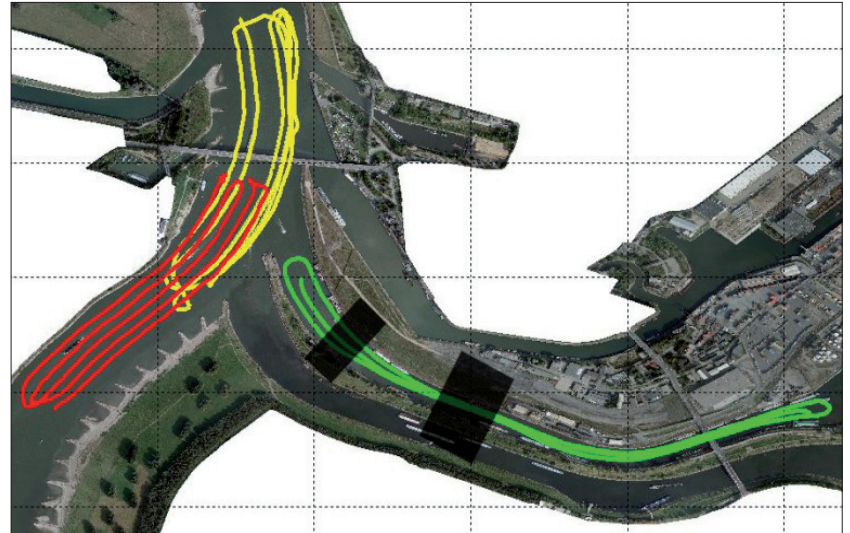


Fig. 2: Area of the test surveys with three different trajectories; the black boxes denote parts of the GNSS trajectories which have been removed to simulate large GNSS gaps (according to Wirth et al. 2015)

before the gap and observations outside the assumed noise floor are detected as outliers. Thus, the estimation is not affected by the outliers due to the huge redundancy. As in such cases, the information for the positioning is taken from other measurements.

In addition to the outlier tests within the parameter estimation, some observations can also be filtered out beforehand due to unmatched quality criteria. This has been done for the GNSS measurements, where the quality indicator (QI), number of observed satellites, and horizontal dilution of precision (HDOP) have been used. These criteria are reported by GNSS receivers. QI is a classification of the GNSS solution and easily allows excluding

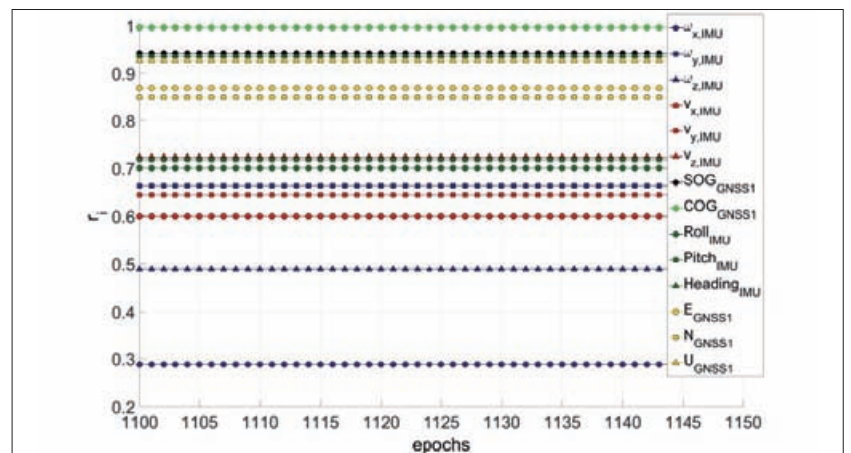


Fig. 3: Redundancy values for a subset of the different sensors, e.g., only one GNSS receiver is shown as it is representative for all of them

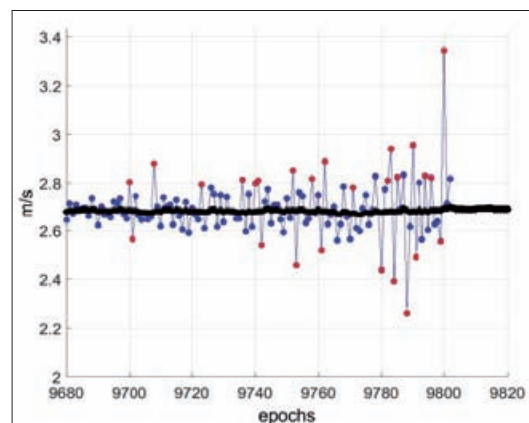


Fig. 4: Speed over ground measurements from a single GNSS receiver (blue) with marked outliers (red dots) and estimated speed over ground from the EKF solution (black)

GNSS 1	Survey 1		Survey 2		Survey 3		Survey 4	
	shading	others	shading	others	shading	others	shading	others
0–1.0 s	–	3	0	4	0	2	–	1
1.0–10.0 s	–	2	0	9	0	2	–	2
10.0 – 30.0 s	–	0	10	0	4	1	–	0
30.0–60.0 s	–	0	1	2	0	0	–	2
> 1 min	–	0	0	4	0	2	–	1
sum	–	5	11	19	4	7	–	6

positions without fixed ambiguities. DOP values permit an assumption of the quality of a GNSS solution (Langeley 1999). Applying these criteria reveals that even in unshaded areas on average 5 % to 8 % of the GNSS positions are not usable or even not recorded. A significant amount of these gaps last longer than 10 s, the absolute occurrences of gaps for one of the GNSS receiver during the four surveys are listed in the table. By utilising HydrOs, accurate positions can be determined in these regions.

3.2 Filter results

For an initial solution, the observations of one GNSS receiver and the IMU have been used. Fig. 3 shows the estimated height trajectories for this example. The EKF is not able to rectify these simulated gaps by only integrating a minimal sensor configuration, so, the trajectory is drifting away. However, the situation can be improved by adding rudder propeller revolutions as well as water-level and squat models (see Fig. 5). An assimilation of these models eliminates the drift of the EKF solution. When these EKF results are compared to the original values (without simulating the gaps), maximum deviations of about 5 cm are revealed (not shown here).

These examples demonstrate clearly the gain of using HydrOs for hydrographic surveys. Due to consistently combining the available sensors in the EKF process, a high redundancy can be achieved. Hence, outliers can be easily detected and the elimination does not harm. This way, the robustness of the solution is significantly improved. Furthermore, it has been proven that GNSS gaps of up to 60 s can be bypassed by including models into

the filtering process. The same could be achieved by implementing a backward smoother (Wirth et al. 2015).

4 Conclusions

One major issue of hydrographic measurements under the patronage of the WSV is the accuracy and reliability of the vessel's position and orientation, i.e., the GNSS-RTK solution. Within the project HydrOs, a multi-sensor system was developed which uses several on-board measurement systems (GNSS receivers and GNSS/INS system) to increase the robustness of the trajectory. In addition, hydrodynamic models and further information, i.e., a squat and a water-level model, were combined with the real measurements by means of an EKF. Especially the use of the water level model provides a reliable height solution during GNSS gaps. Furthermore, a DVL was mounted to the vessel, and the revolutions of the rudder propeller were successfully integrated.

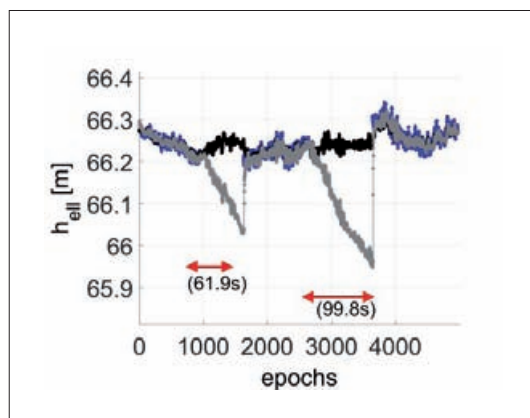
Within the investigation, a thorough statistical analysis of the measurements is performed. As a result, it was shown that the failure rate of GNSS-RTK measurements is at the level of up to 8 %, and thus, significantly higher than expected. As a consequence, the loss of the correction signal for the RTK solution does not only lead to gaps in the trajectory, but also to position errors, which have only been determined in the past if they reached a level of several decimetres. In contrast, these discrepancies are now directly detected if HydrOs is used.

Due to the status of the project, no assessment of the net process time can be made. However, it has been demonstrated that manual corrections of the position estimates are needless when using HydrOs especially by implementing outlier detections and eliminations during the filtering process. As all the entire on-board information is used, e.g., with redundant GNSS receivers, almost all observations are well controlled which has been shown by analysing the redundancy values. The only type of measurement which is prone to undetected outliers is the angular IMU roll velocity.

Furthermore, HydrOs is providing integrity information to the users, leading to a more robust product. This is a fundamental component for warranting traffic security by WSV. [↕](#)

...
 Scheider, Annette; Harry Wirth; Marc Breitenfeld; Volker Schwieger (2014): HydrOs – An Integrated Hydrographic Positioning System for Surveying Vessels; FIG Congress 2014, 16–21 June 2014, Kuala Lumpur, Malaysia
 Scheider, Annette; Aiham Hassan; Volker Schwieger; Marc Breitenfeld; Thomas Brüggemann (2016): Erweiterte Echtzeit- und Postprocessing-Verfahren zur Optimierung der GNSS-Ortung in Abschattungsbereichen an BWaStr; BfG-Bericht, Bundesanstalt für Gewässerkunde, <http://doi.bafg.de/BfG/2016/BfG-1892.pdf>
 Wang, Jian-Guo (2008): Test Statistics in Kalman Filtering; Journal of Global Positioning Systems, 7(1), pp. 81–90
 Wang, Jian-Guo (2009): Reliability Analysis in Kalman filtering; Journal of Global Positioning Systems, 8(1), pp. 101–111
 Wirth, Harry; Marc Breitenfeld; Annette Scheider; Volker Schwieger (2015): HydrOs – Ein integriertes Ortungssystem kombiniert mit hydrologischen Daten; Hydrographische Nachrichten, HN 101, pp. 6–12

Fig. 5: Height component from GNSS-only (blue), EKF with GNSS and IMU input (grey) and EKF with GNSS, IMU and model input (black). Simulated GNSS gaps are indicated by red lines

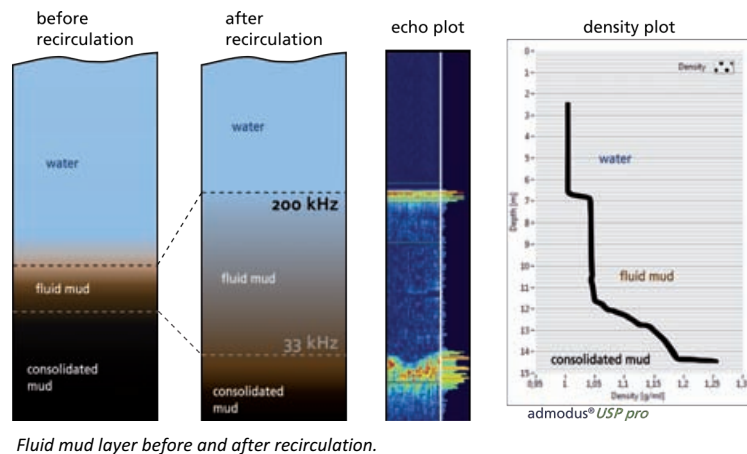
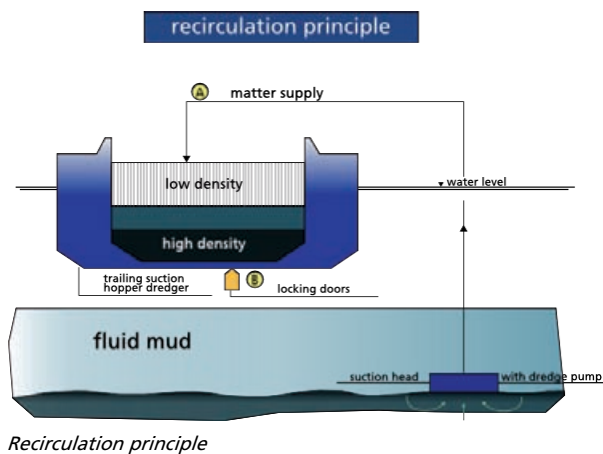


DENSITY matters...

Port of Emden, Germany
reducing dredging costs by 90%

In many of the world's largest harbours, appropriate hydrographic survey is a necessary requirement in order to keep dredging costs low. The port of Emden succeeded in reducing the dredging costs by 90% with the help of a new dredging management and hydrographic survey using the density probe admodus® *USP pro*.

In 1994, after many years of research, the port authority managed to maintain the fluidity of suspended sediments, which were carried into the harbour basin by the river Ems. This so called "sediment conditioning" is mainly based on the prevention of the fluid mud's reconsolidation process by a regular treatment (recirculation). As a result, these sediments no longer have to be removed from the harbour basin and a lot of disposal costs can be saved.



The challenge:

How to monitor the density of this 'fluid mud' or measure the nautical depth in the harbour basin in a fast and reliable way, in order to guarantee navigability?

After 10 years of experience and development, admodus® MARITIME DEVICES released the new admodus® *USP pro* in 2013, with improved precision, ruggedness, better software and easier handling like the one-man-automatic-mode. The port of Emden was the first customer who purchased and still uses this device with great success.



Conclusion

A lot of maintenance costs can be saved by an intelligent dredging management. Investigations in recent years have shown, that ships can navigate safely through fluid mud layers up to a density of 1.15kg/dm³ at the port of Emden. This 1.15kg/dm³ horizon is often much deeper than the 200kHz horizon of an echo sounder. Thus, there is 'more water' under the keel with less dredging.

Offshore unexploded ordnance recovery and disposal

An article by JAN KÖLBEL and DAVID ROSE

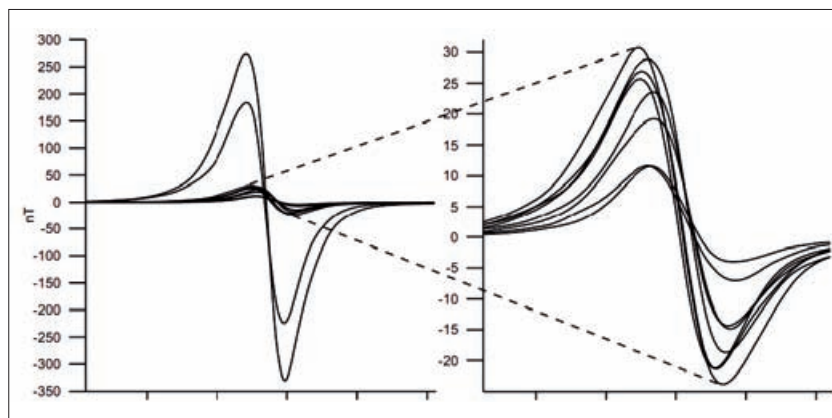
Millions of tons of unexploded ordnance (UXO) and discarded explosive remnants from war can be found in European waters and beyond. Many of them are next to the shoreline, dispensing toxics to the environment. Dumping of ammunition, military practice and warfare are the main source for this large amount posing a risk for the offshore industry besides the undeniable impact this also causes to the environment. With increasing utilisation of offshore areas, the activities in offshore UXO clearance have increased. Due to the governmental commitment and planning of increased usage of offshore wind energy in Germany, research has been conducted to solve the technical question of unexploded ordnance recovery and disposal. Within the last five years, the market for offshore UXO detection and removal has multiplied as well as experience increased, research has also led to better analytical results during the UXO survey campaign which has helped achieve fewer false alarms. Better techniques and the development of specialist equipment for the removal results in smaller time frames in which the clearance can be done as well as lower risk for equipment and personnel. Research is also being conducted on how to handle ammunition safely which is classified as not safe to transport without the normal demolition procedure.

Authors

David Rose and Jan Kölbl
work for Boskalis Hirdes EOD
Services in Hamburg.

david.rose@boskalis.com
jan.koelbel@boskalis.com

Fig. 1: Results for measuring ten identical 2 cm projectiles



© Winkelmann and Fischer 2009

UXO | unexploded ordnance | investigation | metal detector | recovery | disposal | underwater positioning

1 Introduction

Boskalis Hirdes is currently removing UXO on several offshore projects in Germany. Also a growing amount of new UXO removal projects is expected to be related to the increasing industrial and touristic use of coastal offshore areas. Besides UXO at offshore locations, dumped World War II munitions all over the world and in particular within German waters will become a greater concern. The high density of these World War II dump locations, large amounts of contaminated material, the deteriorating condition and close vicinity to ports and places of interest in German waters make these locations the most feasible for munition dumpsite cleaning programs.

2 Technique

A complete UXO removal campaign consists mainly of three different stages.

The first stage is a desk study, the UXO survey campaign, which results in the generating of a list of possible UXO targets. Different survey techniques with varying capabilities are used to obtain

a target list which covers the possible UXO types relevant to that specific area as identified in the desktop study.

In the second stage, the recovery and identification of the potential hazard will take place. Therefore, a precise relocation of the anomalies is necessary. After positive identification, the Explosive Ordnance Disposal Technical Advisor (EOD TA) classifies whether the UXO is safe for transport or not.

In the third stage, depending on type and condition of the UXO, the safe disposal either in situ or by recovery to shore is conducted.

2.1 Survey

Magnetometer survey

Fig. 1 shows some results from a trial carried out by Dr. Kay Winkelmann, formally of Sensys GmbH using ten identical 2 cm projectiles (Winkelmann and Fischer 2009). The results clearly show the magnetic response from each item, even though identical are different for each one. There are many factors which influence the permanent and induced magnetic fields on an object, and therefore trying to reproduce the size and shape of a UXO using modern materials cannot replicate the magnetic signature of UXO.

This results in a very careful processing of magnetic data and indicates also the unnecessary for testing with surrogate items. Nevertheless, the magnetometer survey in combination with a multibeam and side-scan sonar is very popular. Surfaced objects can be found by the high-resolution side-scan sonar and verified by the magnetic response.

However, experience has shown that especially in sandy and muddy maritime environments, the

majority of objects are not found on the seabed surface. Almost 90% of these objects are completely buried. In areas with a minor tidal influence these objects are buried no deeper than 1.5 m below the surface. Nevertheless, a careful survey design with sufficient line spacing as well as the magnetometer altitude is a key element. The table shows the expected minimum anomaly amplitudes for certain ferrous UXO.

This means that a 155 mm shell with up to 20 kg of explosives, can only be found in one metre depth with considerable luck or with a very precise survey design. As shown in Fig. 2, the setup would be difficult to achieve. Under consideration of the table, the maximum height would be around 2 m and the line spacing should not exceed 3 m using a TVG with 1.5 m separation.

Metal detector survey

A metal detector uses pulse induction to generate a secondary field in conductive materials. Such systems are usually mounted on work class ROVs and the survey is conducted very close to the ground since the detection depth range is considerably less than the one from magnetometers. This type is usually only used to relocate magnetic targets, however, it is also the only commercial type of detector currently available in the case of non-ferrous targets like German aluminium naval mines, or very cluttered areas.

Advanced metal detector

The Advanced Boskalis Metal Detector (ABMD) system is a new and specific kind of metal detector, using as other metal detectors the transient electromagnetics or time domain electromagnetics to generate magnetic fields in the three spatial directions. Measuring the decay of these fields also in all spatial directions allows deduction of the geometry and thus a much more efficient discrimination between clutter and UXO (Fig. 3).

The ABMD system is able to make continuous measurements and can be towed next to the seabed like a conventional magnetometer array. Furthermore, exact mapping of the conductive background, the ability to work in cluttered areas and the ability for depth of burial surveys makes the ABMD system a much more advanced tool which far exceeds the current technical standards.

Acoustic survey

The broad range of possible acoustic surveys depends on application. Side-scan sonar and multi-beam echo sounder are usually applied as auxiliary sensors on each magnetometer survey.

However, these systems are unable to detect or map buried objects. Other types of bottom penetrating acoustic systems operating at low frequencies suffer from limited resolution and have a very limited capability to distinguish between buried UXO and false alarms.

Magnetometer Altitude above Object [m]	Total Field Amplitude Observed for Object Oriented S-N with only Induced Magnetization					
	Shell 105mm	Shell 155mm	Bomb 100lbs	Bomb 250lbs	Bomb 500lbs	G.Mine MKIV
2	11 nT	41 nT	75 nT	160 nT	300 nT	1,350 nT
3	3 nT	12 nT	23 nT	49 nT	91 nT	485 nT
4	<2 nT	5 nT	10 nT	21 nT	40 nT	223 nT
5	<1 nT	2.5 nT	5 nT	10.5 nT	20 nT	120 nT
6	<0.5 nT	<2 nT	3 nT	6 nT	12 nT	70 nT
8	<<0.5 nT	<1 nT	1 nT	2.5 nT	5 nT	30 nT
10	<0.1 nT	<0.5 nT	0.5 nT	1 nT	2.5 nT	16 nT
	Clearly detectable and distinguishable from geogenous objects					
	Still detectable but not distinguishable from geogenous objects					
	Undetectable even in good offshore magnetometer surveys					

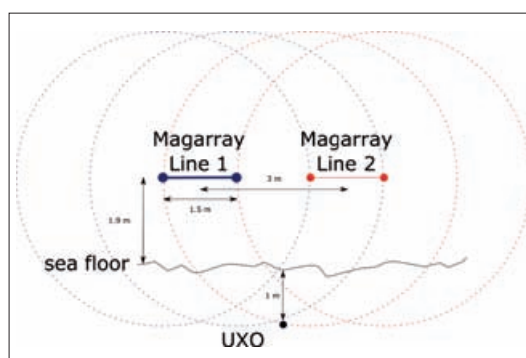


Fig. 2: Magnetometer array with 3 m line spacing to detect 150 mm shell in 1 m depth of burial

2.2 Recovery

In the last decade the increasing amount of UXO surveys and the shorter time frames for the removal lead to an exclusive use of work class ROVs on many projects. ROVs have several advantages over divers, namely elimination of exposure of the human element to unexploded ordnance, longer endurance, and higher weather criteria, as well as more versatile tools (acoustic sensors and imaging systems, cameras and lights, metal detector, magnetometers, manipulators) and higher lifting capacity.

While in some cases inspection class ROVs may be sufficient for simple camera inspections in calm waters, work class ROVs (WROV, Fig. 4) have been found to be a more reliable, robust platform for offshore UXO inspection, recovery and removal operations because of their higher weather criteria (in particular waves, current), and more versatile usability (multiple tools and sensors).

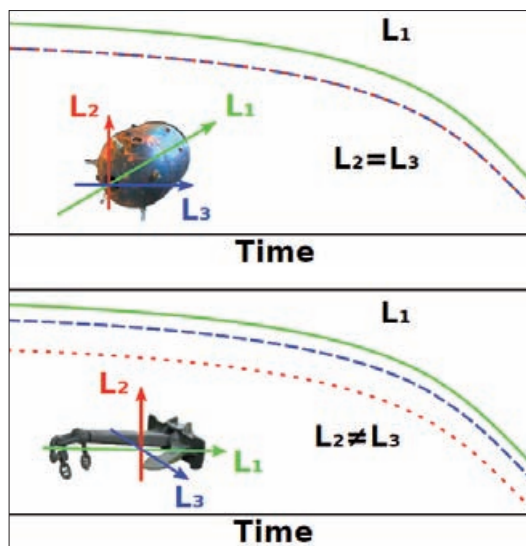


Fig. 3: Schematic decay of the magnetic field along three different axes for a symmetric and an unsymmetrical object

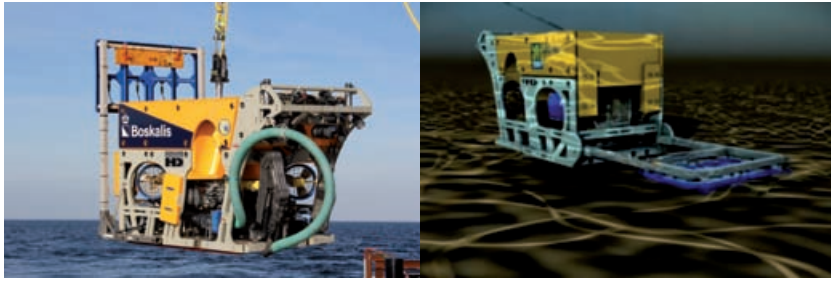


Fig. 4: Heavy duty work class ROVs

References

Schmidtke, Edgar (2010): Schockwellendämpfung mit einem Luftblasenschleier zum Schutz der Meeressäuger; DAGA Conference Berlin, 2010
 Winkelmann, Kay; Andreas Fischer (2009): »Tiefenreichweite« bei der Kampfmittelsuche mit Magnetometern; Fachaufsatz für Kunden der Firma SENSYS Sensorik & Systemtechnologie GmbH, Bad Saarow

Based on the target coordinates given by the client each target will be approached by the ROV installed on the ROV support vessel. A survey grid of 6 x 6 m is placed over the target coordinate on the navigation screen, which is then systematically investigated in a track distance of 2 m, while the readings of the TSS-440 pulse induction detector are recorded. If the target is measured, the WROV only has to rotate 180 degrees and the identification of the target can begin right away. In the event the target is not measured at given location, the survey grid can be extended in 1 m steps, in close liaison with the clients representative on board.

The WROV-pilot has a permanent view of the investigation area so that any surface contacts can also be visually identified and recorded on video. To avoid direct contact with objects lying on the surface we have equipped the WROV with a forward-looking sonar system in addition to its HD video cameras.

After detection, the measurement data is verified, and the list of objects utilised as a basis for identification/recovery is updated accordingly.

In case the target is covered with sediment and thus not visible on the seabed, a dredge pump fitted on the WROV will be employed which enables us to remove any sediment covering the relocated target.

After identification of the EOD TA the UXO can either be left in situ, or wet stored in a known location or brought to deck if safe for transport.

2.3 Disposal

UXO disposal is a key element in the removal campaign. Depending on federal law, different dis-

posal techniques are available, but a demolition is normally the method to deal with UXO which is classified as not safe for transport.

In order to keep the risk to personnel and technology as low as possible demolition operations are conducted without the use of divers. For this reason, the actual placement of the demolition charge is made with the project ROV support vessel and directly with the WROV.

Hereby, demolition charges especially produced for this purpose are used, which can be flexibly and variably scaled to fit the type of ordnance to be destroyed. Once the UXO has been identified and prepared for demolition and with all the information gathered from the investigation, the EOD TA will decide which explosive charge, in his professional opinion will produce the optimum results in the destruction of the UXO. It is at the sole discretion of the EOD TA on which explosive charge is to be utilised. This decision will also be based on several factors which include the type, state of deterioration and position of UXO to be destroyed.

With the demolition of non-transportable ordnance, such as mines, torpedoes, depth charges, etc., by underwater explosion local shock waves are produced with significant amplitude.

In order to minimise the possible damage to the marine environment by these shock waves as much as possible, bubble curtains to dampen the shock waves are used. This is also normally requested from the relevant regulatory agency as we have experienced in the past.

To verify the effectiveness of these bubble veils extensive tests were carried out in 2010 with good results (Schmidtke 2010) (Fig. 5).

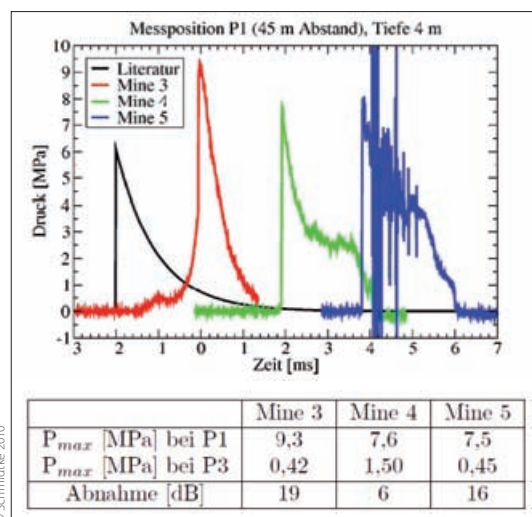
The dampening degree of the shock pressure signals from the demolition of three anchor mines each with 300 kg explosive material (45 % TNT, 5 % hexanitrodiphenylamine, 20 % aluminium powder, 30 % ammonium nitrate) was investigated on passage of the shock signals through an air bubble curtain. By the passage through a fully developed bubble curtain a reduction of the pressure peaks of 16 dB to 19 dB could be achieved, even with an incomplete bubble curtain a reduction of peak pressure of 6 dB were achieved. Spectrally at frequencies greater than 500 Hz a dampening of at least 5 dB with the full-blown bubble curtain in comparison with the incomplete which demonstrated that reduction of the equivalent continuous sound level is in these cases at 7 dB to 8 dB.

Maximum shock reduction is achieved with the placing off a bubble curtain at a diameter of 90 m being provided around the target object.

Nevertheless, demolition is not an option for chemical warfare or dump sites were big amounts of DMM can be found next to each other.

For these cases research is currently in progress and cycles are being developed for each different type of munitions to disarm and salvage them without demolition.

Fig. 5: Time courses of the shock waves of three blasts in comparison with literature values. The time zero points of the individual measurements are for clarity arbitrarily shifted against each other. The table shows the pressure peaks and their reduction. The shock wave loss has already been eliminated



Tailor-made surveys for customers needs

Meritaito is one of the Northern Europe's largest marine survey companies. We provides hydrographical, geophysical and geotechnical survey services in offshore, near shore, inshore and inland water areas.

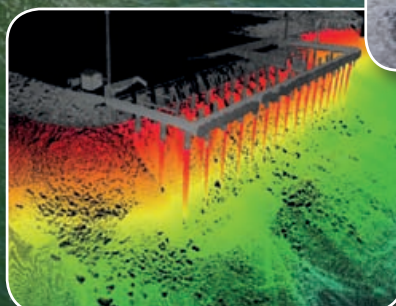
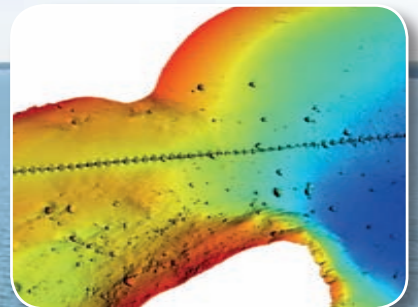
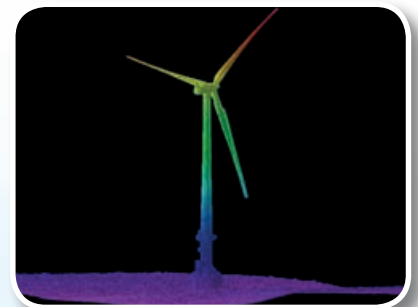
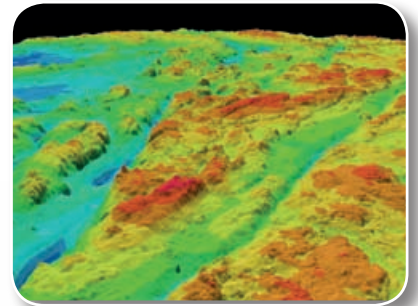
Our certified services meet the highest international quality standards (IHO S-44) and the most demanding customer needs and charting authorities expectations.

Meritaito has a team of highly skilled professionals in hydrographic surveying, marine geology, engineering and data processing. This team of internationally certified hydrographic surveyors and shallow water experts provides tailor-made surveys for your needs.

Meritaito operates in the Mareano bathymetry surveying project which can be called one of the most demanding survey projects in the world.

Further information:
Sales Director Kari Pohjola, Tel. +358 40 571 3193

“Come and visit our stand 64
at Hydro 2016 Exhibition!”



The search for Malaysian Airlines flight MH370

An article by MELANIE BARTH

Even today, hydrographic surveys can reach the boundaries of what is technically possible, and project sizes as presented in this case study will push our ingenuity. The size-challenge can be defined by the extent of the project area, the water depth, the number of vessels/equipment involved, the data volume or all of the above. On 8 March 2014 the Malaysian airplane MH370 scheduled on a flight from Kuala Lumpur to Beijing with 239 people on-board went missing. This tragedy started a marine search and rescue mission, which turned later into the largest aircraft accident investigation in history. This case study presents a summary of the underwater search of this investigation. The mainly uncharted search area in the southern Indian Ocean of 120,000 square kilometres reaches water depths of up to 6,000 metres. The operation was planned in three phases: a deep-water multibeam survey to map the seafloor and enable a detailed search, the detailed survey to find the aircraft, and at last a recovery survey.

Author

Melanie Barth is Delivery Excellence Manager at Fugro NV in Leidschendam, The Netherlands.

m.barth@fugro.com

aircraft search | ultra-deep survey | deep-tow system | Indian Ocean

1 Introduction

On 8 March 2014 the Malaysian airplane MH370 scheduled on a flight from Kuala Lumpur to Beijing went missing. On board the aircraft were 239 people. A marine search and rescue mission was started shortly after the disappearance, which turned later into an aircraft accident investigation to understand the circumstances leading to the tragedy and hopefully bring closure to the families.

The case study will present a summary of the underwater search of this investigation.

2 Project overview

2.1 The search area

The Australian Transport and Safety Bureau (ATSB) is leading the search and recovery operation in the southern Indian Ocean. One of the first steps of the investigation was the identification of the most likely location of the missing aircraft. Available information and simulations were studied

and produced a probability heat map of the aircraft location (Fig. 1), which was used to specify the search area.

The underwater search area is in a remote location approximately 1,000 to 1,500 nautical miles west of Fremantle, Australia; a sailing time of four to six days at 10 knots to reach the location by survey vessel.

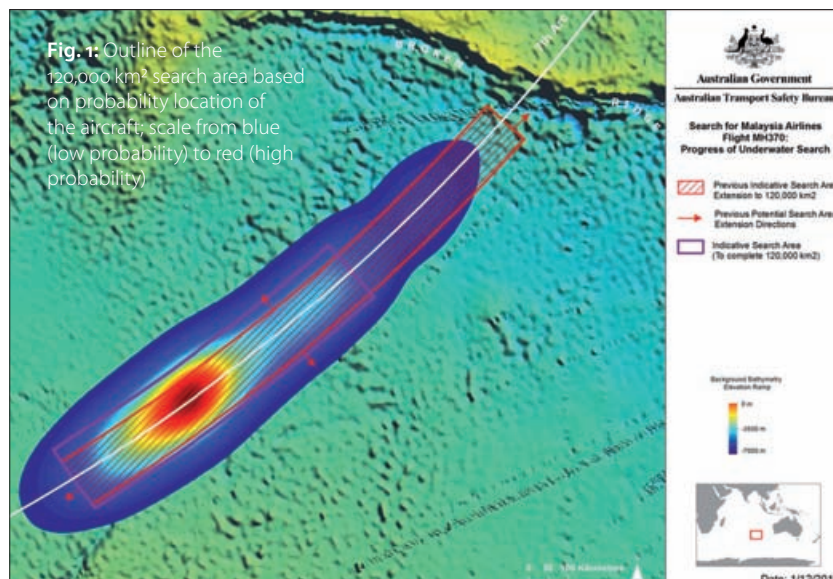
The size of the search zone measures 120,000 square kilometres with water depths up to 6,000 metres. The morphology of the seafloor was relatively unknown previous to the search operation. Satellite radar altimetry data gave an indication of the expected water depth and aided with the planning.

2.2 Search parameters

From previous aircraft accidents it is understood that an aircraft can break up on contact with the water surface, e.g. the accident of the AF447 flight in June 2009 revealed a debris field of 600 metres by 200 metres on the seafloor with one of the turbine engines as the largest located piece (BEA 2012). This experience was used to specify the parameters for the MH370 search. The operation had to be designed to identify debris fields with individual maximum target size of two square metres, while full coverage of the entire priority search area was required.

2.3 The survey

The operation was split into three phases (see table) and started with the deepwater multibeam echo sounder investigation to map the seafloor with a hull-mounted Kongsberg EM302 system of the »Fugro Equator«, which was later joined by three further Fugro vessels. The bathymetry revealed a challenging morphology with underwater volcanoes and canyons, e.g. at the Greelink Fracture Zone an up to ten kilometre wide canyon



Survey phases	Method	Coverage rate
Map the seafloor to enable save mission planning for detailed search	Deepwater multibeam survey with hull-mounted echo sounder	1,200 km ² /d, cross track resolution: 104 m
Detailed survey to identify the aircraft and map/ photograph the debris field	Deep-tow (DT) & AUV survey; with multibeam echo sounder, side-scan sonar, sub-bottom profiler, camera, USBL positioning	DT: 133 km ² /d, cross track resolution: 0.7 m; AUV: 17 km ² /d, cross track resolution: 0.1 m
Find and recover (phase not started yet)	ROV survey	24 km ² /d, cross track resolution: 0.1 m

was observed with an almost one kilometre high perpendicular wall.

Based on the bathymetry the detailed survey plan was designed. The deep-tow system was selected as primary solution for the second phase. The altitude of the deep-tow system was set at 150 metres above the seafloor to ensure the required resolution and maximal possible coverage. This resulted in a towed distance of approximately nine kilometres behind the vessel (Fig. 2), which limited the manoeuvrability of the spread.

As secondary system an AUV («Echo Surveyor VII», a Kongsberg Hugin 1000) was selected to cover the areas that could not be reached by the deep-tow system and for detailed inspections of recorded targets of interest. The AUV was deployed from the stern of the vessel on pre-programmed missions flown at 100 metres altitude, hence the necessity of the high-resolution bathymetry from the first phase of the project.

The deep-tow systems as well as the «Echo Surveyor VII» were depth rated to 6000 metres. The systems were equipped with state-of-the-art sensors: Edgetech 75 kHz side-scan sonar, Kongsberg EM2040 multibeam echo sounder, Edgetech sub-bottom profiler, cameras, hydrocarbon sniffer (only at the beginning of the investigation) and positioning systems such as Doppler Velocity Log (DVL), altimeter, sound velocity sensors, HAIN motion sensors and Ultra Short Baseline (USBL) systems (HiPAP 101 for the deep-tow systems, HiPAP 501 for the AUV respectfully).

Data from the deep-tow system was transmitted directly via an umbilical to the vessel, while the data on board the AUV was recorded on board the vehicle and uploaded after each mission. Missions were limited by battery power to approximately 30 hours. Data was copied immediately to a secondary server system for backup and then transmitted via satellite systems to shore in near real time to enable access to the authorities to all information and allow coordination and control of the operation. Processing of the data was split over various processing centres to increase efficiency. The data was reviewed by minimum of four independent geophysicists (ATSB and Fugro) to ensure that no target was missed.

3 Implication of the remote location

It was mentioned before that the search area was defined in a remote location. There are two main challenges with the remote location: number one is the distance to the nearest port and hence long sailing times, number two is that so little is known about the investigation area.

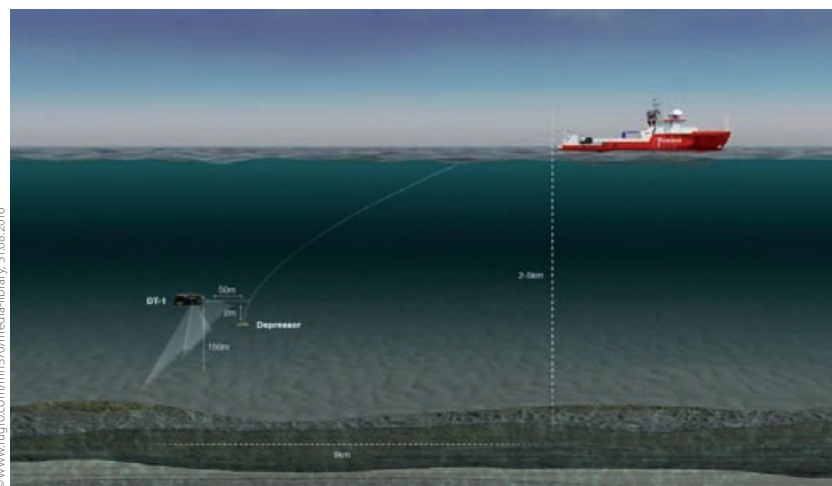
3.1 Distance to shore and sailing time

Vessel mission periods are limited by the fuel consumption and food supplies that a vessel can carry. During the MH370 search operation Fugro vessels with a length between 65 and 93 metres were involved in the project. Even though missions were usually planned for maximum duration of each vessel, effective survey time was always limited by the sailing time from and to the search area, which averaged ten to twelve days per mission. Using up to four survey vessels attempted to minimise this impact on effective survey time.

The long distance to shore also has an impact on each interruption of the operation. It was clear that unplanned mission breaks had to be avoided. Therefore, all vessels had a doctor on board and remote tele-medicine to reduce the likelihood of medical emergency breaks. Even though the medical risk was considered it could not be totally avoided. In the two years operation there were two emergency port calls due to illnesses, though no injuries.

Another risk was exposure to weather extremes. The risk was mitigated by six-hourly weather forecasts to ensure safe mission planning. Though equipment could be recovered on board in time,

Fig. 2: Schematic representation of the deep-tow system of the «Fugro Equator»



References

- ATSB (2015): ATSB Transport Safety Report – MH370 – Definition of Underwater Search Area, AE-2014-054, 3 December 2015
- BEA (2012): Final Report – On the accident on 1st June 2009 to the Airbus A330-203 registered F-GZCP operated by Air France flight AF 447 Rio de Janeiro – Paris (Update: 27 July 2012)

there was no shelter close by and therefore the vessels had to stay out at sea. During the project there were four tropical cyclones at the search area which resulted to largest recorded wave heights of 17 metres, and wind up to 78 knots (~150 km/h).

Not only weather extremes were a limitation to the survey also standard wave heights in the Indian Ocean had an impact on the operations as the AUV had to be launched and recovered on a regular basis. When wave heights increased above the safe operation limits missions had to be postponed until safe operations were possible again. During the project a new launch and recovery system was installed on board one of the vessels used during the survey, the »Harvila Harmony«, which increased the AUV weather window to wave heights of up to 3.5 metres.

3.2 Unknown of the investigation area

Even though hydrographic surveys have been carried out for centuries the main research areas of interest are near to shore in national territories or along popular shipping routes. In general, the further the operation area is away from shore the less information is available. Although satellite radar bathymetry becomes more and more available the details of the collected data reduce

with increasing depths. The MH370 search area is not only located far away from shore, but also in deep water, which resulted in sparse available information before operations started. This made it necessary to commence the operations with the mapping of the survey, before the detailed search could start to reduce the likelihood of losing the survey equipment.

4 Close-out

Flight MH370 has not been located yet. The authorities have indicated that the search will be suspended after completion of the priority area until new information becomes available which warrants continuation of the search. Until such time, the tragedy remains a mystery.

However, data that was collected during the search mission will be made available and might support future studies on tectonics or other earth science topics and increase our understanding of the earth, especially of the seafloor of the Indian Ocean.

Experiences gained during the operation will assist in future projects, e.g. the newly designed launch and recovery system will make operations safer and remote processing becomes a common practice. 



At home in water

Within the Hülskens Company Association, **Hülskens Wasserbau is the expert for hydraulic engineering challenges.** With state-of-the-art technology and innovative processes, we realise demanding **large-scale water construction and port engineering projects ourselves.** Reliably. Meeting deadlines safely. Professionally. So it is not a surprise that Hülskens Wasserbau is one of the leading companies in the sector.

Handling the element water doesn't necessitate any miracles – but simply know-how, creativity and experience.

Culvert construction • Pile driving work • Work on piling walls • Dredging work • Hydrography • Bedload management • Shore redevelopment • River engineering • Bank protection & grouting • Special techniques



www.huelskens-wasserbau.de

The challenge of choosing the right method for surveying power cables

An article by OLIVER ANDERS

The rising number of wind parks, and thus the demand for new survey tasks, results in continuous development for companies working in the renewable energy sector. Building a wind park requires laying inter-array and export cables. Those cables are buried or covered to protect them, bringing environmental changes to a minimum. A

cable tracking | depth of burial | HVAC/HVDC | survey power cables

1 Subsea power cables

There are many offshore constructions that need power cables to either supply energy or, more common, deliver produced energy to the beach. The ever-growing renewables industry is building many wind farms. Many cables are laid in the vicinity of wind farms. There are two kinds of cables, inter-array and export cables. The inter-array cables connect the single windmills with the transformer station. The export cable transports the energy to shore.

Other fields where subsea power cables are used, are islands like Norderney or Heligoland that connect the islands to the mainland's power grid. Furthermore, countries are linked by power cables to level load and overproduction like Norway and Germany.

Subsea power cables can be anything from 70 mm to, exceeding, 210 mm in diameter and there exist two kinds: high voltage AC (alternating current), HVAC, and high voltage DC (direct current), HVDC. The selection criteria which type of cable to use, is heavily dependent on the route length, voltage and transmission capacity. When offshore wind developers decide between HVAC and HVDC cabling, the overall system must be taken into consideration – including cables and transformers/converters. There is a break-even distance between HVAC and HVDC, generally considered between 40 and 80 km, where economic reasons outweigh the building of a HVDC connection. AC cables are three-phase cables, and are laid either as a bundle in a three-core formation, or as three separate cables. The configuration of DC cables is dependent on the DC system. There are two main types: monopolar and bipolar. Generally speaking, they consist of two conductors, either laid separately, bundled together or in a coaxial arrangement.

In 1954 the world's first subsea HVDC cable, Gotland 1, was installed. It was 98 km long, stretching from Gotland Island to the Swedish Mainland and with a capacity of 20 MW. This changed the world's view on submarine electricity transmission as it was realised that it was now possible to connect to other countries overseas that were previously thought unreachable.

Currently, the longest interconnector is the NorNed cable between Norway and the Nether-

lands. With 580 km, it is the longest subsea power cable in the world, with a capacity of 700 MW. However, the very latest cable technology has the potential capability of reaching up to 1.500 km.

2 Burial of cables

Subsea cable damage most often arises from two areas. The first are faults caused in the open sea by anchor strikes, dragging fishing nets and erosion. Second area is poor planning and building at the start of the project, coupled with inadequate risk identification, sub-standard design, and deficiencies in how procedures have to be applied. Around 70 % of insurance payouts for wind farms relate to cable damage. Around 80 % of these incidents occurred in shallow water depths of less than 50 m. Internal faults are relatively rare, external damage is the key reason for repairs: 41 reported failures were the result of external impact by third parties namely anchor dragging and fishing nets. Shifting sediment or rock account for around 5 % of all external cable faults.

As a result the burial of cables decreases the risk of external damage and furthermore fixes the cable to its projected position. Additionally, the heating and electromagnetic field of cables have less impact on the environment.

3 Tracking systems

Submarine power cables need to be located and surveyed for several reasons. Cables need to be inspected after lay to ensure the laying (and burial) specification has been met. It may be necessary to routinely inspect the cable in order to certify its suitability for continued service. It will be necessary to positively locate existing cables prior to carrying out works such as installation of structures, dredging and similar projects before commencing work or to locate them for repairs.

There are several technologies which may be used for the task of surveying, all of which have advantages and disadvantages (see table). The key task is to identify which system is suitable to fulfil the task in a certain configuration. The cable tracking systems can be categorised in either active or passive systems, meaning the procedure of how the systems detect the cables.

common depth of burial ranges from 1.5 m to 3 m. The challenge of surveying those buried power cables is choosing the right method.

Author

Oliver Anders works as a hydrographic surveyor at Fugro OSAE GmbH in Bremen.

o.kuempel@fugro.com

System	Technology	HVAC	HVAC	HVDC	HVDC	widely tested	easy to operate
		in operation	out of service	in operation	out of service		
Teledyne TSS 350	tone detection passive	✓	✓	✗	✓	✓	✓
Optimal Ranging Field Sense	tone detection passive	✓	✓	✗	✓	✗	✓
Teledyne TSS 440	pulse induction active	✗	✓	✗	✓	✓	✓
Innovatum Smartrak 9	gradiometer passive	✓	✓	✓	✓	✓	✓
Pangeo SBI	acoustic active	✓	✓	✓	✓	✓	✗

3.1 Passive systems

Passive systems detect the location of the cable by tracking the cable's own electrical frequency. It is in the nature of AC cables that, due to alternating current, a sinusoidal oscillation takes place with a certain frequency. Most commonly is a frequency of 50 Hz predominant in nearly all European cable grids. The other type of energy transmission, namely direct current, always flows in one direction and therefore does not emit a frequency. There are dominant harmonic frequencies called sidebands. In HVDC applications, the sideband frequency which can be tracked, is typically around 1 to 2 kHz. Another option to track DC passively is by taking them out of service and injecting an artificial frequency by a tone generator.

3.2 Active systems

Instead of tracking what is there by its own, active systems emit either electromagnetic or acoustic signals to locate cables. EM pulses are capable to induce a current flowing in the cable and emit a magnetic field which can be measured again. By using multiple coils, a horizontal and vertical position of the target may be obtained. The system performance is dependent on the target material, the target diameter and the transmitted power. The diameter of the target is the main physical factor governing the maximum detection range. The two-way data path means high losses.

Acoustic systems work similar to sub-bottom systems but visualise a 3D acoustic image of the sediment below seafloor.

Fig. 1: Radial symmetric EM-field of HVAC power cable

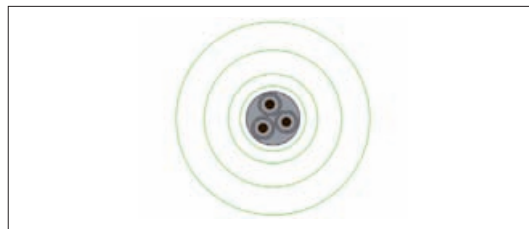


Fig. 2: EM fields for HVAC cables

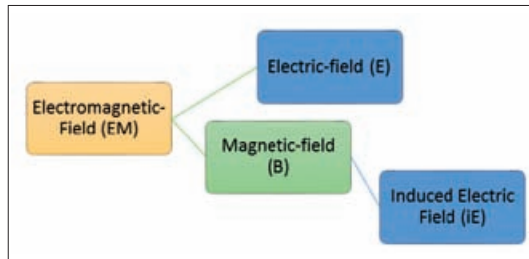
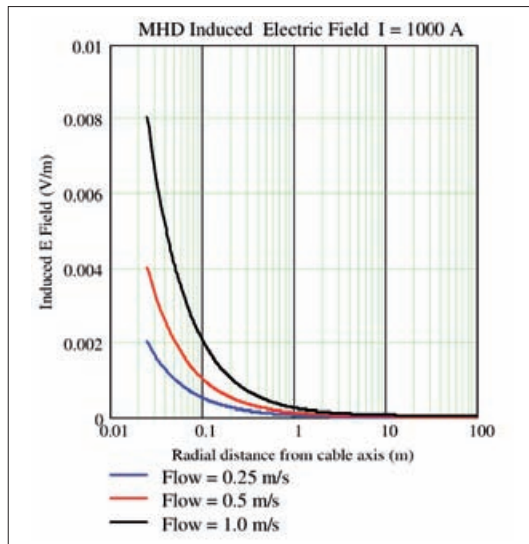


Fig. 3: Induced EM fields



4 Challenge of surveying

Passive systems use at least two or more sensors on a fixed baseline to calculate the frequency's origin by triangulation. All of these triangulated systems assume that a radial symmetric EM field is emitted (Fig. 1).

The most common cable type of subsea three-phase power transmission is the triaxial, or trefoil cable, where three conductors are laid up in the form of an equilateral triangle. The magnetic permeability of the seabed and seawater are approximately equal, as both are non-ferromagnetic, thus burial of the cable into the seabed will not change the magnetic field surrounding the cable. Whilst the sheaths of the cable provide good shielding to the electric field, they cannot shield the magnetic fields. As passive systems track electromagnetic fields, the assumption of a radial symmetric field needs to be looked at closer. The function of earth in which the sheath is, is to set the absolute electric potential of a conducting material to be zero – the same as the earth. Earthing the sheath should reduce any leaked fields further down to zero (earth). Thus, we should expect very little electric fields leaking to the outside of the cable. Apart from direct EM fields, one might wrongly conclude that if the cable is properly earthed, there would be no E field generated outside the cable. Dealing with an HVAC power system, Maxwell's equations for a time-harmonic case shows that the changing magnetic field B (against time) also generates an induced electric field. E and B fields exist around a typical wind power cable even when well shielded (Fig. 2).

If this magnetic field is induced in flowing sea-water, then an electric field will be induced in the sea by magneto-hydrodynamic (MHD) generation (Fig. 3).

Many researches in EM field propagation around submarine cables were conducted during the last years with a special focus on environmental or mammal effects. These studies give a good insight of EM field propagation for submarine cables. Results demonstrated that a variety of factors, such as topographic, bathymetric, and geologic conditions contribute to the natural generation and propagation of EM fields. Thus, a radial symmetric field can be distorted and result in wrong depth calculations (Fig. 4).

In case of a bipolar conductor the electromagnetic field is formed in an elliptical shape. If this is not corrected by postprocessing, wrong depth calculations are the result.

5 Indirect depth of burial survey by seabed difference

As laid data gathered by the laying vessel is just valid for the time directly after cable lay, re-surveys are necessary at a later point of time to ensure a constant monitoring. The cable operator is interested in the change of the burial depth. Cable surveys with cable trackers require special equip-

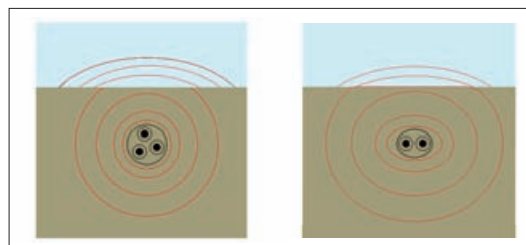
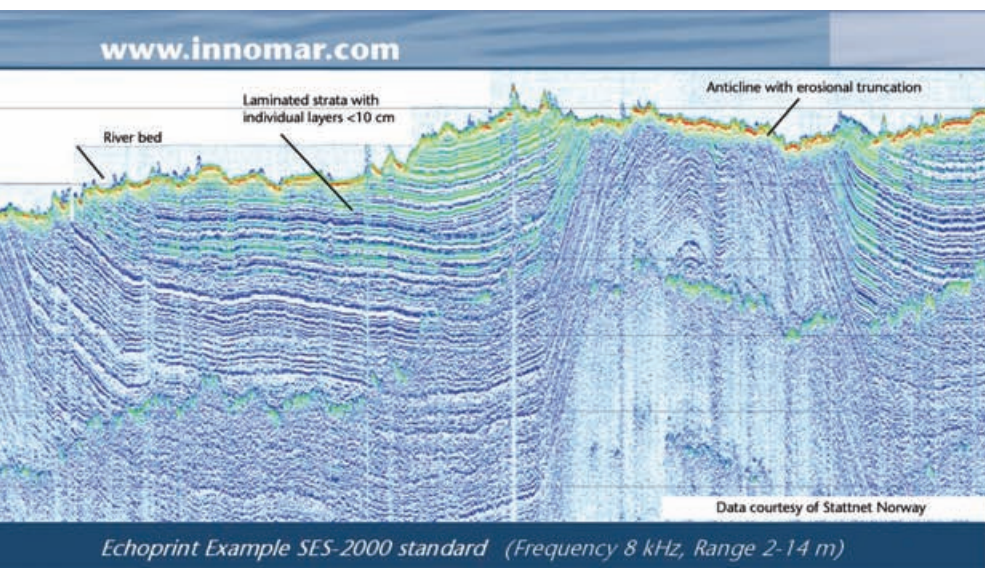


Fig. 4: Distorted radial symmetric EM-field trifoil and bipolar

ment, are expensive and slow compared to multi-beam measurements. Once the cable is in a stable condition (no hardening, no heating-up phase) an indirect cable survey by multibeam sediment difference will give a quick and cheap depth of burial result. For a first initial primal measurement, the cable is located by one of the standard pipe and cable tracking systems. The results give a direct map of the absolute depth of the cable and its burial state. This data also contains absolute seabed height. At the stage of another survey epoch a multibeam survey provides absolute seabed depths as well. By comparing the two multibeam depth information and considering the cable as stable, a change of the burial state can be derived. The aim is to provide quicker and cheaper information about the burial state of the cable. This combined cable tracking and multibeam seabed difference can be used to fulfil that aim. [↕](#)



SES-2000 Parametric Sub-Bottom Profilers

Discover sub-seafloor structures and embedded objects with excellent resolution and determine exact water depth

- ▶ Different systems for shallow and deep water operation available
- ▶ Menu selectable frequency and pulse width
- ▶ Two-channel receiver for primary and secondary frequencies
- ▶ Narrow sound beam for all frequencies
- ▶ Sediment penetration up to 200m (SES-2000 deep)
- ▶ User-friendly data acquisition and post-processing software
- ▶ Portable system components allow fast and easy mob/demob
- ▶ Optional sidescan extension for shallow-water systems



Burial depth determination of cables using acoustics

Requirements, issues and strategies

An article by JENS WUNDERLICH, JAN ARVID INGULFSEN and SABINE MÜLLER

Depth-of-burial (DOB) surveys are well-known in the oil and gas business to obtain the exact position and burial depth of pipelines or cables after dredging and for regular maintenance. With expanding offshore wind farming in the wake of the »Energie-wende« site explorations, route and cable DOB surveys become increasingly important in this industry, too. Various geophysical methods like magnetic, electro-magnetic and acoustic sensors are used to detect and track buried cables. For best detection probability of buried cables to date mostly lines crossing the expected cable route are surveyed. Although this is suited to detect the cable and get its position with high accuracy, survey companies require more efficient technologies, accounting for both, operational and processing costs. Thus they are looking for easy to operate equipment that follows the cable along its actual route, works at different water depths, weather and seabed conditions and gives immediate and reliable results to produce deliverables with high accuracy of XYZ cable positions.

Authors

Dr. Jens Wunderlich is R&D Manager at Innomar Technologie GmbH in Rostock. Jan Arvid Ingulfsen is Senior Advisor Survey & AUV Operations at SWIRE Seabed AS in Bergen, Norway. Sabine Müller is Managing Director at Innomar Technologie GmbH in Rostock.

jwunderlich@innomar.com

detection of buried objects | acoustic cable tracking | depth of burial – DOB | sub-bottom profiler – SBP

1 DOB survey requirements

In shallow waters the cables are buried into the seabed to avoid damages by ships, waves, anchors or other impact. The burial depth depends on the cable location and is mostly between one and three metres for inter-array cables (connections within the wind farm) and power export cables (connections to shore). In areas with heavy fisheries or very dynamic seabed morphology burial up to ten metres or additional rock dumping may be needed.

Requirements for the cable position density along the cable route depend on the survey type. For surveys immediately after the cable was laid, positions of at least every metre are required while for maintenance surveys positions every 50 to 200 metres are sufficient. For cable-tracking systems a position density of up to 25 cm may be requested.

Horizontal (XY) cable position accuracy requirements are mainly based on the accuracy of the positioning system used (DGPS/RTK for surface vessels, USBL for subsea vehicles). Burial depth (vertical position Z) accuracy requirements vary from 5 % of slant range from sensor to 10 % of burial depth with limits of 5 to 10 cm RMS. For a sensor at two metres altitude and a cable buried two metres below seafloor these requirements translate into a vertical accuracy of 20 cm.

Operational costs mainly depend on the vessel costs, a vessel with ROV, crew, etc., often costs more than 50,000 € per day. Thus, survey time has to be as short as possible. If a high position density is required the cable detection system needs to go along the cable route and cover a wide across-track swath and should guide the helmsman along the cable to ensure the cable is not falling out of

the survey corridor. If other sensors like multibeam echo sounders or electro-magnetic pipe/cable trackers shall be operated in parallel, there might be additional requirements like sensor distance above seafloor, which in turn affects the across-track swath requirements.

Data processing needs to be done offshore within 24 hours by the standard processing team aboard. Sometimes cable positions are needed immediately after trenching. For instance aluminium-cored cables are known to float in the slurry created by the trenching tool and end up rising behind the vehicle's depressor. So the contractor needs to have burial depth information quite fast to correct the target depth of burial if necessary. Thus for DOB surveys it is essential to have good online data visualisation for quality assurance and fast on-board post-processing with full position accuracy.

2 Cables as sonar targets

Active sonars used for acoustic cable detection emit sound pulses and register echoes of these pulses returning from objects or surfaces within the insonified volume. To estimate the acoustic performance the sonar equation (Lurton 2002; Urick 1983; Waite 2005) adapted for a buried target is used:

$$SE = \frac{\overbrace{(SL - 2 PL - TL + TS)}^{\text{desired signal } (EL)} - \overbrace{(NL_R + RL)}^{\text{unwanted noise}}}{\underbrace{(5 \log d - 10 \log(BT) - 5 \log n)}_{\text{signal processing } (DT)}}$$

To detect the cable (target) the signal excess (SE) has to be positive. The desired echo signal (EL) depends on transmit source level (SL), the propagation loss (PL = PL_W + PL_B) in water

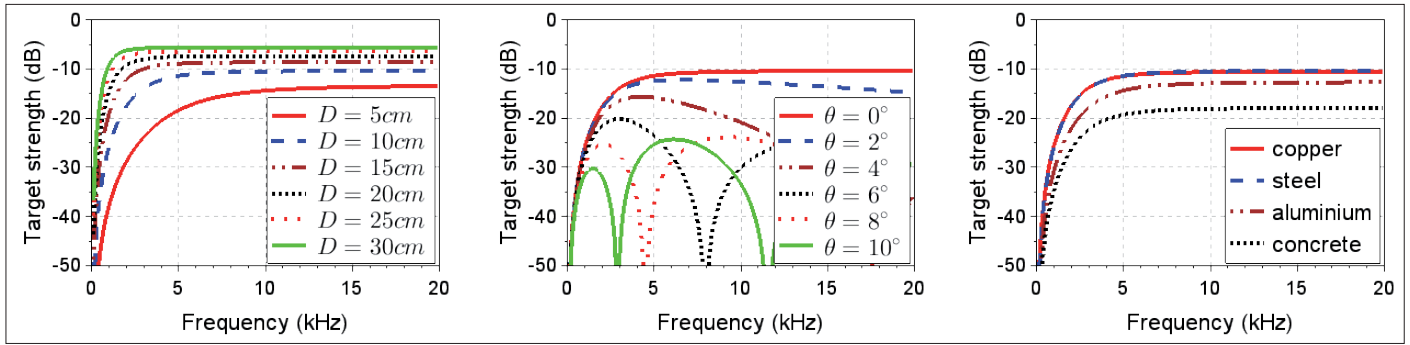


Fig. 1: Target strength depending on frequency of a cable modelled as infinite steel cylinder buried in sand (Stanton 1989) for different diameters D at normal incidence (left), for different incidence angles θ with diameter $D = 10\text{ cm}$ (centre) and for different cylinder materials at normal incidence (right)

and in the seabed (both depending on physical sound attenuation a and travelled distance R : $PL_{W,B} = 20 \log R_{W,B} + a_{W,B}R_{W,B}$), the two-way transmission loss (TL) at the water-seabed interface and the relative amount of energy returned from the target (target strength TS). The received signal also contains unwanted noise and reverberation. The noise seen by the system ($NL_R = NL - DI_R + 10 \log B$) is mainly produced by the survey vehicle and depends on receiver directivity (DI_R) and sound pulse frequency bandwidth (B). The reverberation is caused by backscatter from random voids or objects within the insonified volume and the seafloor roughness. The reverberation level ($RL = RL_W + RL_B + RL_V$) depends on source level (SL), sediment type, the insonified seabed area and volume as well as the angle of incidence. The detection threshold (DT) depends on signal processing parameters to improve the signal-to-noise ratio ($SNR = EL/(NL_R + RL)$) like pulse length (T), pulse bandwidth (B), number of pings per processing ensemble (n) and detection index (d), which depends on detection probabilities as well as signal and noise characteristics (Waite 2005).

At fixed echo (EL), noise (NL) and reverberation (RL) levels the best signal-to-noise ratio will be achieved through a high receiver directivity (i.e. small beam width) and a high number of pings used per processing ensemble. The number of pings which can be used depends on beam width, vessel speed and ping rate. High survey speeds will require high ping rates to ensure pseudo-static conditions for the echo signal.

The reverberation level (RL) can be minimised by keeping beam width and pulse length as small as possible. For the low frequencies required for seabed penetration, narrow sound beams can be

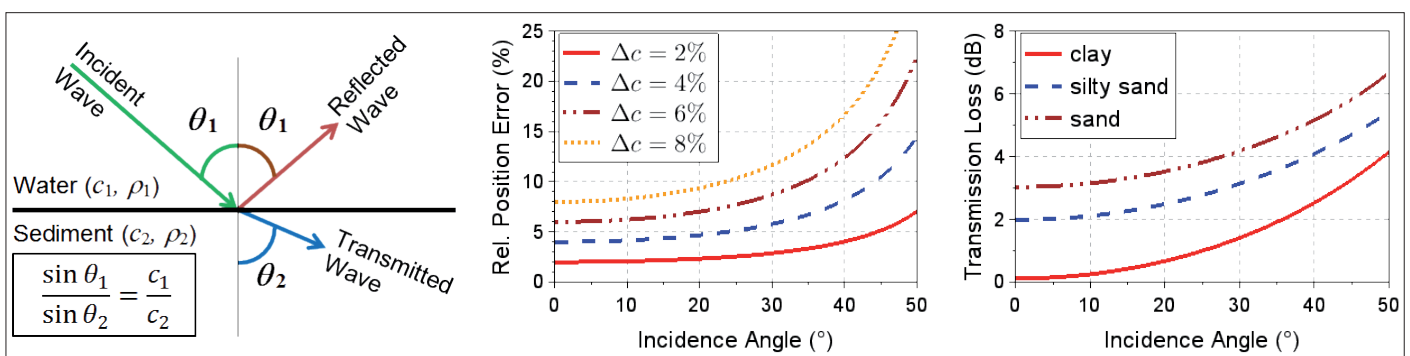
achieved by nonlinear (parametric) acoustics (Lurton 2002).

At fixed source level (SL) and propagation loss (PL) the echo level (EL) can be increased by reducing the transmission loss (TL), which strongly depends on the incidence angle (Fig. 1), and by increasing the target strength (TS). To estimate the target strength, a cable can be modelled as thin straight cylinder of infinite length. For simple shapes various simplified target strength models have been published (Lurton 2002; Stanton 1989; Urlick 1983; Waite 2005).

The target strength depends on frequency, cable diameter, angle of incidence and material (Fig. 1). Typical diameters of wind farm cables range between 5 to 15 cm for inter-array cables and about 20 to 30 cm for power export cables going onshore. For cable diameters of 10 cm and more frequencies down to about 4 kHz can be used. For thinner (e.g. communications) cables higher frequencies are necessary. Especially for higher frequencies it is important to ensure the sound wave incidence perpendicular to the cable. This will be mostly the case at flat seafloors, but at slopes the sound beam direction needs to be adjusted either by tilting the vehicle (ROV/AUV) or by electronic beam steering.

The refraction at the water-sediment interface and at sediment layers is causing errors in the estimated cable position, depending on sediment type and incidence angle. This needs to be addressed during data processing. Sediment properties are mostly unknown and reducing the position error requires time-consuming optimisation algorithms, which will be faster if an educated guess on the sediment sound speed is available and the incidence angle is kept as small as possible (Fig. 2).

Fig. 2: Sound wave reflection and refraction at a flat water-sediment interface with incidence angle θ_1 , the same angle for the reflected wave front and angle θ_2 of refracted wave front transferred into the seabed (left). Position error due to refraction (Euclidian distance between true and mapped cable position related to true burial depth) depending on incidence angle for sand at different sound speed estimation errors (centre). Two-way transmission loss TL (Sternlicht and de Moustier 2003) at a smooth water-seabed interface for different sediment types depending on incidence angle (right)



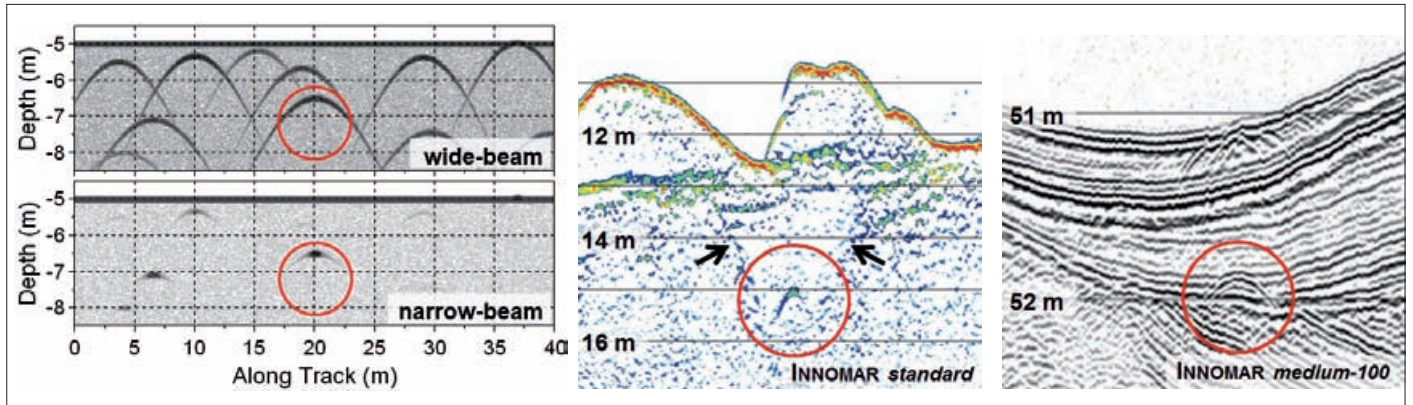


Fig. 3: Model echo prints from a cable (red marks) buried 1.5 m below seafloor surveyed across track and boulders spread in the seabed, for a linear wide-beam and a parametric narrow-beam system; boulders at the same locations for both data sets (left). Data example showing a pipeline approximately 4 m below sand, trench is visible (arrows), original seabed below sand waves (centre). Data example showing a 12 cm-cable buried about 1 m below seafloor at 51 m water depth surveyed shortly after dredging, diffraction hyperbolas visible at the seabed due to remaining trench banks (right)

3 Sonar track crossing the cable

Surveys using acoustics to map buried cables today mostly do survey lines crossing the expected cable route to get diffraction hyperbolas in the echo data, which gives a good detection probability. This method delivers cable positions at the cross points between cable route and survey track only. Thus the cable along-track position density depends on the line spacing. According to section 1 this may be sufficient for maintenance surveys, but higher requirements on position density will cause high operational costs due to the survey time needed. A time-consuming cable position picking in the survey profiles and distinguishing between hyperbolas originating from the cable or from random objects in the sediment, like boulders, result in high processing costs, too. Processing time can be reduced by using narrow-beam sub-bottom profilers (SBPs) instead of wide-beam systems. Narrow sound beams produce much less diffraction hyperbolas from boulders or other objects in the sediment and generate less reverberation (Fig. 3).

Survey tracks crossing the cable route have been successfully applied during DOB surveys for cables buried at water depths down to more than 50 metres using pole-mounted SBPs (Fig. 3). Also during surveys using electro-magnetic pipe/cable tracking equipment, SBP tracks across the cable route are utilised frequently for quality assurance.

4 Sonar track along the cable

This section shows possibilities to obtain the XYZ position of a buried cable while following the

cable route. To get comparable results the same model is used for all configurations (Fig. 4):

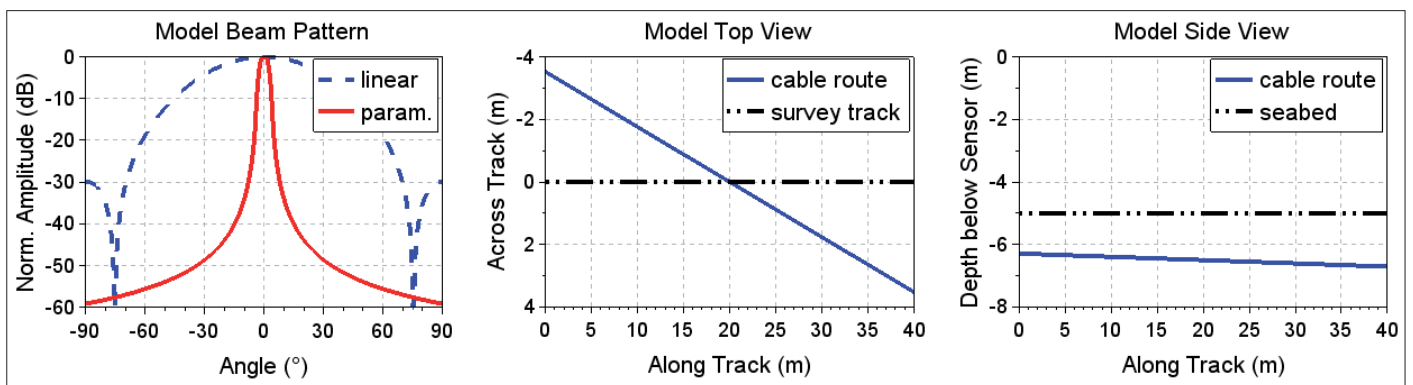
- Flat sandy seabed 5 m below sensor with boulders spread in the sediment volume.
- Cable (diameter 10 cm) buried 1.5 m below seafloor (slightly dipping, angle $\sim 0.6^\circ$).
- Survey vehicle moving not parallel to cable route (angle $\sim 10^\circ$) to simulate the vehicle coming off-track.
- Linear wide-beam projector (beam width 50°) or parametric narrow-beam projector(s) (beam width 5°) of the same size.
- Linear hydrophones with same beam pattern as the linear projector.
- Sonar using CW pulses (centre frequency 10 kHz).

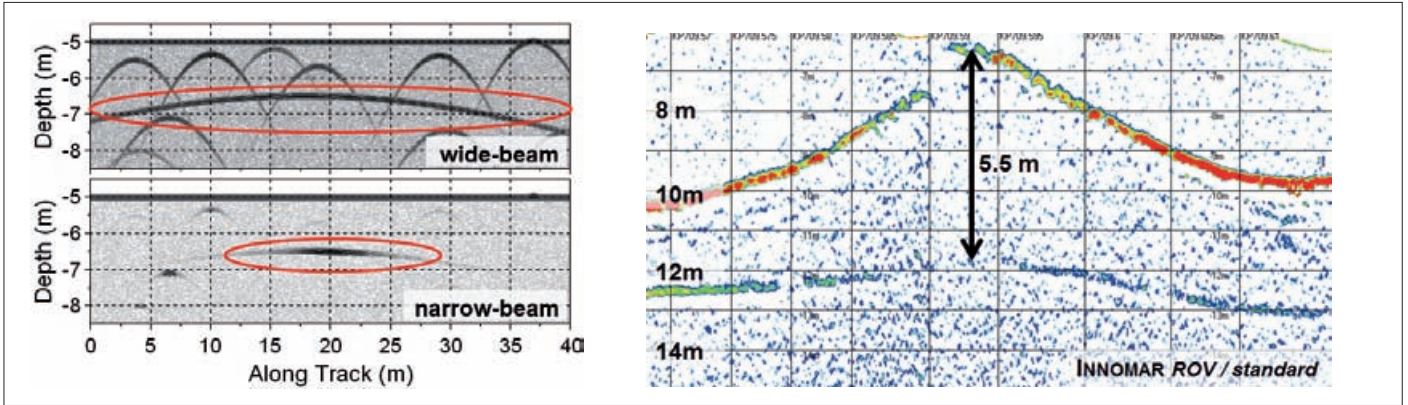
4.1 Projector and hydrophone at the same position

If an SBP follows a cable along track, the cable is seen like a sediment layer and there is no diffraction hyperbola. Burial depth and cable position can be determined assuming the SBP transducer was directly above the cable, but the error might be large depending on beam width and across-track position offset (Fig. 5). If the survey vehicle moves off the cable route, there is no helmsman guidance to correct this.

One idea to improve this situation is to use narrow sound beams pointing into different across-track directions (Schneider von Deimling et al. 2016; Wunderlich and Müller 2007; Wunderlich et al. 2005). Data from oblique beams can guide the helmsman to ensure the SBP stays roughly above the cable, but the localisation error will be still high.

Fig. 4: Model used: linear (blue) and parametric (red) beam patterns, half-power beam width linear 50° and parametric 5° (left); model volume with cable (blue) and survey vehicle track (black) seen from top (centre); model volume with cable (blue) and seafloor (black) seen from the side (right)





4.2 Several hydrophones across track

At least two hydrophones at different positions across the cable track are needed to get the position of a buried cable. The receivers are ideally spread over the entire survey corridor. If only a few receivers are used with an across-track separation longer than half the wavelength, the target position can be obtained from the intersection of travel times from all receivers or by energy focusing of all receiver signals into the cells of a gridded volume. If a large number of receivers shorter than half the wavelength apart is used, phased array beam forming becomes possible and the receiver signals can be combined to a single echo print showing an across-track diffraction hyperbola at the target position. This can be used for online visualisation and quality assurance.

To fully insonify a wide survey corridor across track,

- one wide-beam projector at the swath centre pointing downwards or
- several narrow-beam projectors at the swath centre pointing into different directions or
- several narrow-beam projectors at different across-track positions pointing downwards can be used.

As shown in section 2, wide sound beams will give higher reverberation levels decreasing the cable detection probability and lead to larger incidence angles resulting in larger position errors. Thus, narrow sound beams should be preferred. To avoid high transmission loss and large position errors at large incidence angles (cf. Fig. 2), these narrow-beam projectors are preferably spread across the survey corridor.

Fig. 5: Model echo prints from a cable (red marks) buried 15 m below seafloor surveyed 15 m along track according to the model shown in Fig. 4 (3.5 m off-track at start/end) and boulders spread in the seabed, for a linear wide-beam and a parametric narrow-beam system; boulders at the same locations for both data sets (left). Data example showing a pipeline followed along-track with burial depth up to 5+ m; pipeline echo level is decreased with increasing burial depth due to increasing sound attenuation; echo level reduction might be partly caused by the survey vehicle coming off-track, thus exact pipe position cannot be obtained (right)

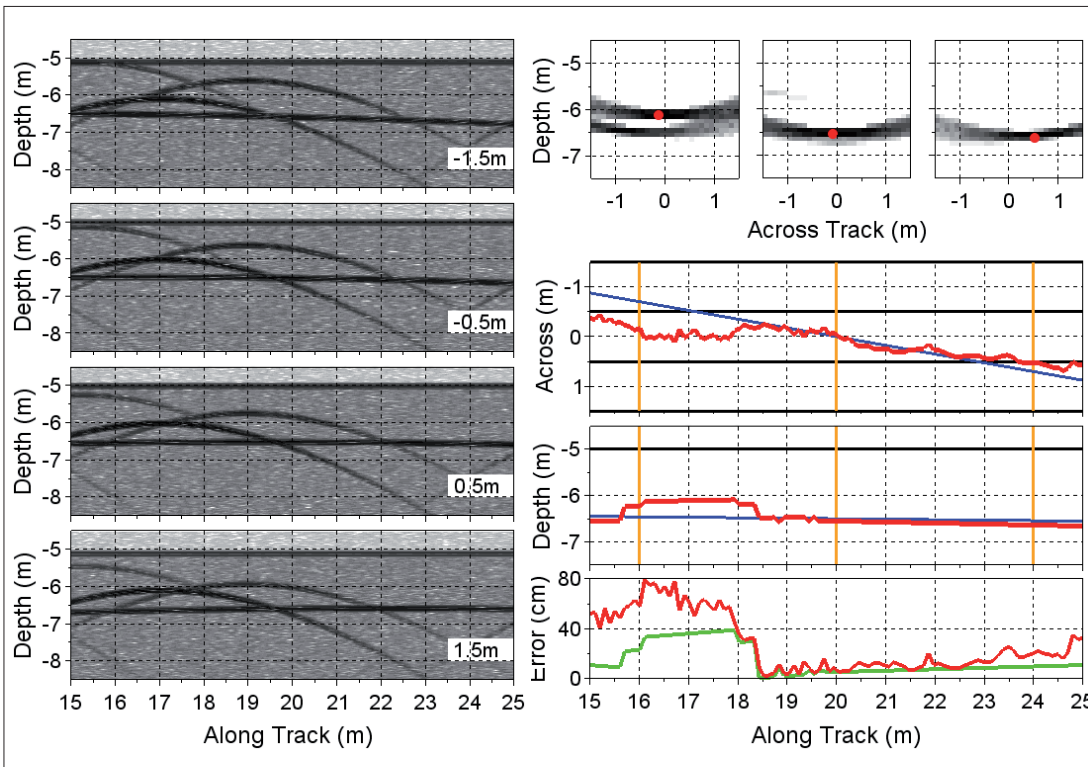


Fig. 6: One wide-beam projector covering the full swath and four hydrophones spread across-track 1 m apart following a cable according to the model shown in Fig. 4: echo prints of the four hydrophones (left); estimated (red) and true (blue) cable positions across track and burial depth; burial depth error (green) and total position error as Euclidian distance (red); receiver positions shown in black (right). Only the central ten metres of the model are shown. Cable position estimated from energy focusing. Large position errors due to boulders and refraction

References

- Lurton, Xavier (2002): An Introduction to Underwater Acoustics: Principles and Applications; Springer, London
- Schneider von Deimling, Jens; Philipp Held; Peter Feldens; Dennis Wilkens (2016): Effects of using inclined parametric echosounding on sub-bottom acoustic imaging and advances in buried object detection; *Geo-Marine Letters*, No. 36, pp. 113–119
- Sternlicht, Daniel D.; Christian P. de Moustier (2003): Time-dependent seafloor acoustic backscatter (10–100 kHz); *Journal of the Acoustical Society of America*, 114(5), pp. 2709–2725
- Stanton, Timothy K. (1989): Simple approximate formulas for backscattering of sound by spherical and elongated objects; *Journal of the Acoustical Society of America*, 86(4), pp. 1499–1510
- Urick, Robert J. (1983) *Principles of Underwater Sound*; Peninsula Publishing, Los Altos
- Waite, Ashley D. (2005): *Sonar for Practising Engineers*; Wiley, Chichester
- Wunderlich, Jens; Sabine Müller (2007): Detection of embedded objects using nonlinear sub-bottom profilers; *Proceedings of the 2nd International Conference & Exhibition »Underwater Acoustic Measurements: Technologies & Results« (UAM)*, pp. 511–516
- Wunderlich, Jens; Gert Wendt; Sabine Müller (2005): High-resolution echosounding and detection of embedded archaeological objects with nonlinear sub-bottom profilers; *Marine Geophysical Research*, 26, pp. 123–133

The next two paragraphs show examples of different projector and receiver arrangements to illustrate advantages and drawbacks.

One wide-beam projector at the centre and several hydrophones across track

If one wide-beam projector at the swath centre is used together with hydrophones spread across the survey corridor, the full ping rate can be used and cable localisation will be possible at high position density and good accuracy (Fig. 6). To ensure the required accuracy across a full swath, extensive processing to reduce the refraction error (cf. Fig. 2) is necessary. This processing is not possible in real-time yet, so online results will be at much lower accuracy. Another issue is the high reverberation level due to the large insonified volume and seabed area. Reverberation can be reduced if two or more tilted narrow-beam projectors are combined to have a wider beam across- than along-track. The receiver signals are very similar and echo plots cannot be used to guide the helmsman to stay along the cable route.

Several narrow-beam projectors and several hydrophones across-track

To reduce reverberation and to avoid large localisation errors caused by oblique sound beams while still having the survey corridor fully insonified across track, several narrow-beam projectors can be used (Fig. 7). Compared to the wide-beam example shown in the previous paragraph,

the reverberation level is much lower and much less boulder echoes interfere with the cable detection. Due to the smaller incidence angles the across-track cable position error is much lower and no time-consuming post-processing to reduce this error is necessary. The echo plots already show rough across-track cable position and can be used for helmsman guidance to stay above the cable.

5 Conclusions

Acoustic equipment is successfully used for cable DOB surveys. SBP survey tracks crossing the cable give the cable position at good accuracy, but position density along the cable track is limited. This position density is sufficient for maintenance DOB surveys and for quality assurance at surveys using electro-magnetic cable tracking equipment. Higher position density is either very costly due to increased survey and processing time or requires equipment following the cable along track. This needs an array of hydrophones spread across track and projector(s) to fully insonify the entire survey corridor. Best signal-to-noise ratio is achieved using narrow-beam projectors spread across track. This also reduces across-track position errors caused by (unknown) refraction at the water-seabed interface and avoids time-consuming post-processing to achieve full position accuracy. Online results can be used for quality assurance and to guide the helmsman. [⚓](#)

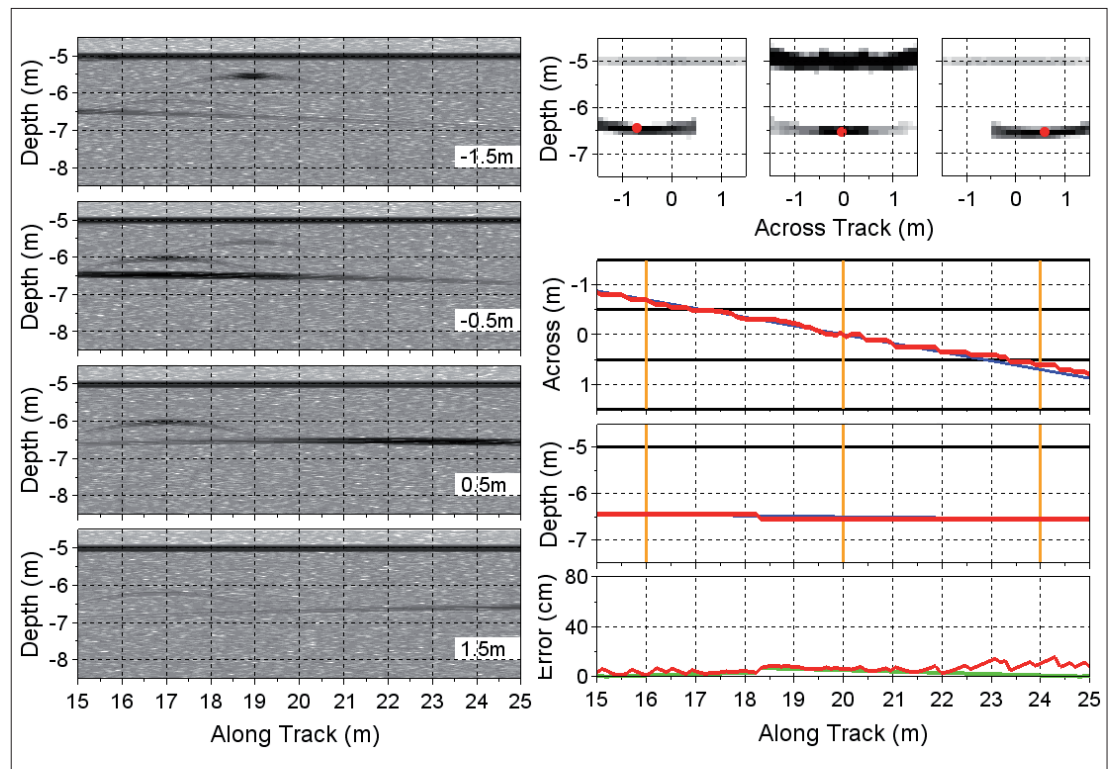


Fig. 7: Four narrow-beam projectors and four hydrophones spread across-track 1 m apart following a cable according to the model shown in Fig. 4: echo prints of the four hydrophones (left); estimated (red) and true (blue) cable positions across track and burial depth; burial depth error (green) and total position error as Euclidian distance (red); projector/receiver positions shown in black (right). Only the central ten metres of the model are shown. Cable position estimated from energy focusing. Much lower position errors compared to Fig. 6

Hydrography at the HCU

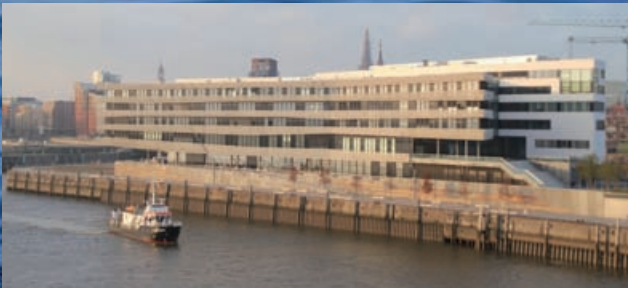
The HafenCity University Hamburg offers as the only German academic institution a full-time course in Hydrography (taught in English). It is a specialization within the area of Geomatics and certified as **FIG/IHO/ICA Category A**.

The course is scheduled to last two years and results - after completing a master's thesis and a final examination - in a Master of Science (MSc) degree.

The modules include hydrography, higher geodesy, navigation, GIS, marine geology and geophysics, oceanography, tide, maritime environment, data processing, and software technology.

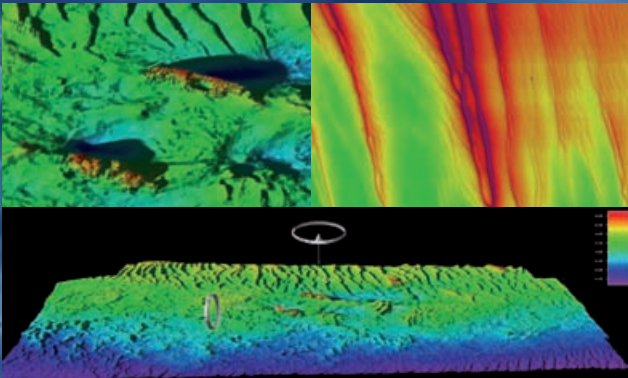
Research (Selected Topics):

- Seafloor topographic modeling
- Data cleaning methods
- Unmanned surface and underwater vehicles
- Subbottom profiling
- Shallow water quality surveys
- Magnetic and side scan object detection
- Multi-sensor systems



Field Training

“RV Ludwig Prandtl” (Helmholtz-Zentrum Geesthacht) in front of the HCU building, 3rd semester.



Results of Seafloor Surveys (QPS Fledermaus & CARIS)



Practical Exercise

Practical training on “Deepenschriewer III” (in co-operation with Hamburg Port Authority and Innomar), 1st and 2nd semester.



HafenCity Universität Hamburg, Überseeallee 16, 20457 Hamburg, Germany



Contact: Prof Dr. Thomas Schramm
thomas.schramm@hcu-hamburg.de

geomatik@hcu-hamburg.de
www.hcu-hamburg.de/en/master/geomatics



A new view on the Elbe

Dynamic and interactive 3D views for public information purposes in news media

An article by TANJA DUFEK, JOHANNES KRÖGER, BRENDON DUNCAN and JOCHEN SCHIEWE

In collaboration with the German newspaper *WELT*, a team of researchers from HafenCity University Hamburg developed new views of the River Elbe, showing the riverbed in a couple of 3D interactive views and videos. These have been integrated into a multimedia special which follows the goal to give people better insights into the complex topic of the fairway adjustment of the Elbe. This contribution describes input data as well as its processing and visualisation.

Authors

Tanja Dufek is research assistant for Hydrography at HCU. Johannes Kröger is research assistant at g2lab, HCU. Brendon Duncan studies M.Sc. Geomatics at HCU. Jochen Schiewe is Professor for Geoinformatics and Geovisualisation, and chair of the g2lab at HCU.

tanja.dufek@hcu-hamburg.de

Multimedia special of WELT

www.welt.de/lesestueck/2016/elbvertiefung

Long video versions

www.geomatik-hamburg.de/g2lab/research-welt.html

DTM visualisation | dynamic views | interactive 3D views | public participation

1 Introduction

Since 2002 the next – the ninth – stage of the fairway adjustment of the River Elbe in Germany is being planned and discussed by various experts, including politicians and lawyers. The adjustment of the navigational channel shall lead to depths of 15.9 m to 17.1 m below Sea Chart Zero (SKN) so that ships with a draught of 13.5 m (independent of tide) and 14.5 m (dependent of tide) are able to reach the Hamburg Port. This process implies deepening and widening at places where the minimum thresholds are not ensured due to the topography of the riverbed. It is expected that in December 2016 the Federal Administrative Court of Germany finally decides on the legitimacy of the planned process.

As this topic has gained significant public attention not only with people living along the Elbe, the newspaper *WELT* came up with the idea to support their readers with a better impression of the status and the plans. The result is a multimedia special in a so-called storytelling format called »A new view on the Elbe«. Core of this special are several dynamic and interactive 3D views of the Elbe riverbed which have been created by a scientific team of the HafenCity University Hamburg.

In the following the process of merging and visualising the data will be summarised as well as selected results together with first public reactions on it.

2 Data

For this project a digital terrain model of the whole riverbed of the Elbe from Cuxhaven up to the eastern boundary of Hamburg was generated. The underlying data was provided by the Federal Waterways and Shipping Administration (WSA) of Cuxhaven and Hamburg as well as by the Hamburg Port Authority (HPA) in XYZ format. The data sets were collected in 2010 by the responsible authorities. Some of the data sets are available from www.portaltideelbe.de and emodnet-bathymetry.eu. Originally derived from a 2 m grid and cross-lines of 100 m distance, the WSA data was delivered in

1 m resolution. The HPA data set was also obtained at 1 m resolution.

2.1 Videos

For the purpose of creating overview videos in the visualisation software *QPS Fledermaus* the data sets were re-gridded to 3 m resolution in order to increase the manoeuvrability and navigation performance.

A publicly available digital terrain model of the whole of Germany in a 200 m grid, made by the Federal Agency for Cartography and Geodesy (BKG) was used as background data, particularly in order to add some aesthetics to the scenes created.

2.2 Interactive 3D surfaces

The data sets for the interactive 3D surfaces of several locations were obtained from different sources with different properties:

- Wrecks: The wrecks are located in the area of Pagensand close to the city of Stade. This data was recorded by students of HafenCity University Hamburg with the SV »Deepenschriewer II« of HPA in June 2016. This digital terrain model features a horizontal resolution of 25 cm.
- Parkhafen and Turning Basin: These data sets were extracted from the data with 1 m horizontal resolution received from HPA, the same data that was also used for video generation.
- Old Elbtunnel: This data set was also provided by the HPA, but in a higher horizontal resolution (25 cm) than the general data set.

3 Data processing

3.1 Video

The data sets for the Elbe were individually imported into the visualisation software *QPS Fledermaus* where they were transformed to the UTM 32N (WGS 84) coordinate reference system with depths related to NHN (Normalhöhennull). Subsequently the data sets were gridded to a 3 m surface using the »Weighted Moving Average« algorithm. Finally, the single surfaces were merged into one surface depicting the entire sea floor from Cuxhaven to

Hamburg. To prevent data distortion when overlaying the detailed Elbe surface data and the coarse background data, a masking was applied.

A tailor-made colour map was also applied to the scene, illustrating the seabed in a blue colour scheme and the land area in brownish colour. To support the perception of depth and to increase the visibility of small scaled underwater features, a vertical exaggeration of approximately 10 times the horizontal scale was used. Using a 3D mouse, a flight path was created and recorded using the software's camera/video function. The recorded flights were rendered as individual frames in 720p HD resolution before using *ffmpeg* to generate a video in *mp4/H264* format.

3.2 Interactive 3D surfaces

In addition to the videos, HCU also provided interactive views for selected subsets of the bathymetry. The plug-in *Qgis2threejs* for the free desktop GIS software *QGIS* was used to generate *WebGL*-based 3D viewers of the data. *Qgis2threejs* also supports texturing, shading, labels and additional geometries such as lines or points. The result is a HTML-page plus a set of JavaScript files which consist of the application logic for display/interaction and the triangulated 3D data. Default interaction methods include zooming, panning, rotating and orbiting.

Qgis2threejs offers two different resampling approaches when triangulating the elevation grid. While the »simple« mode uses a fixed spacing between vertices, the »advanced« mode uses a quad-tree to increase or decrease the geometric detail in user-defined regions. One disadvantage of *Qgis2threejs* is that it will always ignore the topological details but simply creates a regular mesh of triangulated squares. This limits the possible scale or resolution in the viewers quite severely. For more advanced uses other free and open-source software like *SAGA GIS*, *Blender* or even specialised tools like *Instant Meshes* could be utilised to generate optimised topology.

Qgis2threejs also allows the placement of a texture on the surface. To visually enhance the plain geometries a simple divergent colour scale for land elevation (red) and water (blue) depths with a neutral light grey midpoint was used. For displaying purposes a vertical exaggeration of 3 (Wrecks, Parkhafen, Turning Basin) to 5 (Old Elbtunnel) was chosen.

4 Results

4.1 Videos

The flight of the first video (»Medemrinne«) starts at the Elbe estuary close to Cuxhaven, then proceeds upstream towards Brunsbüttel showing the main fairway as well as the Medemrinne north of it. The flight path has a length of approximately 38 km. The main fairway is only a small part of the Elbe in the south, as shallow water zones and tide ways extend to the northern banks. These features can be very nicely seen in the 3D data set. The original video has a length of 2:39 minutes. Its speed was

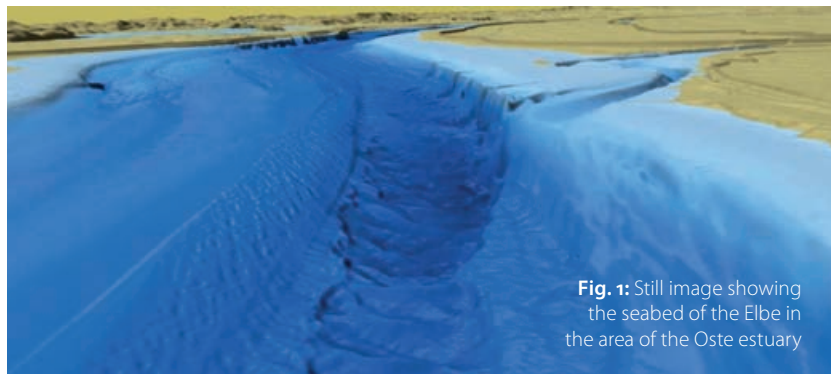


Fig. 1: Still image showing the seabed of the Elbe in the area of the Oste estuary

increased when adding the text by a narrator so that the final length is less than one minute within the multimedia special of WELT. A still image of the video is depicted in Fig. 1.

The second video (»Brunsbüttel to Wittenbergen«) starts in the area of Brunsbüttel and takes the viewer upstream to Wittenbergen. The flight path has a length of approximately 58 km (long video version), leading to a video duration of 2:32 minutes which was reduced to 0:38 minutes within the multimedia special of WELT. A still image of the video in the area of the entrance of the Kiel Canal is depicted in Fig. 2.

Near the end of this video the actual and planned fairways in the area between Wedel and Wittenbergen are visualised by additional vector data (Fig. 3). The respective coordinates were partly provided by the responsible authorities (WSA Hamburg and HPA) and partly derived from the publicly available planning documents (www.fahrrinnenausbau.de). The actual and planned fairway extents were modelled in *AutoCAD Civil 3D*, the resulting DWG files were then imported into *QPS Fledermaus*.

Acknowledgements

The authors thank the team of WELT, namely Daniela Jaschob and Lars-Olaf Preuß, for the productive co-operation in this project.

Furthermore, we would like to thank the WSA Hamburg and Cuxhaven as well as HPA together with the Federal Maritime and Hydrographic Agency of Germany (BSH) for providing the data.

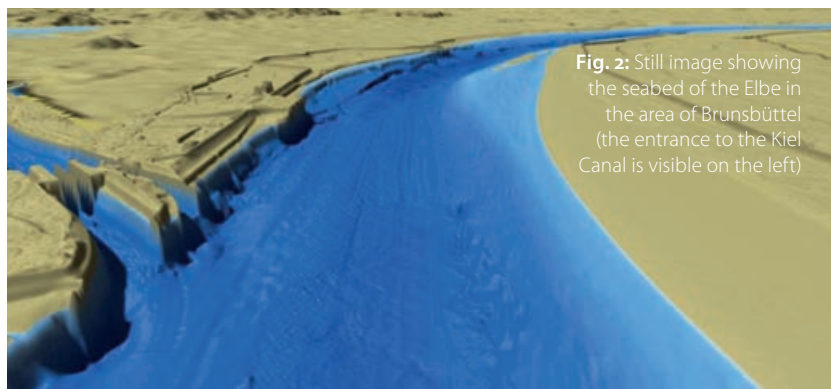


Fig. 2: Still image showing the seabed of the Elbe in the area of Brunsbüttel (the entrance to the Kiel Canal is visible on the left)

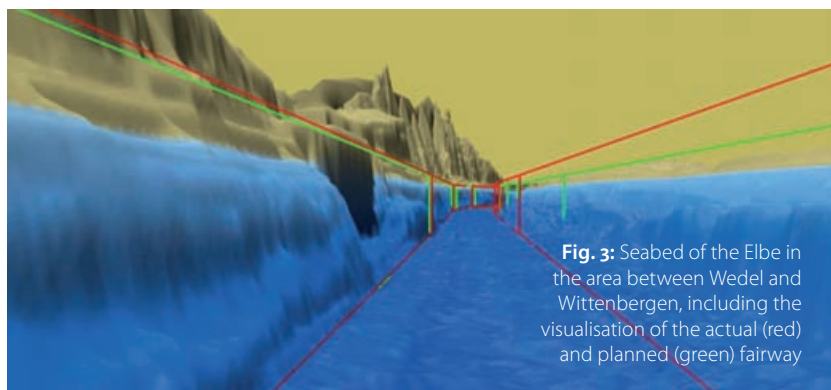


Fig. 3: Seabed of the Elbe in the area between Wedel and Wittenbergen, including the visualisation of the actual (red) and planned (green) fairway

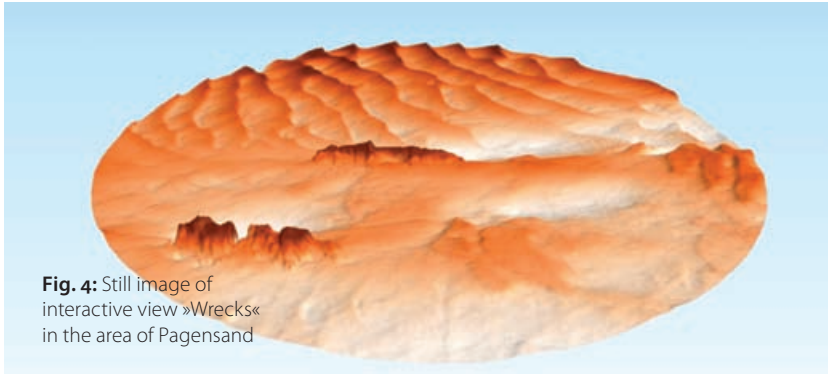


Fig. 4: Still image of interactive view »Wrecks« in the area of Pagensand

4.2 Interactive 3D views

Fig. 4 shows the first interactive prototype focussing on some wrecks. The area was clipped to a circular shape for aesthetic reasons.

The data set »Parkhafen« (Fig. 5) shows the riverbed of the Elbe in the north, the turning circle of Parkhafen in the centre and the entrance to Waltershofer Hafen in the south-east. In the area of the Petroleumhafen dredging scours are visible in the seabed.

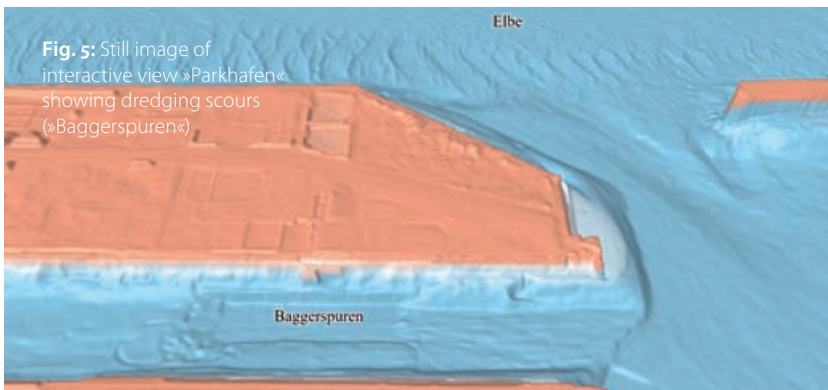


Fig. 5: Still image of interactive view »Parkhafen« showing dredging scours (»Baggerspuren«)



Fig. 6: Still image of interactive view »Old Elbtunnel«

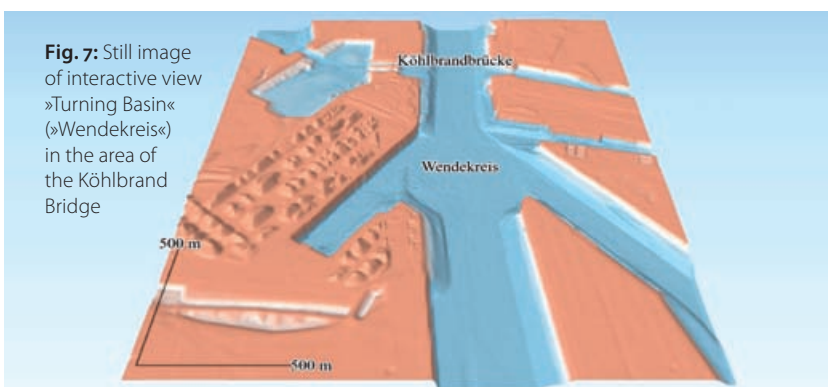


Fig. 7: Still image of interactive view »Turning Basin« (»Wendekreis«) in the area of the Köhlbrand Bridge

As mentioned above, for the area of the »Old Elbtunnel« data of a higher horizontal resolution was used. The selection of an appropriate level of geometric detail in *Qgis2threejs* led to a file size much too big, so a blended hillshade texture based on the high-resolution data was used in combination with a lower-resolution mesh to display the details via the mesh's texture rather than actual geometry (Fig. 6). The viewer shows the material currently placed on top of the Old Elbtunnel to weigh down the structure during ongoing construction works within.

As with the »Parkhafen« example, for the view »Turning Basin« a quad-tree approach was used in order to supply higher geometric resolution for the main area of interest. Looking closely at the »blobs« in the left centre one might be able to see the difference in geometric detail between the high-resolution centre of the image and its borders (Fig. 7). Also shown is a scale bar, simply made of two lines with labels.

4.3 Multimedia special

Finally the WELT team compiled the single elements into the final product, an online multimedia special in a so-called storytelling format. This consists of seven chapters, each of them describing a certain aspect of the adjustment process (like »Elbe without water«, »Elbe upstream«, »Ships' Cemetery«, etc.). These chapters are enriched by the above mentioned videos (with added explanatory narration) and 3D interactive views, together with additional figures and photos. Finally, 360° videos of the Hamburg Port acquired on-board a ship with statements of Jens Meier (Director of HPA) are explaining the importance of the fairway adjustment process.

5 Summary

WELT observed an extraordinary user interest in the resulting multimedia special in terms of visitors. Regarding the impressive impact, Frank Horch, as Senator for Traffic in Hamburg responsible for the Elbe project, stated: »I haven't seen such a representation before. Such 3D views are able to produce a better understanding of infrastructure projects or environmental interventions« (WELT, 01.09.2016).

From a scientific perspective one main challenge within this project was the harmonisation of the huge data sets. In particular, the combination of data with very different horizontal resolutions (in particular, between land and water areas) was not trivial. The second challenge was about the generation of appealing and compact visualisations that should offer both the overview and details like wrecks. Also an appropriate colour scheme had to be chosen, taking into account the fact that some of the areas which are already above the mean sea level (like the Wadden Sea or islands within the Elbe) are widely considered as water area. [↕](#)

Apogee Series

NEW

SURVEY IN ALL SEA CONDITIONS

Apogee makes very high accuracy INS/GNSS affordable for all surveying companies.

HIGH ACCURACY INS/GNSS

- » 0.005° Roll & Pitch
- » 2 cm Delayed Heave
- » 0.02° Heading
- » 1 cm Position

PPK accuracy

Operational up to 200 m depth



OFFICIAL DISTRIBUTOR

M·B·T 
UNDERWATER TECHNOLOGY

 **MBT GmbH**
Wischhofstraße 1-3
Gebäude 11
D-24148 Kiel
Germany

TEL +49 (0)431 535 500 70
FAX +49 (0)431 535 500 99

MAIL info@m-b-t.com
WEB www.m-b-t.com



The liberated organisation

An article by MATHIAS JONAS

The IHO has been working on organisational changes for several years. During the 3rd Extraordinary International Hydrographic Conference (EIHC) in 2005 and the International Hydrographic Conference (IHC) in 2007, the constitutional documents were approved in the meeting but they needed support by 48 member countries. As this now has been reached, changes will be made, entering into force on 8 November 2016.

Author

Dr. Mathias Jonas is National Hydrographer of Germany and Vice President of the Federal Maritime and Hydrographic Agency in Rostock.

mathias.jonas@bsh.de

The International Hydrographic Organization IHO is surrounded by the aura of its extraordinary founding history and residence. In 1921 Prince Albert I. of Monaco, a passionate marine researcher, established the IHO predecessor, the International Hydrographic Bureau IHB at the foothills of the Monte Carlo, from which today you still have a remarkable view onto the famous marina and the Mediterranean Sea.

The prospects of this international technical organisation for welcoming a growing number of new member states with national hydrographic tasks and a corresponding modern organisational structure improved drastically with the international entry into force of the revised IHO Convention, which will take effect as of November 2016. The IHO deals with many hydrographic topics in an up-to-date manner and has gained considerable reputation in the IMO, the International Maritime Organization of the United Nations, with the digital flagship electronic sea chart ECDIS. However, the constitution and organisational body are still characterised by pre-computer era working methods.

The start-up for the announced quantum leap took a long time: In the early years of this millennium a proposal of amendments was elaborated to the IHO Convention by experts for public law, and agreed on unanimously in 2004 after intensive discussions on the Extraordinary Hydrographic

Conference under the chairmanship of the former BSH president Peter Ehlers.

The new IHO Convention, modestly called Protocol of Amendments, enjoys the status of an international contract; for its entering into force many member states needed the approval of its national parliaments. The well-known attitude of many states towards hydrographic significance is reflected in the ratification history of the renewed contractual text. It took twelve years for the last member state – Syria – to send the official ratification approval to its embassy in Paris and thus to obtain the quorum.

Which changes will bring the new IHO Convention taking effect on 8 November 2016 and which benefits will arise for the organisation?

The most significant change concerns the accession of new members. United Nations states are automatically qualified for IHO membership, thus the formerly time consuming procedures for seeking the approval of a two third majority of existing member states is not required anymore. An increase of members does not only imply a greater representation and political importance but also increasing membership fees, which are calculated according to the ship tonnage under the corresponding national flag. Huge flag states like Liberia, Panama and Malta do not belong to the IHO yet. The simplified procedures give hope for the accession of important new entries.

The revisions of the new IHO Convention introduce UN organisations, in particular to the IMO, with regard to the IHO internal administration and organisational body. The International Hydrographic Bureau headquarters in Monaco will now be called IHO Secretariat. It will be led by a future Secretary General replacing the former position of the IHB President. Robert Ward, current President, will take over the new position in this legislative period until 31 July 2017. These changes will show consequences. So far, the President was »first among equals« in the Directing Committee, that comprised a President and two Directors. His main task was to represent the organisation to the outside. However, passing a resolution concerning strategic and operational measures remained in the responsibility of the three nominated IHB Directors. The President had no directive towards the Directors. Based on the amended Convention this right is now given to the Secretary Gen-



eral. Furthermore, it changes the eligibility requirements for candidates applying for one of the three positions. So far, candidates needed to prove a close relation between their professional career, hydrography and practical experience at sea, ideally having worked in hydrographic surveying. However, this IHO relevant qualification doesn't automatically imply the ability to manage an international organisation. Talented managers with an academic, economic or legal background were excluded from the applications until now, as well as candidates older than 65 years seeking a position in the Secretariat. These regulations do not exist anymore.

The most important body of the organisation was the Hydrographic Conference taking place every five years so far. It will be replaced by an Assembly of all member states meeting in a three-year-cycle. A Council made up of 30 states that show highest interest in hydrography will meet annually – an entirely new element. One of the controversial questions is how to measure this interest according to the new convention. In future, ten seats will be given to the states with the greatest national tonnage; the remaining 20 seats will be divided among the 15 regional committees by means of a still untested procedure. The

aim of the three-year-cycle meetings of Council and Assembly is to provide more flexibility in decision-taking processes, choosing topics and use of budget. Additionally, the instrument of voting by correspondence changed in so far as decisions will be taken based on a majority of the member states that cast a vote, instead of the still existing arrangement where a majority of all member states entitled to vote is required. However, it is still unclear whether the Council with its 30 members is allowed to take decisions for the reporting committees for technical standardisation and international cooperation. This IHO working level made up of committees and related working groups had already been restructured in 2009 with regard to the new Convention.

The long awaited new organisation has finally arrived at the Côte d'Azur. It is now up to the Secretary General, the Directors and the Council Chairman to live up to the expectations of the former generation. The time has definitely come for these changes as processes depending on hydrographic information such as sea transportation, energy production, resource extraction and marine conservation speed up globally and call for an organisation that works successfully on international level. [↕](#)



40+

YEARS OF HYDROGRAPHIC EXPERIENCE

Fugro's hydrographic and geophysical surveys inform energy, construction and mining projects around the world.

Our high resolution, large area multibeam surveys - facilitated by Fugro's precise positioning services - deliver IHO compliance, whilst our desktop studies and detailed surveys of cable routes, pipelay and subsea infrastructure, enhance the safety and efficiency of your project.

Fugro OSAE GmbH
+49 4212 239150
info@fosae.de
www.fugro.com
www.fosae.de

In memory of DVW President Prof. Dr. Ing. Karl-Friedrich Thöne

An obituary by HAGEN GRAEFF*

Since the »Declaration of Bremen« (»Bremer Erklärung«) from 2008 the geo societies DVW (German Society for Geodesy, Geoinformation and Land Management) and DHyG (German Hydrographic Society) are friendly connected. On 15 July 2016 the President of the DVW Prof. Dr. Ing. Karl-Friedrich Thöne died unexpectedly at the age of 59 years. At a deeply moving sea burial off the island of Föhr we said farewell.

Author

Hagen Graeff was President of the DVW until 2008.

This text is a shortened translation of the obituary published in ZfV (DVW journal).

Prof. Dr. Ing. Karl-Friedrich Thöne was born 4 August 1956 in Neu-Garstedt (district of Hamburg-Harburg). From 1976 till 1982 he studied Geodesy at the Technical University of Berlin and with a following scholarship he went to Portugal for further studies on agricultural restructuring in the context of the EU accession. Over the years his professional focus was set on land development starting in 1985 in the Administration of Agricultural Structure of Lower Saxony. Further stations in his professional career were:

- 1990: Federal Ministry of Food, Agriculture and Forestry;
- 1996: Head of the Department Land Development;
- 1994: Ph.D. in Engineering, »Die agrarstrukturelle Entwicklung in den neuen Bundesländern. Zur Regelung der Eigentumsverhältnisse und Neugestaltung ländlicher Räume« (»Development of Agricultural Structure in the new Federal States. Regulation of Ownership Structures and Rural Reorganisation«).

In 1998 Prof. Dr. Ing. Karl-Friedrich Thöne started his career in the Thuringian Ministry for Agriculture, Nature and Environment and as head of department he was responsible for 2000 employees. One of his greatest achievements was the creation

of the public-law institution »Thuringian Forestry« (»Thüringer Forst«) showing his deep interest in rural development, forestry and environmental protection. The »Green Belt« (»Das grüne Band«) was another regional project of international significance he was very much engaged in.

Prof. Dr. Ing. Karl-Friedrich Thöne held numerous honorary positions and represented our professional interests in various committees, councils and advisory boards. At the Technical University of Dresden he was honorary professor for international land policy and at the Technical University of Munich he held lectures in the international Master study programme on land management and land tenure for professionals.

On 1 January 2001 Prof. Dr. Ing. Karl-Friedrich Thöne was elected Vice President by the DVW. Eight years later he became President of this society. For almost 16 years he represented, formed and supported the society's interest in an excellent way. This extraordinary engagement was only made possible by the understanding support of his wife Jutta and daughter Mareike.

During these 16 years Karl-Friedrich Thöne was the driving personality behind the DVW's continuous development. Closer cooperation, a sense of community and more intense communication among members and work groups became every-day practice, as well as our presence on Twitter, Facebook, Xing and the *DVW-news*. Preserving and renewing without giving up traditions were significant elements during his presidency. Taking part in Europe and representing national interests in the world association FIG was another passionate goal of Karl-Friedrich Thöne. Also the INTERGEO conference and trade fair stands for his great achievements.

Karl-Friedrich Thöne was not only DVW President, he was a personality who generated ideas and when necessary convinced with unconventional ideas and solutions. The DVW has lost a friend and an advisor, a politically motivated creator and an important geodesist. He leaves footprints, which will be hard to fill. We – the national associations of the DVW, the working groups and the board members – are full of admiration and thankfulness for his achievements.

We will honour his memory at all times. [📍](#)



COME SEE US AT STAND 45 AT HYDRO 2016,
8-10 NOVEMBER IN ROSTOCK-WARNEMÜNDE

Deformation Analysis Solution

- Coastal and waterway analysis
- Vertical quay wall inspection
- Structural model creation
- Conformance and validation analysis
- Combine lidar and multibeam
- 3D visualization and editing
- Map creation and reporting
- Available in CARIS BASE Editor™

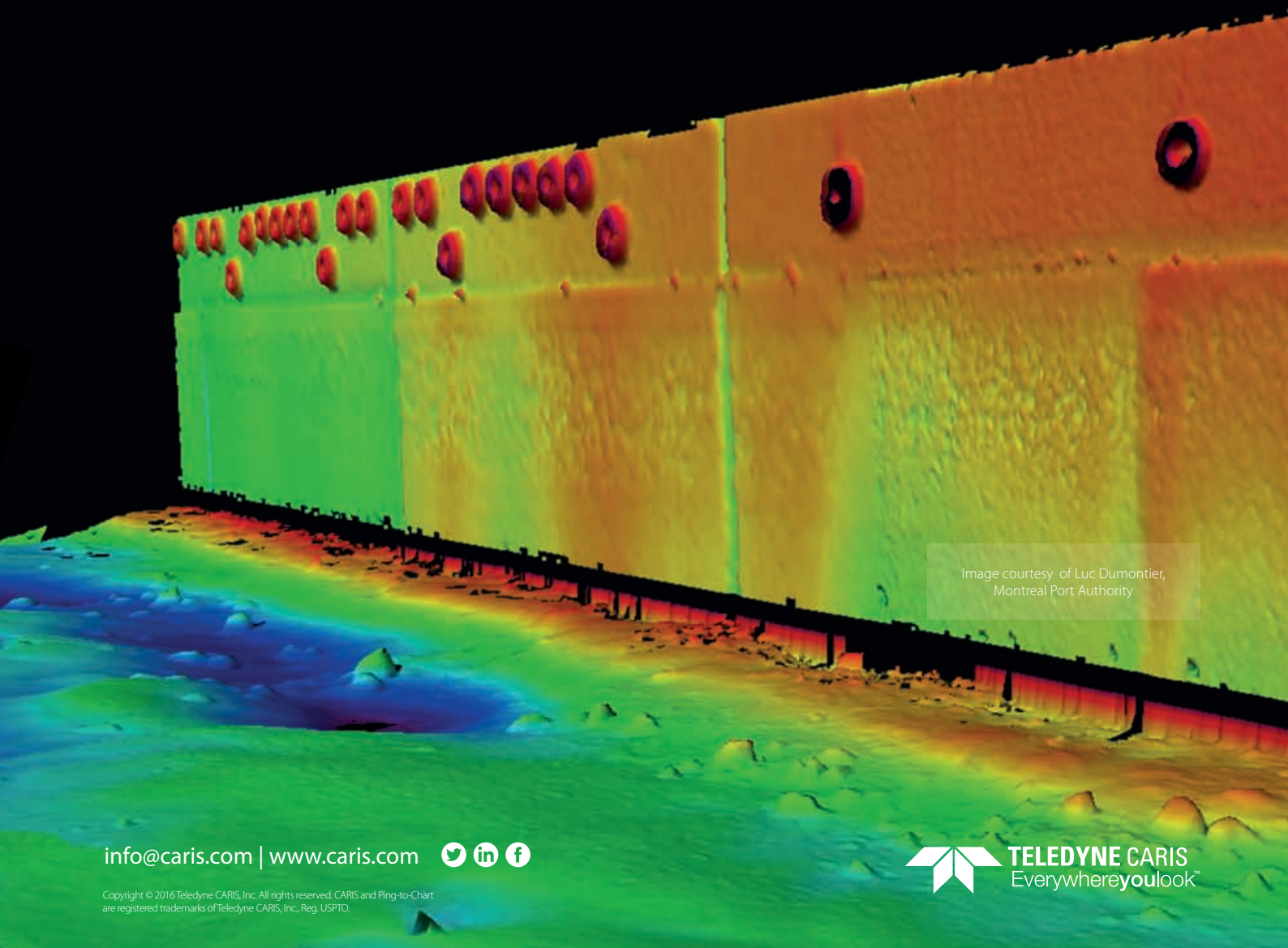


Image courtesy of Luc Dumontier,
Montreal Port Authority

info@caris.com | www.caris.com



Copyright © 2016 Teledyne CARIS, Inc. All rights reserved. CARIS and Ping-to-Chart
are registered trademarks of Teledyne CARIS, Inc., Reg. USPTO.



TELEDYNE CARIS
Everywhereyoulook™

Präzise 3D Positionierung

.. mit GNSS und Polarmessverfahren

Leica Geosystems ist mit nahezu 200 Jahren Erfahrung Pionier in der Entwicklung und Produktion von Vermessungsinstrumenten und Lösungen und gehört zu den Weltmarktführern in der Vermessung. Innovation, absolute Präzision und höchste Qualitätsansprüche kombiniert mit einem umfassenden Service- und Dienstleistungsangebot führen dazu, dass Fachleute auf Leica Geosystems vertrauen.

Die **GNSS Instrumente** von Leica Geosystems empfangen und verarbeiten die Signale der Navigationssysteme von GPS, GLONASS, **Galileo und BeiDou**. Mit diesen GNSS

Instrumenten sind Sie für Ihre 3D Gewässervermessung bis **über das Jahr 2020 hinaus für die Zukunft gerüstet ohne weitere Investitionsmittel einplanen zu müssen.**

Die MS60 **MultiStation** und die TS16 **Totalstation** sind Polarmesssysteme für höchste Präzision und Leistung bei voller Automatisierung der Messabläufe. Der revolutionäre Distanzmesser vereint die Vorteile des Phasenmessprinzips mit den Vorteilen der Zeitmessung. Die Messzeiten sind bis zu 50% schneller, was eine Datenrate bis zu 20 Hz ermöglicht.

Leica Geosystems GmbH Vertrieb
Telefon 0 30/44 02 13 29
e-mail: Frank.Hinsche@leica-geosystems.com
www.leica-geosystems.de



Leica
Geosystems